DESIGN AND APPLICATION OF COMPARTMENTALIZED PLATFORMS FOR NEUROBIOLOGICAL RESEARCH

by

Aysel Çetinkaya Fışgın

B.Sc., Chemical Engineering, METU, 1993

M.S, Medical Systems and Informatics, Boğaziçi Univesity, 2010

Submitted to the Institute of Biomedical Engineering

in partial fulfillment of the requirements

for the degree of

Doctor

of

Philosophy

Boğaziçi University

2016

ACKNOWLEDGEMENTS

I would like to thank all the people who contributed in some way to the work described in this thesis. First and foremost, I would like to express my special appreciation and thanks to my advisor Professor Dr. Cengizhan ÖZTÜRK, for his lead and tremendous support throughout my research, and for his provision of wonderful opportunity in Johns Hopkins University and constant faith in my success.

I would also like to thank Associate Professor Erdem TÜZÜN and Assistant Professor Özgür KOCATÜRK, Associate Professor In Hong Yang and Assistant Professor Esin Öztürk Işık for serving as my committee members. I also want to thank them for letting my defense be an enjoyable moment, and for their brilliant comments and suggestions. Profound gratitude goes to Dr In Hong Yang, who has been a truly dedicated mentor and Professor Ahmet Hoke for his continuous support and guidance.

I am so grateful to the EU Marie Curie Actions IRSES Project 269300 (TAHITI, Improving Therapy and Intervention through Imaging) and Center for Life Sciences and Technologies Grant (09K120520) that funded part of the research discussed in this dissertation.

I want to thank my loving and caring family. I am grateful to my parents for all of their sacrifices and prayers. I am also grateful to them for teaching me to follow my dreams even when they go against the grain. Words cannot express my appreciation and love for my daughters Ece and Eda. The motive of this dissertation was to be a role model for them. My role model was Jonathan Livingston seagull that thought me to push against my personal boundaries and discover what lies beyond.

Finally, but by no means least, I am grateful to my "wise husband" Tamer for his unbelievable support and his soothing effect. He was always there to give me the best advice. Thank you.

ACADEMIC ETHICS AND INTEGRITY STATEMENT

I, Aysel Çetinkaya Fışgın, hereby certify that I am aware of the Academic Ethics and Integrity Policy issued by the Council of Higher Education (YÖK) and I fully acknowledge all the consequences due to its violation by plagiarism or any other way.

Name :

Signature:

Date:

ABSTRACT

DESIGN AND APPLICATION OF COMPARTMENTALIZED PLATFORMS FOR NEUROBIOLOGICAL RESEARCH

Conventional culture systems remain inadequate for comprehensive understanding of injury and regeneration in peripheral neurons that extend axons over long distances and through varying extracellular microenvironments. Therefore, a highly tailorable in vitro system, that allows studying in different in vitro models that mimics axonal injury, regeneration and nerve transplants is required. This dissertation presents the development and application of novel compartmentalized *in vitro* cell culture platforms, where cell bodies are cultured on one side and axons are allowed to grow to the other side through microchannels that connect the two fluidically isolated compartments.First, regenerative effects of members of the glial cell-line derived nerve growth factor (GDNF) family of ligands (GFLs) were investigated in a microfluidic physical injury model and GDNF was most potent in promoting axon outgrowth after axotomy. Next, the first high throughput compartmentalized microfluidic platform (HTCMP) is developed, which is an innovative model for *in vitro* assays in drug screening, where distal axonal degeneration can be modeled by manipulating compartments independently. By means of HTCMP, Flucinolone Acetonide (FA) is identified as a neuroprotective compound *in vitro* and validated *in vivo* that it demonstrates axonal protection from PIPN as well as relieving neuropathic pain. Finally, compartmentalized microfluidic platforms that mimics the isolated *in vivo* environment, are used in an *in vitro* model of stem cell replacement therapy for nerve injuries, and it is demonstrated that that the axons of mESC (mouse embryonic stem cell) derived motor neurons are myelinated by mESC derived oligodendrocytes.

Keywords: compartmentalized microfluidic culture platform, chemotherapy induced peripheral neuropathy, Paclitaxel, GDNF, Flucinolone Acetonide, high throughput drug screening, myelination; embryonic stem cells (ESCs); mouse ESCs derived motor neurons; mouse ESCs derived oligodendrocytes.

ÖZET

NÖROBİYOLOJİK ARAŞTIRMALAR İÇİN KOMPARTMENTALİZE MİKROFLUİDİK KÜLTÜR PLATFORMU TASARIM VE TATBİKATI

Alışılagelmiş hücre kültürleri; aksonları uzun mesafeler katedip, değişken mikroçevresel alanlarda bulunan periferik nöronların dejenerasyon ve rejenerasyonunun kapsamlı bir şekilde incelenmesi için yeterli olmamaktadır. Bu sebeple, akson zedelenmesi, rejenerasyon ve sinir nakli gibi değişik biçimlere uyarlanabilecek bir *in vitro* sisteme ihtiyaç vardır. Bu amaçla sinir hücrelerinin bir kompartmanda yetiştirilip, aksonlarını aradaki mikrokanallar vasıtası ile diğerine uzatabildiği fluidik olarak izole iki kompartmandan oluşan yenilikçi bir *in vitro* hücre kültür platformu tasarlanmış ve uygulaması yapılmıştır. Öncelikle glial hücre hattı türevli büyüme faktörü ligand ailesi'nin rejeneratif etkileri bir mikrofluidik akson kopması modelinde incelendi ve aksonların ortama eklenen GDNF'le en yüksek büyümeye ulaştıkları belirlendi. Bu sonuçlar büyüme faktörüne dayalı periferik akson yenilenme tedavilerine katkı sağlayacaktır. Daha sonra ilaç tarama için axon uçlarındaki dejenerasyonu *in vitro* modelleyebilen ve bu alanda ilk olan yüksek verimli kompartmentalize platform geliştirildi. Bu platform sayesinde Flucinolone Acetonide (FA) *in vitro* analizlerde sinir koruyucu ajan olarak tanimlandi ve paclitaxel kaynaklı periferik nöropatilere karşı aksonları dejenerasyona karşı koruma özelliği *in vivo* nöropati modelinde ispatlandı. Son olarak; izole *in vivo* ortamları andıran kompartmentalize mikrofluidik platformlar, sinir hasarlarının tedavisinde kullanılan kök hücre replasman tedavilerinin *in vitro* modellemesi için kullanıldı ve fare embriyonik kök hücreden türeyen oligodendrisitlerin yine fare embriyonik kök hücreden türeyen motor nöronların aksonlarını myelinle kaplayabileceği gösterildi.

Anahtar Sözcükler: Kompartmentalize mikrofluidik platform, Kemoterapi kaynaklı periferik nöropati, Paclitaxel, Taxol, Fluocinolone Acetonide, yüksek verimli ilaç tarama sistemi, myelinizasyon, fare embriyonik kök hücre türevli motor nöron, fare embriyonik kök hücre türevli oligodendrosit.

TABLE OF CONTENTS

LIST OF FIGURES

LIST OF TABLES

LIST OF SYMBOLS

C	concentration at a point (x,y,z)
D	coefficient of diffusion
v	velocity vector
u	x component of velocity
η	viscosity
ρ	density

LIST OF ABBREVIATIONS

ALS	Amyotrophic lateral sclerosis
ATP	Adenosine triphosphate
BDNF	Brain-derived neurotrophic factor
CIPN	Chemotherapy Induced Peripheral Neuropathy
CMP	Compartmentalized Microfluidic Platform
CNS	Central nervous system
DRG	Dorsal root ganglion/ganglia
EBs	Embryonic bodies
ECM	Extracellular matrix
ESCs	Embryonic stem cells
FA	Fluocinolone Acetonide
FGF2	Basic fibroblast growth factor
FITC	Fluorescein Isothiocyanate
GDNF	Glial cell-derived neurotrophic factor
GFL	GDNF family of ligands
HTCMP	High throughput compartmentalized microfluidic platform
mESCs	mouse Embryonic stem cell
MNs	Motor neurons
MS	Multiple sclerosis
NB	Neublastin
NF	Neurofilament
NT	Neurturin
ONI	Optic Nerve Injury
OPCs	Oligodendrocyte progenitor cells
PDGF	Platelet-derived growth factor
PDL	Poly-D-Lysine
PDMS	Polydimethylsiloxane
PIPN	Paclitaxel Induced Peripheral Neuropathy

PTX	Paclitaxel (Taxol)
Pur	Purmorphamine
RA	Retinoic acid
SCI	Spinal cord injury
SMA	Spinal muscular atrophy
TEM	Transmission electron microscopy

1. INTRODUCTION

1.1 Overview of the Dissertation

Neurons are structurally and functionally unique. Unlike other cells, they extend long processes over long distances and through varying extracellular microenvironments. Therefore, conventional *in vivo* and *in vitro* cell culture methods remains deficient to understand and explore the mechanisms, which differentially affect distinctive parts of the neuron that often occur in neuronal injury and neurodegenerative disease [3].

This dissertation presents the development and application of a two-compartment *in vitro* cell culture platform, where cell bodies are cultured one side and axons are allowed to grow to the other side through microchannels that connect the two compartments. This *in vitro* modeling enables control of local environments and study axonal injury and regeneration of neurons where conventional culture systems remain inadequate in modeling the unique features of neurons.

In chapter 2, the fluidic isolation between two compartments that mimics the different microenvironments of cell body and axon of a neuron is modeled and established. Then the compartmentalized *in vitro* cell culture platforms are used to elucidate the regenerative the effects and site of action of members of the glial cell-line derived nerve growth factor (GDNF) family of ligands (GFLs) in a microfluidic axotomy model.

In Chapter 3, compartmentalized microfluidic cell culture platforms are used to model Paclitaxel induced peripheral neuropathy, where axons are more susceptible to toxic effects of paclitaxel than cell bodies of peripheral neurons. Compartmentalization of axons and cell bodies is an explicit way to elucidate localized effects of Paclitaxel to axons and to seek for potential compounds that protects axons. A high throughput drug-screening platform is developed in order to identify therapeutic targets for pe-

ripheral neuropathies induced by paclitaxel, and FA is identified as a neuroprotective agent. Next, the findings are validated at an *in vivo* mouse model of paclitaxel induced neuropathy.

In chapter 4, by means of compartmentalized microfluidic platforms, the ability of stem cell derived oligodendrocytes to myelinate axons of stem cell derived motor neurons is verified. It is demonstrated that oligodendrocytes have potential as therapeutics for myelination of stem cell derived motor neurons that are transplanted to replace damaged neurons and remyelination of demyelinated axons in the central nervous system (CNS).

Chapter 5 provides summary of the specific aims and provides suggestions for future development and directions for the developed compartmentalized microfluidic platforms and *in vitro* neuropathy and axotomy models.

1.2 Peripheral Nervous System and Peripheral Nerves

An understanding of the general organization and components of the nervous system is necessary for insight into *in vitro* modeling of degeneration, regeneration and myelination of peripheral nerves, which is the scope of this dissertation.

The nervous system is categorized into the central nervous system (CNS) and the peripheral nervous system (PNS). The CNS serves as a control center, conducting and interpreting signals, and consists of the brain and spinal cord, while the PNS consists of ganglia and nerves, both motor and sensory, that transmit signals between the CNS and the rest of the body. Neurons are the functional units of the nervous system and do not undergo mitosis, while glial cells are the support cells of the nervous system and much more plentiful than neurons. Schwann cells are the principle glial cells of the PNS, while oligodendrocytes, astrocytes, and microglia are the glial cells of the CNS.

The cell bodies of the sensory neurons are located in dorsal root ganglia (DRG) located along the dorsal root while the cell bodies of motor neurons are located within the spinal cord and exits through ventral root as can be seen in the schematic in Figure 1.1. The peripheral nerve is composed of both motor and sensory neuron axons. As axons can be on the scale of meters long in the PNS, the cell bodies of these peripheral neurons may experience drastically different environments from their distal axons.

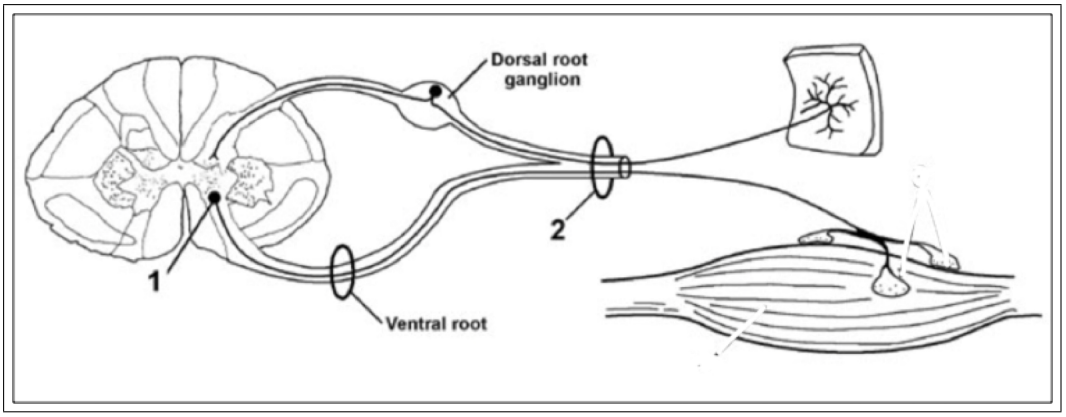

Figure 1.1 The peripheral nerve (2) has both motor and sensory branches [1].

Whereas the central nervous system (CNS) usually cannot regenerate, peripheral nerves regenerate spontaneously after injury because of a permissive environment and activation of the intrinsic growth capacity of neurons. One important feature of axon regeneration is the activation of the intrinsic growth ca- pacity by peripheral nerve injury. This is best studied in the dorsal root ganglion (DRG) primary sensory neurons. The DRG neurons are pseudobipolar neurons and have only one axon stemming from the cell body. However, the axon branches out to two axons: The peripheral branch innervates the sensory organs in the peripheral tissues, and the central branch enters the spinal cord and ascends the dorsal column terminating in the brain. The two axonal branches from the same cell body are fundamentally different in their responses to injury. The peripheral branch re-generates spontaneously after injury, resulting in functional recovery, but the central branch does not. This difference in regenerative potential is largely due to their environments [4]. Therefore an understanding of the local mechanisms at the axonal environments through *in vitro* is essential.

1.3 Microfluidic Compartmentalized Platforms for Neurobiological Research

Microfluidics is a technology that features the manipulation of small amounts of fluids in channels with dimensions of tens to hundreds of micrometer. Microfabrication is the process of fabrication of these miniature structures of micrometer scales and smaller.

Microfabrication and soft lithography techniques are used to compartmentalize neurons, the cell bodies from axons. Compartmentalization made it possible to investigate axonal injury or regeneration. Moreover, compartmentalization facilitated new research methods, which is not possible in /textitin-vivo or traditional cultures, such as high throughput drug screening, visualizing and manipulating the distinct neural segments i.e. cell bodies, axons, dendrites, or synapses and biochemical analysis of axons [3,5,6]. Additionally, it facilitates axon harvesting and analyzing its biochemical composition [5,6]. Campenot chamber is the first device developed for the axonal isolation of neuron, which facilitates to study the cellular parts of neurons [7]. However, Campenot chambers required great skill, as leakage between chambers is a common problem, limiting efficiency and reproducibility.

In particular, polydimethylsiloxane (PDMS) based microfluidic devices have been shown to be potent to isolate axons of both CNS and PNS neurons [8, 9]. In these devices, cells are plated directly into the area close to microchannels or cells are plated through a loading inlet and the cells are randomly dispersed throughout a cell reservoir. Neuronal cells that are in close proximity to the microchannels extend axons through the channels and into adjacent compartments. Application of hydrostatic pressures between microchannel-connected compartments can induce fluidic isolation between axon and cell body. However, there is no report how molecules diffuse in between the compartments and how hydrostatic pressure should be regulated. The diffusion of the molecules through the microchannels and the procedure to hinder this diffusion in order to maintain fluidic isolation is investigated and explained in detail at

Chapter 2.

1.3.1 Microfabrication of Compartmentalized Platforms

The fabrication procedure for the compartmentalized platforms in our experiments consists of three main steps; where, a master wafer is created using standard photolithography techniques and replicas created from the mold using PDMS soft lithography.

1.3.1.1 SU-8 Master Wafer Fabrication and Preparation for Molding

Photolithography is the most widely used micropatterning technique. It is essentially based on the selective exposure of a thin film of a light-sensitive organic polymer (photoresist) to light. Generally, photoresist solution is dispensed onto a flat substrate, usually silicon or glass wafer, spun into a thin film, and dried [10]. When this photosensitive layer is exposed to UV light through a photomask, which is a transparent plate with the desired opaque pattern on its surface, the regions of the photoresist exposed to the light undergo a chemical modification. In the case of a "positive" photoresist, the irradiated polymer molecules break down and become much more soluble in a specific developer solution than the unexposed regions. In the case of a negative photoresist, light induces photochemical crosslinking of the photoresist, which renders the exposed regions virtually insoluble in the developer. The viscosity of the solution and the spin speed controls the height of the photoresist features. The negative photoresist SU-8, which has been specifically developed for applications requiring high- aspect ratios in very thick layers, is used in the photolithography processes in this dissertation. SU-8 (Microchem Corp.) is a negative, epoxy-type, near- UV photoresist having mechanical and chemical stability and excellent coating, planarization and processing properties.

The master mold was constructed using standard SU-8 photolithography with two-layer microfabrication process. (Appendix 1) The first resist layer (h = 2.5 μm)

defined an array of microchannels while the (b) subsequent step (h = 150 μm) defined larger fluidic ports and reservoirs. (Figure 2.1)

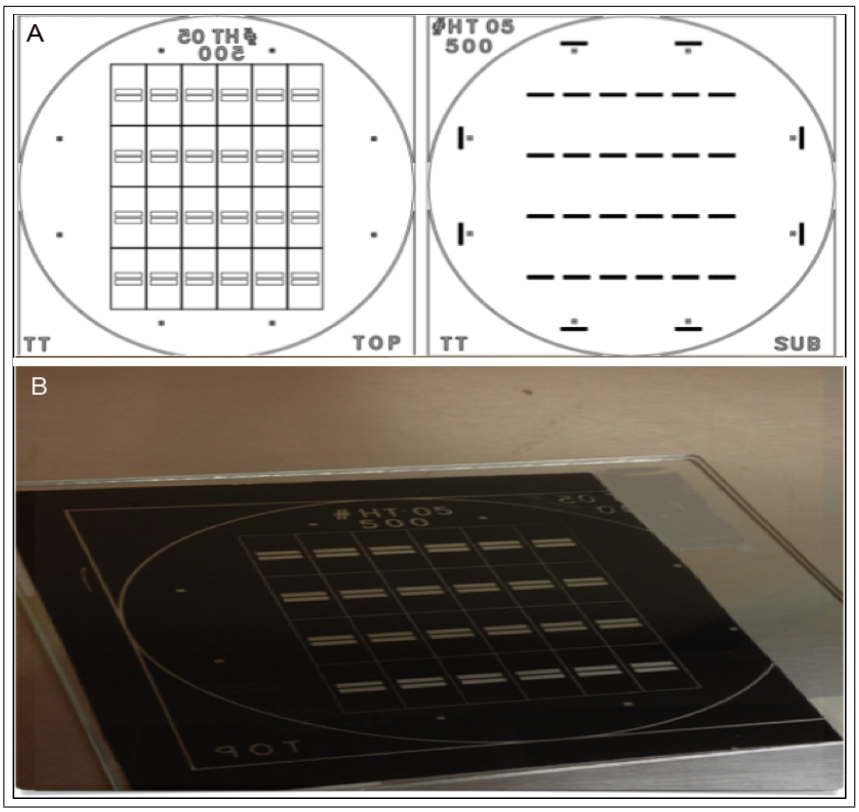

Figure 1.2 A) The "photomask" designs of the two step photolithography process B) the master wafer that is used in soft lithography.

1.3.1.2 PDMS Casting, Curing and Peeling from the Mold

In the fabrication of multi-compartment platforms, one of the cornerstones is Soft Lithography that is all based on the replica molding of microstructures in polydimethylsiloxane (PDMS), a transparent silicone rubber. The silicon wafer, which is patterned with SU-8 by photolithography, is used to mold the PDMS. Soft Lithography made microfluidics attainable to biomedical research because both the material and the straightforward molding process is inexpensive and do not require clean room facilities. All PDMS protocols involved standard 10:1 base to cross-linker ratios by mass. PDMS is very suitable for biological applications, because it is biocompatible, transparent, permeable to gases and amenable to surface modification that can be used to change the chemical or biological functionality of the PDMS surface. PDMS can

replicate submicron features with high fidelity, can form a reversible seal with smooth surfaces and when oxidized by simple exposure to oxygen plasma, it can be irreversibly bonded to itself or glass [10].

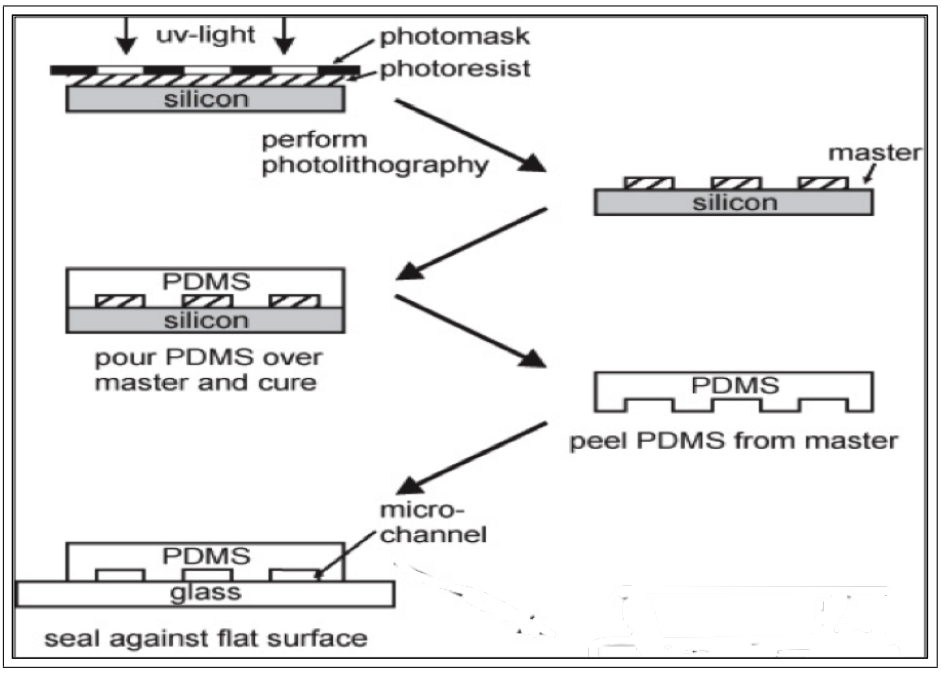

Figure 1.3 Schematic of typical device fabrication using contact photolithography for structuring and PDMS as the device material [2].

1.3.1.3 Punching the PDMS Molds and Bonding on Glass Substrate to Produce Wells and Microchannels

Dermal biopsy punches are used to fabricate the compartments. Then the PDMS with wells and microchannels are bonded to glass substrate with Oxygen plasma bonding. Oxidative treatment with oxygen-containing plasma chemically modifies the surface of PDMS allowing it to permanently adhere to glass, quartz, PDMS and other silica-based substrates. The glass substrate also allows better imaging with the microscopy.

1.3.2 Neuronal Cell Cultures for Microfluidic Platforms

Embryonic DRG sensory neurons are well suited for compartmentalized cultures, and the use of embryos allows the culturing of a high content of cells with higher efficiency in isolating neurons in comparison to post-natal animals [2]. Compartmentalized microfluidic platforms with embryonic DRG neurons have been successfully used to study mechanisms of axonal degeneration in disease models [3, 8, 11].

DRG neurons of pregnant rats at gestational age of 15 were plated on the cell body site of the HTCMP's where the micro channel dimensions are 10 μm in width, 500 μm long and 2.5 μm in depth. The average size of rat DRG neurons is about 29 μm so the neuronal cell bodies will not be able to migrate through the channels, only the axons that have a diameter of 1 μm will pass through. Also the compartments are fluidically isolated, that micro channels have such a small cross-sectional area, that they allow axons to grow from one compartment into another but attenuate the diffusion of molecules from the compartment of lower hydrostatic pressure in the channels compared to the hydrostatic pressure in the compartments.

Neurons are highly sensitive to the surrounding environment. Establishing cell cultures of dispersed neurons and glia can require reagents of high purity and refined protocols. Furthermore, for most cell lines, and especially for post-mitotic neurons, substrate coating is necessary before seeding. Addition of adhesion molecules prior to cell culture is a two-step process. It is extremely important that induced cell-surface adhesion be greater than naturally occurring cell-cell adhesion to avoid large aggregates of clumped cells [12]. These cell clumps are problematic in that they tend to promote retraction of networks from the adhesive surface. The microfluidic platform surfaces and microchannels are coated with PDL and Laminin, in order to promote neuronal viability and neurite growth.

2. FLUIDIC ISOLATION AND AXON REGENERATION BY GLIAL CELL LINE DERIVED FACTORS IN COMPARTMENTALIZED MICROFLUIDIC PLATFORM

2.1 Introduction

The GDNF family of ligands (GFLs) plays important roles in neural development and different neurological diseases [13–18]. These growth factors have been shown to promote survival and differentiation of dopaminergic neurons, motor neurons and sensory neurons of DRG [19–24]. GDNF in particular has been investigated due to its therapeutic potential. Previous studies have evaluated the role of GDNF in the nervous system in settings of disease and traumatic injury [25–27]. In addition to GDNF, other members include neurturin (NT), neublastin(NB) (also known as artemin), and persephin [25]. It has been demonstrated in both clinical trials and animal experiments that GDNF enhances myelination [28–30]. GDNF also enhances survival of motor neurons in models of amyotrophic lateral sclerosis [31–33], and dopaminergic neurons in models of Parkinson's disease [34, 35]. Similarly, neurturin has been shown to increase survival of motor and dopaminergic neurons [36–38] and neublastin was found to be effective in reducing neuropathic pain [39–41]. Persephin showed effective in the treatment of stroke [42, 43]. In peripheral nerve system, all GFLs showed enhancement of axon growth after the axotomy [23, 24]. However, the site of action of GFLs in axon regeneration is not well characterized. Identification of biochemical mechanisms involved in axonal injury can be difficult in a complex *in vivo* experimental setup. In addition, standard cell culture does not allow for the compartmentalization of axons from neuronal cell bodies, thus making it difficult to delineate axon-specific mechanisms. Several injury systems have been incorporated within microfluidic culture devices in order to investigate axon-specific mechanisms in injury and regeneration. These systems include simple aspiration of the distal compartment, two-photon laser ablation, and hydrodynamic shear based axotomy [5, 44].

The diffusion of GFLs between the compartments and the regenerative effect of GFLs on the injured axons by measuring the regrowth of them after axotomy are identified in this chapter.

2.2 Materials and Methods

2.2.1 Cell and Adult DRG Preparation

All experiments involving animals were conducted according to protocols approved by the Animal Care and Use Committee of the Johns Hopkins University School of Medicine.

DRG neuronal cultures were prepared as previously described.127 Briefly, DRG from Sprague-Dawley rats at 15th day of gestation were aseptically dissected and isolated, and the cells were dissociated enzymatically with collagenase and trypsin and suspended in Neurobasal medium (Gibco 21103-049), with 1% FBS (Hyclone 3H30071.3), 0.5 mM L-Glutamine (Gibco 25030-081), 10 ng/ml GDNF (Amgen), 2% B27 supplement (Gibco 17504-044), and 0.2% glucose. One day after seeding cells, neurobasal media containing anti-mitotic agents (either 10 μm of cytosine arabinoside, or a combination of 50 μm each of uridine and 5-fluoro-2- deoxyuridine) was added to the cultures in order to arrest the division of glial cells, and then removed the following day.

DRG explants were harvested from sacrificed adult Rosa mice expressing red fluorescent protein in sensory neurons, ranging from spinal levels L3-L6. For a subset of experiments, spinal origin level was noted, with a focus on L4-L6. Once explants were obtained, they were placed in dissection medium, containing Hanks Balanced salt solution (HBSS) (Gibco, Grand Island, NY), 4.3 mM sodium bicarbonate, 10 mM HEPES 2-[4-(2-Hydroxyethyl)-1-piperazinylethanesulfonic acid, 33.3 mM D-glucose, 5.8 mM magnesium sulfate, 0.03% BSA and penicillin/streptomycin (Gibco, Grand Island, NY). Explants were then cleaned to remove any remaining dura, and placed on a transwell membrane filled with media underneath. Median and ulnar nerves were

obtained from wild type donor mice (C57B16) in the age range of p3 to p5 and abutted next to DRG explants to allow axons to traverse through for approximately one week to allow grafts to re-innervate.

2.2.2 Microfluidic Platform Fabrication

A two-step photolithographic process was utilized to create the master mold. Silicon wafers (WRS Materials, San Jose, CA) were coated with SU-8 2002 (Microchem, Newton, MA), spun, and soft baked using parameters specified by the manufacturer to yield a resist thickness of 2.5 μm. An array of microchannels was defined by UV light exposure through a high-resolution transparency (Cad/Art, OR). The dimensions of each microchannel for standard devices were: width = 10 μm, length = 500 μm. The exposed substrate was once again baked, to enhance polymer cross-linking post exposure, and developed as stated in the resist technical sheet to fully define the microchannels. The process was immediately repeated with SU-8 3050 (Microchem, Newton, MA) to define the fluidic reservoirs with dimensions: width = 3 mm, length = 13 mm. The master mold was then treated with trichlorosilane (United Chemical Technologies, Lewistown, PA) for 30 minutes to create a nonstick surface for subsequent processing. Standard soft lithography was performed using Sylgard 184 polydimethylsiloxane (PDMS) (Dow Corning, Midland, MI). After curing, the PDMS was carefully removed from the master and access ports were created using dermal biopsy punch tools (8 mm) (Huot Instruments, Menomonee Falls, WI).

2.2.3 Characterization of Growth Factor Diffusion

Prior to GFL experiments, the fluidic isolation in the microfluidic devices was characterized. First, a theoretical profile of growth factor diffusion was developed incorporating the experimental parameters of the system. Next, computational simulations were performed to further characterize and visualize diffusion within the devices. Finally, experimental verification of small molecule isolation was performed by observing

the diffusion of a comparably small fluorescent molecule over time.

2.2.4 Collagen Gel Preparation

Collagen gels were prepared using a PDMS mold of roughly 50-100 microns in thickness. The collagen gel solution was prepared by mixing Collagen I, Rat tail (Gibco, Grand Island, NY), 7.5% sodium bicarbonate, and 10X PBS in a 8:1:1 ratio. If laminin (Invitrogen) was used, 10 μg/ml was added to the solution. All solution preparation was carried out on ice and under sterile conditions. Once the mixture was vortexed, in order to limit bubble formation, it is left for 20 minutes before loading the solution into PDMS molds. Gels were placed in 37° C incubator for 2 hours to allow adequate time for gelation of the thin films. Gels were then cut to dimensions as needed from the formed sheets and placed under transected nerves.

2.2.5 DRG Cell Experiments

DRG neurons were loaded into the soma side of devices and grown for sufficient time to allow axons to grow through channels and into the axonal compartment. Phase contrast imaging was used for a majority of experiments. Representative axon images and a certain subset of experiments were performed by labeling axons with viral GFP for enhanced visibility. Axons were transected at the base of the microchannels by gently scratching the surface of the glass with either a glass pipette or syringe tip, and neurotrophic factors (GDNF-Amgen, Neurturin-Peprotech, Neublastin-Biogen) were applied to axonal or neuronal cell body compartments at a concentration of 100 ng/ml, a commonly used peak concentration for various neurotrophic factors. For GDNF and cytochalasin D (Sigma) experiments, 100 ng/ml of GDNF was added to the axonal compartment concurrently with 10 nM of cytochalasin D. Regeneration of axons was monitored by daily imaging of the axonal side and measuring the length of longest axon coming from each microchannel. A minimum of 10 axons per experimental condition was measured and experiments were done in triplicates for GFLs. A minimum of 5

axons was measured for GDNF and cytochalasin D.

2.2.6 DRG Explant Experiments

After approximately one week in culture, allowing for enough time for nerve grafts to fully reinnervate and with a minimum of 2 days without GDNF, grafts were transected in order to mimic a nerve injury. Collagen gels with or without laminin were placed under transected grafts in order to overcome the intrinsic directionality of transwell membrane. When with or without the presence of laminin is noted, this refers to the presence or absence of laminin within the context of the collagen gel. GDNF was then either added or withheld after transection and during media exchange every two days, depending on the experimental condition. Explants were imaged under a fluorescent scope daily for 5 days. These images were stitched and quantified using a superimposable radial grid. This grid is adjustable and starts at a radius of 250 μm, continuing in 250 μm increments. In this way, axons that cross over at different lengths can be binned.

2.3 Results

In this study, fluidic isolation of somal and axonal compartments is characterized and the site of action of three neurotrophic factors in an *in vitro* axotomy model of sensory axonal regeneration is examined. To characterize fluidic isolation, parameters essential to growth factor diffusion are examined and verified. In order to confirm small molecule isolation through theoretical, computational, and experimental means, the diffusion profile of growth factor within the devices is determined. Once characterized, the growth factor experiments are performed.

2.3.1 Theoretical Profile of Growth Factor Diffusion

In order to identify whether growth factors can diffuse from the axonal to cell body compartment, models to simulate this experimental setup were developed. The central idea behind the compartmentalized platform is to have fluidic isolation between compartments facilitated by high resistance microchannels. If the microchannels contain a small cross-sectional area ($< 30\ \mu m^2$), the device paradigm allows axons to grow from one compartment into another but attenuates the diffusion of molecules from the compartment of lower hydrostatic pressure to the compartment of higher. In this experiment, a small differential pressure gradient was established with a higher pressure in the axonal compartment as compared to the cell body compartment. As a result, a low velocity retrograde flow was created in the microchannels to prevent molecular anterograde diffusion. Theoretically it is demonstrated that chemical isolation is achieved when working with the aforementioned parameters. First, the diffusion-advection problem is formulated (Figure 2.1).

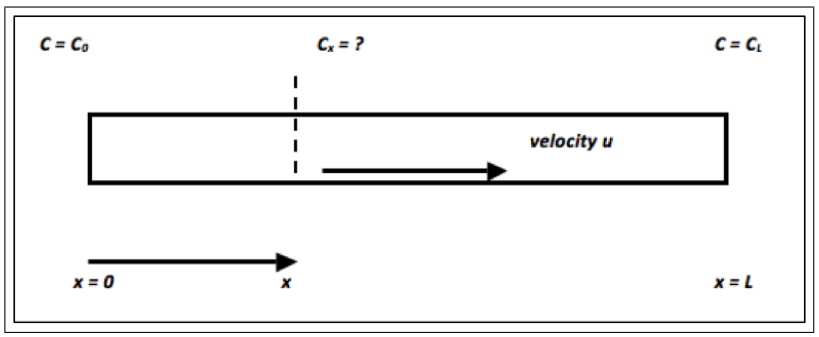

Figure 2.1 Formulation of the diffusion advection problem.

The diffusion of any molecule in a fluid medium is governed by the diffusion-convection equation. The first term including spatial derivatives of concentration describes passive diffusion while the second term including the velocity of the medium describes active diffusion (or the convective element):

$$\frac{\partial C}{\partial t} = D \cdot \nabla^2 C - \vec{v} \bullet \nabla C \tag{2.1}$$

Where C is the concentration at a point (x,y,z) at time t, D is the coefficient of diffusion, $\vec{v}$ is the velocity vector at the point (x,y,z) at time t. The pressure and concentration gradients driving the dynamics are mainly along the groove (x-axis) and hence, this can be approximated as a one-dimensional problem. Steady state is achieved when:

$$D\frac{d^2C}{dx^2} = u\frac{dC}{dx} \tag{2.2}$$

where u is the x-component of the velocity. Solving this with appropriate boundary conditions yields the following solution:

$$C_x = C_L \cdot e^{-\frac{u}{D}(L-x)} \quad \text{and} \quad C_0 = C_L \cdot e^{-\frac{uL}{D}} \tag{2.3}$$

For pressure (gravity) driven flows, Co can be expressed as

$$C_0 = C_L \cdot e^{-\frac{\rho g \cdot \Delta h \cdot a^2}{16\eta D}} \tag{2.4}$$

For the purpose of simplifying calculations, media is approximated as water. In this equation, Δh is the height difference of the water column at inlet and outlet that leads to the pressure difference which drives flow, ρ is the density and η is the viscosity of water (saline) and a is the channel height (the most critical dimension for laminar flow). Due to the geometry of the system, Δh is limited to approximately 2 mm, and a is limited to 2.5 μm, which is the height of the groove. The other constants used are g=9.81 m/s^2, η=0.00089 m^2/s, and ρ =1000 kg/m^3.

The diffusion coefficient D is calculated indirectly from its inverse dependence on the square root of molecular weight of the diffusing species. Doxygen is known to be 2 x 10-9 ^{2}m/s. The molecular weight of oxygen (M_{Oxygen}) is 16 Daltons.

$$D_{growthfactor} = D_{oxygen} \cdot \sqrt{\frac{M_{oxygen}}{M_{growthfactor}}} \tag{2.5}$$

Table 2.1
Growth factor molecular weights and calculated diffusion coefficients.

Name of Growth Factor	Mol Weight (Daltons)	Calculated Diffusion Coef.
Human GDNF	21 kDa [45]	5.5x10$^-$11 m^2/s
Rat Neurturin	19.5 kDa [27]	5.7x10$^-$11 m^2/s
Rat Neublastin	4.5 kDa [46]	1.2x10$^-$11 m^2/s

The smallest molecule has a mass of 4.5 kDa, which also has the highest tendency to diffuse. It is sufficient to use this molecule for the calculations, as the amount of GDNF diffusing to the somatic compartment will also be less than the amount of rat neublastin diffusing to the somatic compartment. So, considering the diffusion of rat neublastin:

$$\frac{C_0}{C_L} = e^{-\frac{1000X9.81X0.002x(2.5X10^{-6})^2}{16X0.00089X1.2X10^{-10}}} = 6.8X10^{-32} \tag{2.6}$$

Thus, there is negligible diffusion from the axonal compartment to the somatic compartment at steady state. Care must be taken that while performing experiments utilizing these culture systems that the height difference in the two compartments must be achieved before adding the growth factor to the axonal compartment so that there is always an anterograde flow preventing diffusion of species in the retrograde direction. This height difference must be maintained throughout the experiment.

2.3.2 Computational Simulations to Study Diffusion Patterns of Growth Factors

Simulations were done in Comsol Multiphysics (Formerly FEMLAB; Comsol Inc., MA), a finite element-modeling package. The geometry was simplified to study the diffusion pattern in only one of the microchannel grooves. Each microchannel has a plane of symmetry passing though the middle (a plane going from floor to ceiling all along the length halfway between the two vertical walls). Further simplification of the geometry was performed using such symmetric considerations, so that only half of a microchannel needed to be simulated (Figure 2.2).

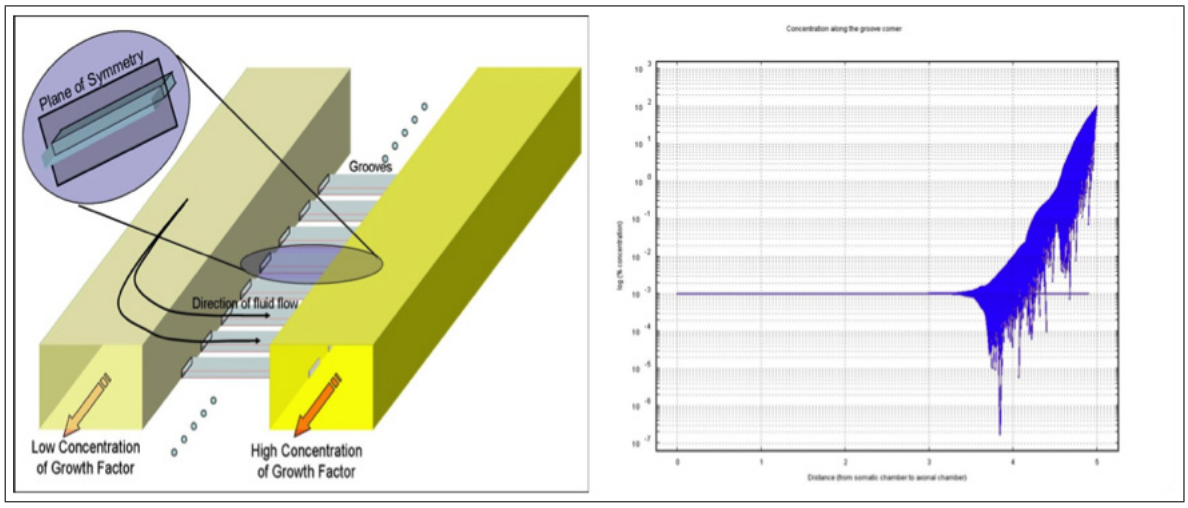

Figure 2.2 Handling of the groove geometry for computational simulations. Half the groove is meshed for computational solutions of fluid dynamics and diffusion-convection equations. P plot showing the concentration drop along the groove from the axonal side (right side) to the somatic side (left side). The profile along the middle of the groove shows the profile along one of the edges of the groove.

Simulation consisted to meshing the architecture into a grid of smaller elements. The aspect ratio of such finite elements was tailored to suit the aspect ratio of the microchannel, that is, elements were longer along the length (x-axis) than along the width or height (y and z axes respectively). The geometry was first solved for fluidic parameters such as velocity and pressures at all points. This was done by solving the continuity and Navier-Stokes equations for the microchannel. While all three cases were simulated as described above, the results of rat neublastin (the smallest molecule we used) diffusion are presented in Figure 2.3. This simulation suffices to demonstrate

the paucity of small molecule diffusion through a microchannel.

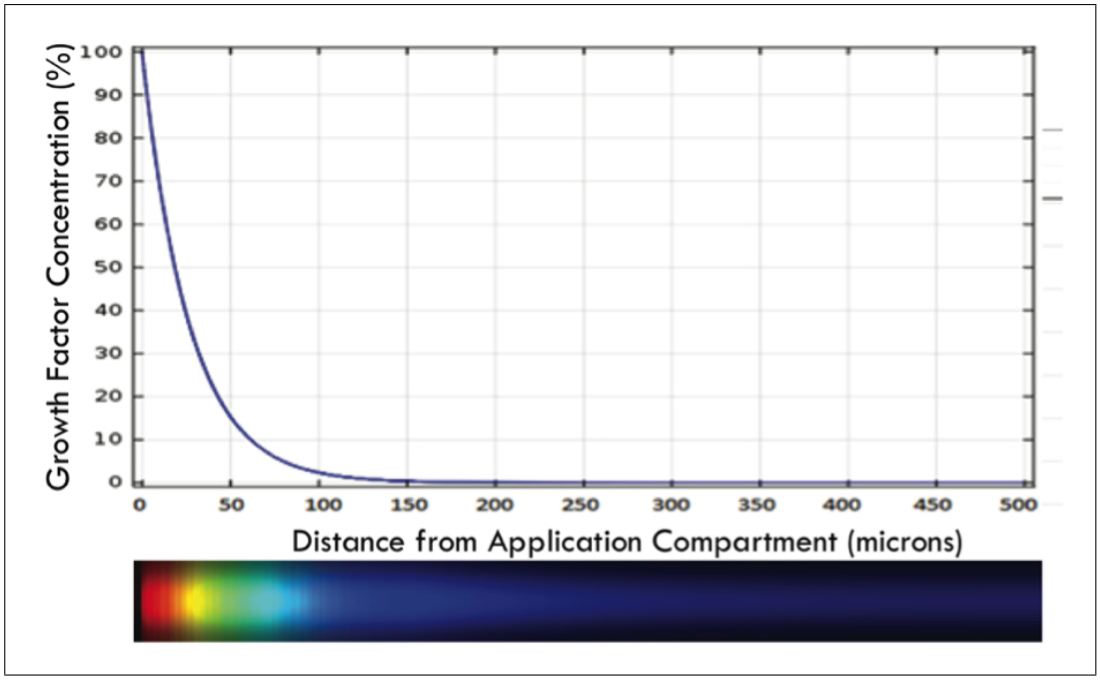

Figure 2.3 Computational simulation of the diffusion profile of growth factor along a microchannel groove. The plot demonstrates that when growth factor is applied to the axonal side, the concentration along the groove drops to negligible amounts within approximately 100 μm in a 500 μm channel.

2.3.3 Restriction of Fluorescent Molecules

Experimental verification was performed in order to confirm our theoretical and simulation findings pertaining to small molecule diffusion within our microfluidic chambers. A hydrostatic pressure was established between the compartments by establishing fluid volumes such that the somal compartment was of lower fluidic height than the axonal compartment. This hydrostatic pressure created a small flow to counteract diffusion. A bolus of 1 microliter fluorescein isothiocyanate (FITC) (Sigma, St. Louis, MO) dye was introduced to the somal compartment and was imaged over the course of 24 hours. Empirically, a fluid height difference $>$ 2 mm was sufficient to prevent a low-molecular weight compound (700 Da) from diffusing from the axonal compartment to the somal compartment, which matches both the theoretical and simulated conclusions. In Figure 2.4, it is seen that under these conditions, the diffusion of the dye was approximately 100 μm after 24 hours, well under the channel length and very close

to the theoretical prediction. This height difference was maintained by adding 5μL of media to the higher volume compartment daily, allowing for localization of an applied compound for longer periods. After verifying growth factor isolation theoretically, in a simulation, and experimentally, the experiments to investigate the effect of GFLs on axonal regrowth following axotomy are performed.

Figure 2.4 Analyte restriction maintained for 24 hrs. Diffusion of a small (MW 700) fluorescent analytes was examined under high hydrostatic pressures. Microchannels (region between dashed lines) connect compartments of unequal fluid height. Establishment of fluid heights >2 mm prevented entry of dye (solid white lines) into the compartment of higher fluid height.(Scale bar 100 μm).

2.3.4 Axotomy and Axonal Regeneration by Neurotrophic Factors

In order to identify the regrowth of axotomized axons, neuronal processes are allowed to grow into the axonal chamber and then the axons are transected using either a glass pipette or metal syringe. In Figure 2.5, a representative device is seen, seeded at lower density in order for enhanced visualization of single axons, before and after axotomy. These neurons were transfected with viral green fluorescent protein GFP [47] to enhance visualization. While axons are cut slightly farther from opening, there is some retraction and degeneration. For the experiments, recombinant GDNF, neublastin, or neurturin to either axon or cell body compartments of cultured DRG neurons for 72 hours are added. Multiple images of the axons were captured using

phase contrast microscopy. ImageJ (NIH; Bethesda, MD) was used to calculate percent changes in axon lengths before and after axotomy in the application of growth factors.

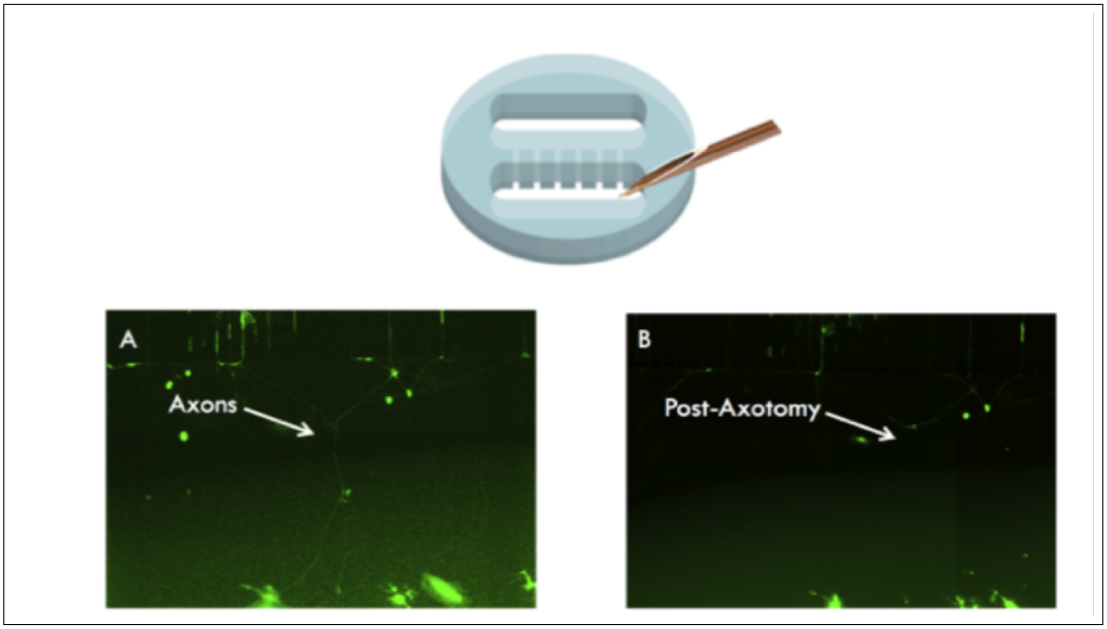

Figure 2.5 A schematic of axotomy performed by needle within the device is presented above. A and B are the representative images of axons: A) before axotomy and B) after axotomy.

In Figure 2.6, representative images of the DRG axons before and after different neurotrophic factor treatments, all taken at the same magnification are demonstrated. In these images, the axons exiting channels and traversing into the axonal compartment on the right are seen.

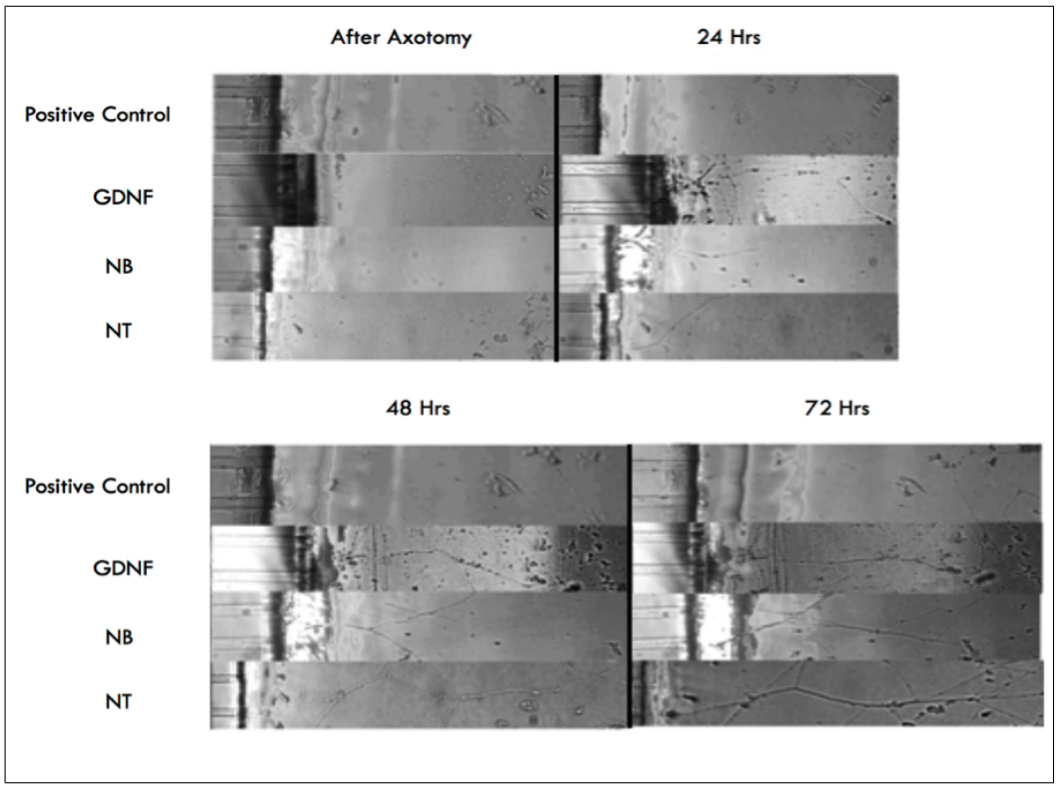

Figure 2.6 Representative phase contrast images of regenerating axons where neurotrophic factors were administered into cell body compartment. Images were taken every 24 hours for 3 days after injury. Immediately after axotomy no difference can be seen between the conditions. Over the next 72 hours, there is very little growth in the positive control compared to the growth factor treated conditions.

As summarized in Figure 2.7, all of the neurotrophic factors enhanced axonal regeneration, whether they were applied to the axonal or somal compartments but GDNF was most potent. Furthermore, there was a slight benefit to applying GDNF to the somal compartment. In order to verify if the enhancement effect of adding GDNF to the axonal compartment was due to local mechanisms, experiments are carried out with concurrent application of GDNF and cytochalasin D. In Figure 2.8, the results indicate ($p < 0.05$) that this enhancement is diminished with the application of the retrograde transport blocker, indicating a need for GDNF to be transported into the cell.

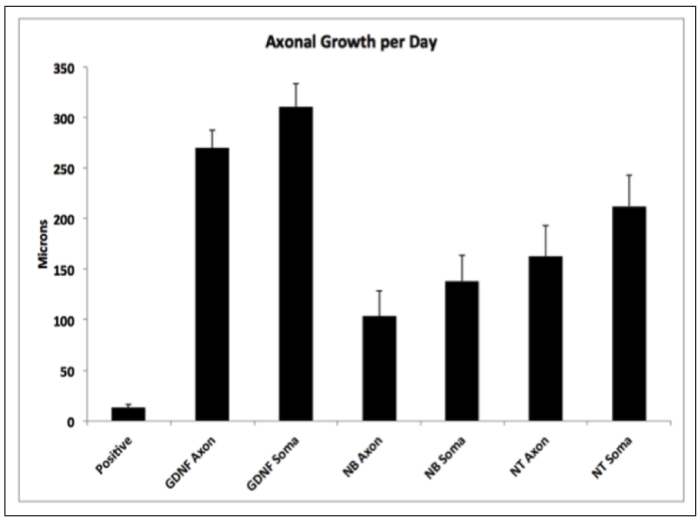

Figure 2.7 Axonal regeneration by GDNF, neurturin (NT) and neublastin (NB) after the axotomy. Rate of axonal regeneration induced by the neurotrophic factors over 3 days. All tested growth factors enhance axonal outgrowth compared to the positive control, applied to either location (n=3).

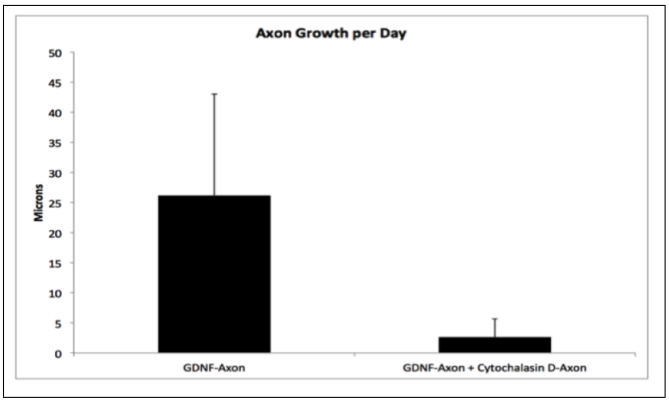

Figure 2.8 Axon regeneration with Axonal GDNF application compared with Axonal GDNF application concurrently with cytochalasin D.

2.3.5 GDNF Effects at the Tissue Level

Explant cultures are more reflective of the *in vivo* environment than dissociated cultures as the DRGs can be cultured with support cells such as Schwann cells and macrophages. In order to determine if the enhancement of growth by GDNF translates to the tissue level, DRG explants with or without GDNF, and with or without the presence of laminin are cultured. A representative culture immediately after transection and 5 days later with a radial grid superimposed to demonstrate the quantification

technique could be seen in Figure 2.9. In Figure 2.10, axon counts at the different radii compared are seen. These graphs indicate that there are more axons that are at least 250 μm for both GDNF conditions (with or without laminin) and this effect diminishes over time. For the larger axon lengths, particularly for axons at least 2000 μm, there are more axons for the GDNF without laminin condition, potentially due to the initial boost. Viewed another way in Figure 2.11, growth over several days compared between our four conditions of GDNF and laminin, GDNF without laminin, control with laminin and control minus laminin can be observed. An upward slope within the growth curve implies increased branching since this indicates there are more axons present at the next larger radii.

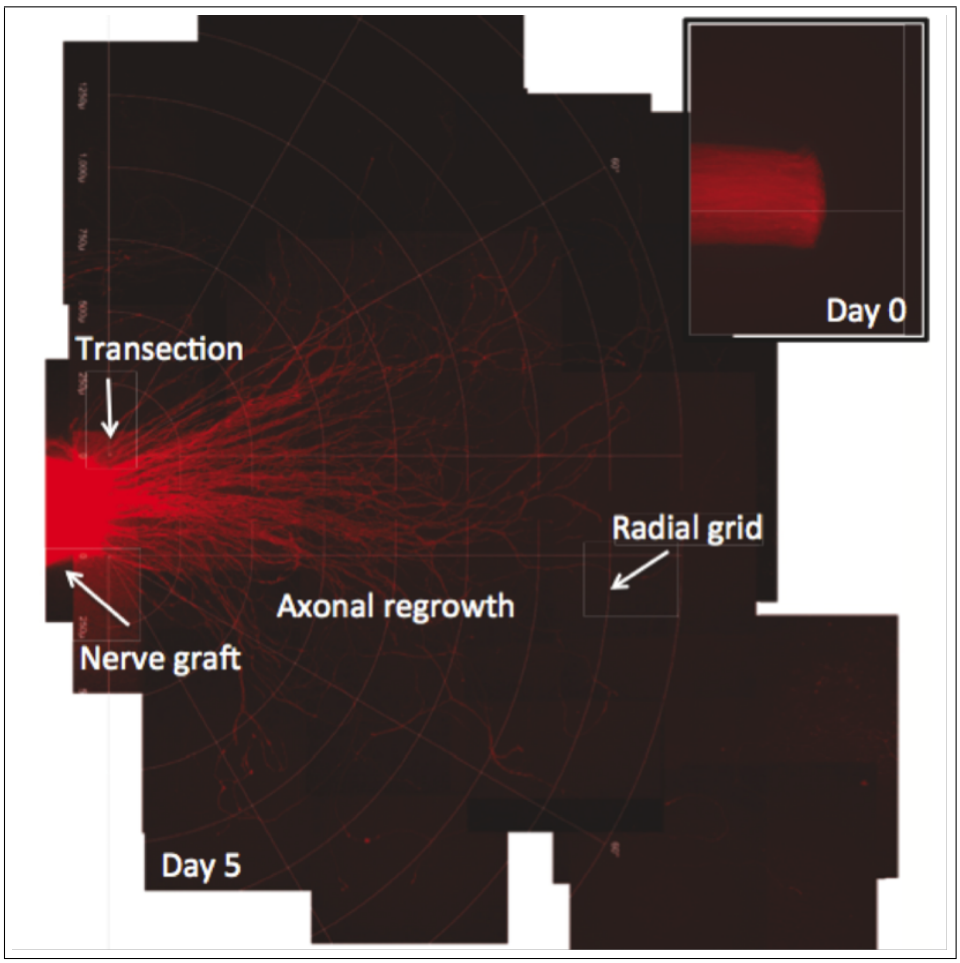

Figure 2.9 An example of a nerve transection and DRG explant culture inset showing initial nerve transection (Day 0) and the same culture 5 days after transection and DRG explant abutment with a template superimposed to demonstrate how axonal growth was quantified. The grid is adjusted around the nerve graft, starting at the site of transection. The template starts at an inner radius of 250 μm from the site of injury and increases in 250 μm increments. All axons to the right of the point of transection are axons regrowing post-injury.

GDNF without laminin proved to have the largest amount of growth on the first day, particularly as compared to both controls ($p < 0.05$). This effect is not as strong over the remaining days, until day 5, where there is again a significant ($p < 0.05$) difference between GDNF without laminin and control with laminin.

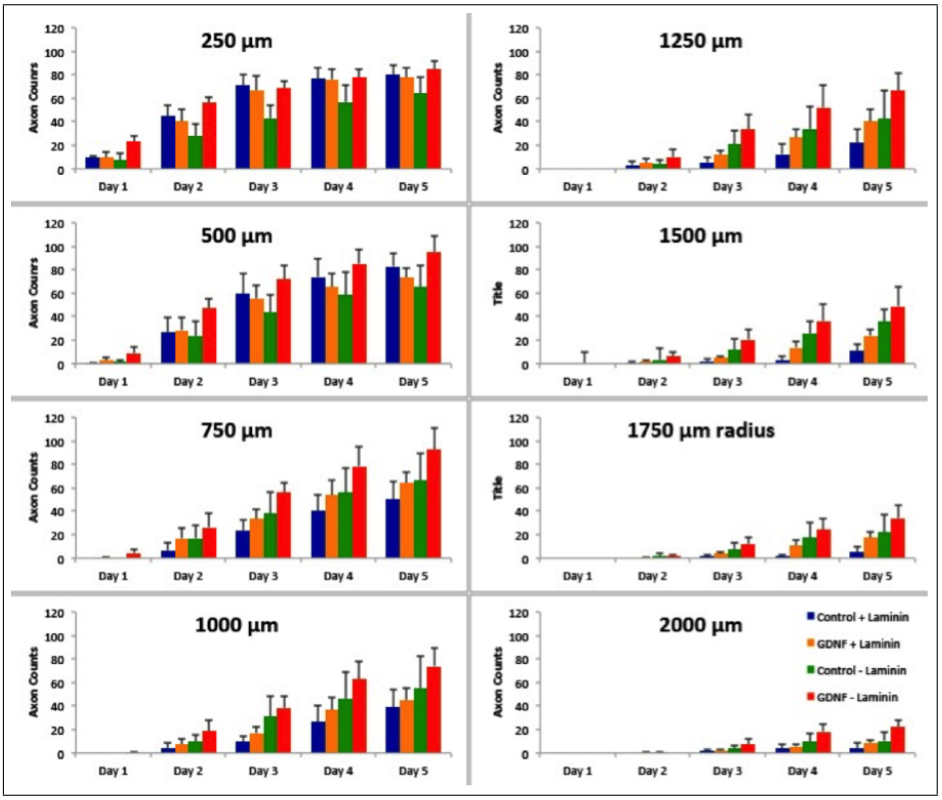

Figure 2.10 Quantification of axon counts separated by axon lengths, over 5 days in each graph. There are significantly more axons that are at least 250 μm by Day 1 and at least 2000 μm by Day 5 for the GDNF without laminin condition particularly as compared to either control condition.

2.4 Discussion

Compartmentalized microfluidic culture systems have been utilized in a variety of neuronal studies, from examining the effects of toxins and neuroprotectants on axons versus soma, to enhancing spatial and temporal control of neurons and other cultures, and performing axon-glia co-culture studies [3,8,48]. In order to elucidate regenerative effects and to determine the site of action of each GFL, an *in vitro* axotomy model is performed by transecting axons simply and easily by scratching the surface of the glass with a sharp pipette or syringe, and then the regenerative effects of GFLs to soma and

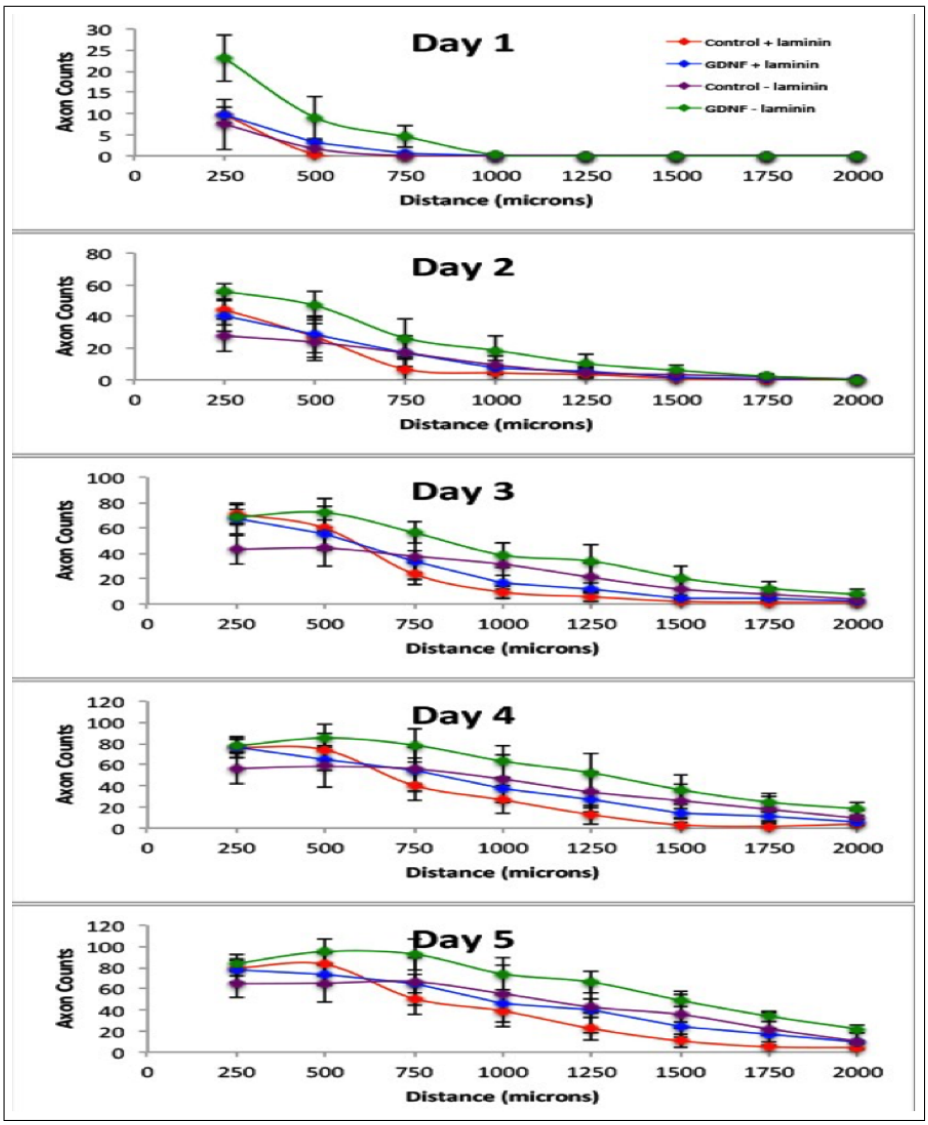

Figure 2.11 Axon counts at different lengths separated by day, allowing for visualization of growth curves, with the most pronounced difference occurring on Day 1 for GDNF without laminin.

axons of the axotomized DRG's are observed by measuring the regrown axons.

Compartmentalized microfluidic culture devices have become ubiquitous, however, there is no report how molecules diffuse between the compartments and how hydrostatic pressure should be regulated. Therefore appropriate characterization of the diffusion properties within the devices would not only be beneficial, but necessary. This study demonstrates a potential pitfall in designing and carrying out microfluidic experiments with neuronal cultures. Unless proper hydrostatic pressure is maintained, there is no true fluidic separation of the axonal and neuronal cell body compartments.

Experiments studying the effects of individual local manipulations of axons and neuronal cell bodies will have to take these observations into consideration. This is especially true for small molecular manipulations, as they are more likely to diffuse through the microchannels and confound the findings of an experiment.

Neurotrophins have traditionally been known to play integral roles in neuronal survival during development, but only relatively recently has their function in regeneration been explored [49]. GDNF and its family of growth factors, neurturin, artemin, and persephin, represent a class of novel neurotrophic factors. These growth factors signal through a two-receptor complex consisting of and a glycosylphosphatidylinositol (GPI)-linked GFR-α. The growth factors GDNF, neurturin, artemin, and persephin preferentially bind to GFR-αl, GFR-α2, GFR-α3, and GFR-α4, respectively. GDNF has been shown to provide neuroprotection and promote axonal regeneration but the role of the other family members is not as clear.

Injury to peripheral nerve reactivates its intrinsic growth capacity, and the retrograde transport of injury signals has been suggested to be one of the essential mechanisms for regeneration [50]. The retrograde transport of GDNF has been postulated to act as a positive injury signal for induction of regeneration [51]. The enhancement of regeneration by GDNF within the developed *in vitro* system is consistent with previous studies. It has previously been demonstrated that GDNF selectively promotes regeneration of injury-primed sensory neurons, both *in vitro* where GDNF caused enhancement of neurite outgrowth in preconditioned DRG neurons, and *in vivo* where GDNF administered directly to cell bodies in lesioned spinal cord, facilitated the preconditioning effect and enhanced regeneration further [52]. In this study, it is observed that GDNF acts as a more potent inducer of regeneration than the other GDNF family growth factors that are examined, and this finding is consistent with previous studies. GDNF and its receptor GFR-α1 are upregulated in the distal denervated segment of injured nerve, suggesting that GDNF may provide trophic support for injured peripheral neurons. No analogous upregulation of neurturin, persephin, and artemin or their receptors was found following injury [53]. However, all growth factors promote regeneration.

The finding that GDNF administered to cell bodies produced better results than GDNF administered to distal axonal compartments is interesting. A previous study utilized compartmentalized cell culture devices to study the role of GDNF as a retrograde survival factor, as well as its ability to promote survival over long distances to cell bodies [54]. In this study, it was found that GDNF promoted survival of DRG neurons equally well from either distal axon or cell body application. However, this study was not done within an injury model, and the DRG neurons were relatively healthy, and thus the reason for this discrepancy in the potency of GDNF depending on location of application may be due to the fact that injured DRG neurons are used. It is important to note that the mechanism of action of GDNF may be different in these two systems, indicating the need to study the role of growth factors in both injury and developmental systems separately. It has been demonstrated that GDNF and GFR-α1 are retrogradely transported in peripheral axons, but these studies were also done in relatively healthy neurons [55]. Axonal injury may have an impact on protein turnover and retrograde transport, and this may impair some of the retrograde pathways for GDNF transport, making the direct application of GDNF to the cell bodies more effective. The experiments in this dissertation, comparing axonal GDNF application alone and together with cytochalasin D demonstrate the important role of retrograde transport of GDNF, and further indicate that the enhanced regeneration effect may be cell body specific rather than at the localized axon.

Due to several environmental differences *in vitro* versus *in vivo*, including the enhanced presence of endogenous growth factors as well as the presence of more substantial support cells and ECM components, it is expected that the *in vitro* and *in vivo* results may not be identical. In order to investigate the role of GDNF at the tissue level, experiments with adult DRG explants are performed. Laminin is prevalent throughout the body within ECM and is known to have axonal growth promoting properties both *in vivo* and *in vitro*, and thus experiments were performed with and without the presence of laminin [56, 57]. The results will help to further elucidate GDNF's role in regeneration following injury as well allow for further factors for consideration in its potential use as a therapeutic treatment.

The experiments at the tissue-level were done with GDNF, which elicited the highest response in the cellular studies. The results demonstrate that the regeneration enhancement effect of GDNF translates to an extent at the tissue level, but not nearly as dramatically, as the control explant cultures regrow much better than the control cell cultures. The fact that the enhancement effect seems to be most pronounced on Day 1 immediately following injury and application on non-laminin coated substrates can have implications for timing of future therapy applications of growth factors. It is important to note that after axotomy, there will be an upregulation of endogenous growth factors after injury that is more pronounced in a tissue-level model as compared to cellular, and this may be why the effect of exogenous GDNF is either diminished or hidden. As GDNF is necessary for development, future studies involving DRG explants from conditional knockout mice may elucidate GDNF's role further. The demonstration of a slight increase in branching is consistent with other studies in which GDNF increases branching in different types of neurons to varying extents [58, 59].

While laminin is widely known to promote axonal outgrowth, it is interesting to see that the effect of GDNF when there is no laminin in the collagen gel is significantly higher than not only the control without laminin but also the control with laminin, as this indicates that laminin alone may not be sufficient to achieve optimal growth. This finding may also have implications for future treatments of nerve injuries in which the basal lamina is disrupted. While some studies indicate the necessity of laminin to promote axonal outgrowth in the presence of growth factors in *in vitro* studies [60], the results here indicate that laminin may be a confounding factor.

It is also important to note that other significant data may not be as readily apparent due to large error numbers associated with these DRG explant cultures. This may be due to inherent differences not only in absolute numbers of DRGs, but differences in the distribution of subpopulations of DRGs that are responsive to GDNF. A comparison between DRGs of the same spinal level may level the playing field to produce lower error. Preliminary experiments were performed noting spinal level of origin of the DRG explants, in this case L4-L6 (Lumbar level 4 to Lumbar level 6), and without the presence of laminin. The results from these experiments indicated that

spinal level might be important in determining responsiveness to GDNF as well as intrinsic axonal outgrowth; however, a larger scale study is needed. This is an important area for future study, not only as it seems to be most appropriate to compare DRGs at the same level, but also because a relationship between spinal level and responsiveness to different growth factor treatments can affect an eventual outlook for functional recovery based on corresponding level of injury. These findings can lead to treatments tailored for particular nerve injuries based on spinal level origin of the nerve. In addition, performing these experiments within a tissue-level compartmentalized platform will help tease out if there are differential effects based on exposure to either solely the distal axon or cell body at the different spinal levels.

Neurotrophic factors are a promising area of research for understanding regeneration. Their role in providing trophic support during development and in maintenance of neurons has long been known, but elucidating their roles in regeneration may prove fruitful in the development of therapies for overcoming neural degeneration and for enhancing regeneration post-injury. Understanding axon specific or cell body specific effects of growth factors and being able to distinguish between local effects and retrograde signaling will be necessary for any future therapies. Compartmentalized microfluidic culture devices may be instrumental in these studies, but caution must be exercised to better characterize the devices to ensure true microfluidic separation of chambers. Progression of cellular studies to the tissue level brings the researcher one step closer to actualizing clinical therapies for traumatic peripheral nerve injuries.

2.5 Summary

Compartmentalized microfluidic platforms (CMP) are functional devices to study local effects of chemicals and factors associated with axonal regeneration and degeneration in neural cultures. The regenerative effects of Glial cell derived nerve growth factors (GDNFs) post-axotomy in a physical axotomy model are examined. CMP's contain high fluidic resistance microchannels where hydrostatic pressure is utilized to create a small but sustained flow to counteract any diffusion. This property is inves-

tigated further by characterizing the diffusion profiles of molecules in the device both theoretically and experimentally. A fluidic height difference of 2 mm is required to localize fluorescent molecules in one side of the compartment. Using the 2 mm height different media, the diffusion profile of GDNFs and site of action of GDNFs are identified in an *in vitro* model of sensory axonal regeneration. Three members of GFLs, specifically neublastin, neurturin, and GDNF are investigated in order to compare their ability to promote regeneration of the axons of DRG neurons. GDNF is found to be the most potent in promoting axon outgrowth after axotomy, although all explored growth factors demonstrated some effect. Application of GDNF to either cell body or axon side is effective in enhancing regeneration. To further investigate the regeneration potential, experiments within microfluidic cultures with concurrent application of GDNF with a retrograde transport blocker, cytochalasin D are performed. To examine the effect of GDNF at the tissue level, GDNF is applied to adult DRG explant cultures, both with and without the presence of laminin. The effect of GDNF was the strongest during the initial days following injury and application, and this effect was most pronounced without laminin. These results contribute to developing growth factor based treatments for enhancing/promoting sensory axon regeneration.

3. IDENTIFICATION OF NEW THERAPEUTIC TARGETS FOR PACLITAXEL INDUCED PERIPHERAL NEUROPATHIES

3.1 Introduction

1 in 2 males and 1 in 3 females are at risk of developing cancer in their lifetime, and the majority of patients with cancer are treated with chemotherapy. Increasing numbers of patients are experiencing excellent outcomes from chemotherapy, with prolonged survival [61]. However, chemotherapeutic agents often create CIPN, a serious, painful, and dose-limiting complication [61, 62] .The incidence of CIPN can be as high as 80 to 90% of patients receiving chemotherapy [63, 64], and the number is increasing due to two main reasons. First, more neurotoxic drugs are being developed, which are combined into multiple chemotherapy regimens that patients receive. Secondly, because of prolonged survival, patients are receiving more treatments that increase both the risk and severity of CIPN. Due to the destructive and dose-restricting nature of CIPN, patients are sometimes unable to complete their treatment schedules [62–65].

Up to now, no drugs capable of preventing the occurrence of CIPN or ameliorating its long-term course are currently available, and chemotherapy schedule modification is often required to limit CIPN severity, which prevents patients from receiving the most effective treatment for cancer. Moreover, symptomatic therapy is often largely ineffective in reducing painful CIPN symptoms [65]. Although the pain and paresthesia can completely resolve months or years after stopping chemotherapy, in some cases the effects of CIPN are only partially reversible and are permanent [62]. In addition, CIPN also creates economic issues, since cancer patients with CIPN have significant excess health care and resource costs [61]. CIPN is caused since the chemotherapy drug acts locally and has better access to the peripheral nervous system, thus resulting in peripheral rather than central neurotoxicity [63]. The mechanisms underlying CIPN are controversial.

PTX, often called by its brand name Taxol, is an anti-mitotic agent that is widely used as a chemotherapeutic agent for the treatment of breast [66], ovarian [67], lung [68], and liver cancer [69], as well as leucopenia [70]. As a microtubule stabilizer, PTX enhances the polymerization and protects against disassembly of microtubules, thus blocking mitosis in the late G2 phase of the cell cycle and inducing cell death, which is the reason for its anti-neoplastic activity [71, 72]. One hypothesis is that this disrupts fast axonal transport, which relies on microtubule polymerization [63, 73, 74]. The dying back pattern observed in CIPN, which is when the degeneration starts distally and proceeds proximally, supports this idea. It is also supported by the selective vulnerability of sensory neurons bearing the longest axonal projections [75, 76]. Longer axons are more susceptible to disruption of axonal transport, and drug effects tend to accumulate and cause more damage at the distal end of axons. Thus, PTX produces length-dependent axonal damage. The resulting neuropathy is distally predominant, with symptoms beginning in the lower limbs and appearing later in the upper limbs. Alternative hypotheses have been proposed, such as mitochondrial dysfunction, changes in gene expression and membrane excitability, and inflammation [62, 77, 78]. In fact, it is possible that these mechanisms involved in CIPN may be interrelated rather than independent [79].

Dorsal Root Ganglion (DRG) cells are simple and well-accepted models for studying peripheral neuropathy induced by anti-neoplastic agents [11, 80, 81]. Furthermore, these cultures are a valuable tool in the validation of molecular targets for neuroprotection and axonal regeneration that were identified in high throughput drug screens.

It has been shown in *in vitro* experiments that axons are much more susceptible to neurotoxic effects of PTX than the cell bodies are [8]. When PTX was applied to the axonal side, there was a clear degeneration of axons. However, when it was applied to the soma side, there was no significant change in the axon lengths. There were also no pathological changes seen in the neuronal bodies of the spinal cord, nor in the DRG cells [65]. Thus, compartmentalized microfluidic culture systems combined with embryonic DRG can be effectively used for studies aimed at understanding axonal

degeneration, neuroprotection, and the development of the nervous system [8].

Animal models are critical to understand the mechanisms underlying CIPN as well as the related neuropathic pain. Development of these models, mostly through rodents, contributed in the development of new therapeutic agents for neuropathic pain management. Furthermore, preclinical data obtained from these models have been successively translated to effective pain management in clinical setup [82–84]. PIPN is modeled in the A/J strain of mice by means of tail vein injections [85]. A consistent pathological finding in patients receiving PTX treatments is the loss of intra-epidermal nerve fibers (IENF) that innervate the epidermis [86]. IENFs are particularly important in transmitting noxious mechanical and thermal information, [87] and the loss of IENFs are highly correlated with painful neuropathy [88]. PTX induced neuropathy models showed mechanical hyperalgesia and allodynia, as well as thermal hyperalgesia [83]. The mechanical and heat hypersensitivity is suggested as a result of spontaneous discharge due to the axonal degeneration [89, 90].

In this study, a phenotypic screening of the Thermoscientific Spectrum Collection (120606), which contains a total of 2322 FDA, approved agents, for the identification of therapeutic drugs for CIPN is made (Figure 3.1).

The initial screening was made with embryonic rat DRG cultures at a gestational age of 15 days, an embryonic stage in which the neurons are post-mitotic cells that differentiate and mature under the influence of nerve growth factor (NGF) [91]. A novel HTCMP (Figure 2.2) that enables the consolidated validation of axon protection and the study of sites of action, for 30 pharmacologic agents is developed. The fluidic isolation of the somal and axonal compartments enabled selective application of drugs to different components of cultured neurons. The axonal protection ability of the drugs and the site of action are elucidated by the preservation potential of the drugs against PIPN. FA is identified *in vitro* and *in vivo* as a neuroprotective agent to prevent PIPN without preventing PTX's efficacy.

The endogenous polyamines, spermine, spermidine and their diamine precur-

sor putrescine are ubiquitous polycations that exist at all organisms. They interact with negatively charged molecules, such as DNA, RNA or proteins and are involved in many functions, mostly linked with cell growth, survival and proliferation. Polyamines also exhibit a number of neurophysiological and metabolic effects in the nervous system. They have a pivotal role on nervous system development [92], increase the rate of peripheral nerve regeneration [93], accelerate regeneration of superior cervical sympathetic ganglia neurons following axotomy [94], enhance neuronal survival after injury [95, 96], and promote both neurite elongation [96] and regeneration of injured axons in cultured rat hippocampal neurons [97].

Polyamines act on axonal injury that; one of the earliest biochemical changes following axonal injury is the transient up-regulation of polyamine-producing enzymes (ornithine decarboxylase, transglutaminase) [98]. This has been linked to an increase in mRNA metabolism and protein synthesis [99, 100], resulting in the polyamines putrescine, spermine and spermidine, which show a strong enhancing effect on neurite outgrowth both *in vitro* and *in vivo* [101–103].

The effect of FA on cellular polyamine levels of DRG neurons, whether its neuroprotection comes from the polyamine levels is investigated.

3.2 Methods

All experiments involving animals were carried out according to protocols approved by the Johns Hopkins Institutional Animal Care and Use Committee.

3.2.1 Cell Cultures

DRG from Sprague-Dawley rats at 15th day of gestation were aseptically dissected and isolated, and the cells were dissociated enzymatically with collagenase and trypsin and suspended in Neurobasal medium (Gibco 21103-049), with 1% FBS (Hy-

clone 3H30071.3), 0.5 mM L-Glutamine (Gibco 25030-081), 10 ng/ml glial cell line derived neurotrophic factor (GDNF, Amgen), 2% B27 supplement (Gibco 17504-044), and 0.2 96 well sterile tissue culture plates were coated with first with 100 μg/ml Poly-D-Lysine Hydrobromide (PDL Sigma- Aldrich P7280) and then with 10 μg/ml Laminin (Invitrogen 23017-015). The DRG cells were cultured at a density of 6000 cells/ well, and incubated in a humidified 37 °C, 5% CO2 incubator. Their neurite growth and differentiation was visible under an inverted light microscope after 24 hours of culture.

3.2.2 ATP Assays

PTX (Sigma T7402) was dissolved in DMSO, and the drugs were in DMSO and further diluted in Neurobasal Medium (Life Technologies 21103-049). PTX and drugs were added to the wells with 100 nM and 1 μM final concentrations, respectively. Each plate contained one column of wells with cells only as negative control and one column with cells and PTX served as positive control. The cells were incubated for another 24 hours, and then the therapeutic effect of drugs together with PTX was evaluated by the ViaLight Plus Cell Proliferation and Cytotoxicity Bioassay Kit (Lonza), according to the manufacturer's protocol on L-Max (Molecular Devices, Sunnyvale, CA). Each drug screen was performed in duplicate and repeated at least twice and their percentage of cytotoxicity/neuroprotection was calculated, based on the cellular ATP levels of positive and negative controls.

3.2.3 Microfabrication of compartmentalized platform

Compartmentalized microfluidic platforms were fabricated by means of standard photolithography and soft lithography techniques [8]. The silicon wafers (University Wafer, MA) were coated with SU-8 photoresist (MicroChem), spun, and soft baked according to manufacturer's parameters to yield a resist thickness of 2.5 μm. Then the wafer was exposed to UV light through an exposure mask with the desired microfluidics pattern to generate an array of microchannels with 10 μm width and 500

μm length. The substrate was baked again, and then developed with SU-8 developer. This process was repeated with a thick layer of SU-8 3050 (Microchem; MA) and an exposure mask with the defined fluidic reservoir patterns with dimensions of 3 mm width and 3 mm length. Standard soft lithography was performed using Sylgard 184 polydimethylsiloxane (PDMS) (Dow Corning, MI). A 10:1 ratio of cross-linking agent to Silicone Elastomer Base was referenced to add in the agent, then the mixture was degassed under a vacuum, poured onto the master wafer to reach a thickness of 5-7 mm, and allowed to bake for 3-4 h at 80 °C until it became transparent and fully cross linked. After curing, the PDMS was removed from the master and access ports were created using a suite of dermal biopsy punch tools (3-6 mm) (Huot Instruments, WI). Then the PDMS slabs were plasma bonded to glass coverslips to generate HTCMP, which facilitate screening 30 drugs in one plate (Figure 1.2). Since the microfluidic chambers were plasma bonded to a glass substrate, it is possible to investigate the axons with light microscopy.

Embryonic DRG cells were plated on one side of the HTCMP, and were allowed to grow axons through the microchannels to the other compartment; Uridine (Sigma U3003) and 5-Fluoro-2-deoxyuridine (Sigma F0503) at 50 μM concentrations were added in culture in order to prevent excess proliferation and invasion by Schwann cells and fibroblasts. The media was changed after 24 hours. PTX was added to the axonal side and therapeutic candidates were added to the axonal side, or to soma side. Neuroprotection was qualitatively evaluated with light microscopy after 24 hours.

3.2.4 Axon Length Measurement

E15 DRG neurons were cultured in 24-well plates on collagen coated glass coverslips, and incubated in media for 24 hours to allow axons to grow. Drugs along with PTX were then added, and the plates were incubated for another 24 hours. Each plate contained both positive and negative controls. Then the cells were fixed with 4% paraformaldehyde and stained with anti-βIII-tubulin antibody (Promega). The axon lengths of the control group, PTX group, and drugs with PTX group were mea-

sured. Each experimental condition was done in triplicate wells and repeated twice. 30 isolated axons were measured per well and their average axon length was calculated.

3.2.5 PTX Efficacy Interference Test

Eventually 4 different cancer cell lines: SUM 159 breast cancer, MOSEC cancer, ES2 ovarian cancer, and cervical TC-1 cancer cells were plated on 96 well plates in DMEM-F12 (Cellgro 15090) media containing 5% FBS, 500 μl of 10 mg/ml insulin (Sigma I0516) and 25 μl of 10 mg/ml hydrocortisol (Sigma H-4001) and the varying drug amounts along with 100 nM PTX were administered. ATP levels of these groups were measured using the ViaLight Plus Cell Proliferation and Cytotoxicity Bioassay Kit (Lonza), according to the manufacturer's protocol on L-Max (Molecular Devices, Sunnyvale, CA).

3.2.6 In Vivo PTX and Drug Treatment

In order to model PTX induced sensory neuropathy *in vivo*, PTX was administered by tail vein intravenous injections (25 mg/kg) on days 1, 3 and 5, to A/J strain of female mice of 8 weeks old [104]. Each group consisted of 5-10 mice. One group received only saline as the vehicle and served as the negative control. 500 μg/kg FA (Fluka F8880) was injected into the intraperitoneal cavity on a daily basis to one of the PTX injected groups. One group only received PTX (25 mg/kg) by tail vein injection, and one group only received 500 μg/kg FA intraperitoneal injections.

3.2.7 Nociception Assays

Daily intraperitoneal injections of drugs were done at around 10 am with standard rodent injection techniques. On day 19, two weeks after the first administration of PTX, and the last day of IP injections of FA, the plantar surface of the right hind

paw is tested for heat hyperalgesia according to the Hargreaves method [105]. Two days after, Von Frey monofilaments (Stoelting, Wood Dale, IL, USA) were used for the assessment of mechanical allodynia [11,106]. Baseline sensitivity to the monofilaments and heat was already assessed 2 days before the start of injections.

3.2.8 Intra Epidermal Nerve Fiber Density Analysis

After the behavioral tests were done, animals were euthanized under deep inhalation anesthesia, and the footpads were harvested for the evaluation of intra-epidermal nerve fibers. 2mm punch biopsies of medial plantar footpads were fixed with paraformaldehyde-lysine-periodate fixative up to 24 hours at 4degC, kept in a cryoprotective solution, and cut serially with a freezing microtome with 50 μm thickness. Then the sections were stained with pan-axonal marker anti-protein gene product 9.5 (Bio-Rad 7863-0504). For quantitative analysis, IENFs were counted with a microscope at 40X magnification as described [86]. Three sections from each biopsy were examined. The length of the section along which IENF were counted was measured with ImageJ [107]. IENF density was determined as the total number of fibers per mm of epidermal length. The IENF density was calculated for each section and averaged for a group [108, 109].

3.2.9 HPLC Analysis for Polyamine Levels

Immortalized DRG cell line 50B11 cells are plated to T- 75 flasks in Neurobasal medium (Gibco 21103-049), with 10% FBS (Hyclone 3H30071.3), 0.5 mM L-Glutamine (Gibco 25030-081), 2% B27 supplement (Gibco 17504-044), and 0.2% glucose. After they were confluent, the culture medium changed with reduced serum (0.2%) and differentiation and axonal elongation was induced by addition of forskolin (Sigma F6886) with a final concentration of 50 μM and incubated for 24 hours. Then taxol and FA in varying concentrations are added and the cultures are incubated for another 24 hour.

The cells are harvested with trypsin and suspended in ice-cold ODC breaking

buffer (25 mM Tris-Cl, 0.1 mM EDTA, 2.5 mM DTT) and quick freezed. Polyamines were quantitated by HPLC separation of dansylated derivatives by use of an internal standard [110].The HPLC analysis is performed by Tracy Murray-Steward, SOM Onc Cancer Biology, JHU, Baltimore, MD. Each measurement is made in duplicates and repeated three times.

3.3 Results

3.3.1 Identification of Neuroprotective Drugs In Vitro

Primary cultures of E15 DRG neurons are used to make a phenotypic screening for compounds that exhibited protective effects from PTX induced neuropathy. 2322 FDA approved pharmacologic agents (Thermoscientific Spectrum Collection - 120606) were added to neuronal cultures and PTX, and cellular ATP levels were measured 24 hours after. Since reduction in ATP levels is correlated with axonal degeneration, the neuroprotection potentials of the drugs were evaluated by comparing the cellular ATP levels to positive and negative controls. Through this process, 40 pharmacologic agents that exhibited 50% or more neuroprotection are identified. Further evaluation with varying doses of 1 μM, 500 nM, 100 nM, 10 nM and 1 nM of each compound showed that they exhibit the highest neuroprotective levels in between 10-100 nM concentrations. More specifically, among all, varying doses of FA showed that FA has the highest neuroprotection of 96% at a concentration of 10 nM (Figure 3.3A).

3.3.2 Validation of neuroprotective drugs in HTCMP and Site of Action of FA

The Embryonic DRG cells that were plated on soma side of the HTCMP, Uridine (Sigma U3003) and 5-Fluoro-2'-deoxyuridine (Sigma F0503) at 50 μM concentration were added in order to prevent excess proliferation and invasion by Schwann cells and fibroblasts. The media was changed after 24 hours and the cultures were incubated

for 7-10 days to facilitate axonal growth through microfluidic channels to the axonal compartment. Then the 40 therapeutic candidates that were identified by ATP assays were added, in their optimum neuroprotective concentrations, either to the soma side or to the axonal side. PTX is always added to the axonal side because it was demonstrated in previous findings that PTX causes axonal degeneration only when it is applied directly to the axonal side. Addition to the soma showed no significant axonal degeneration [8]. The degree of neuroprotection was qualitatively evaluated by light microscope after 24 and 48 hours.

Our HTCMP studies showed that when 10 nM of FA was added together with PTX to axonal compartments, there was a significant level of distal axonal neuroprotection. However, addition of FA to the somal compartment and PTX to the axonal side resulted in neurodegeneration (Figure 3.4).

Next, CMPs are used again to further ensure the neuroprotection of FA and the site of action of FA. In order to determine that the increase in ATP was due to actual axonal protection, rather than the promotion of glial cell proliferation, E15 DRG neurons were cultured in CMPs. PTX was then added to the axonal compartments, and FA was added to either the somal or axonal compartments.

3.3.3 Validation of FA on actual Neurite Degeneration

In order to validate the protective effect of FA on actual neurite degeneration induced by PTX, E15 DRG neurons are cultured on collagen-coated coverslips to measure axon lengths. Varying doses of FA along with PTX were added to the cultures, and then they were immunostained to delineate axons. Isolated axons from each coverslip were identified during fluorescent microscopy, and their lengths were measured. FA exhibited a high degree of neuroprotection where the average axon length of the PTX + 10 nM FA group was 76% greater than that of the PTX group.

3.3.4 Effect of neurotective drugs on PTX's efficacy to cancer cells

In order for FA to be clinically feasible, it must not interfere with the ability of PTX to kill cancer cells. To study this, 4 different cancer cell lines are used: SUM 159 breast cancer cells, MOSEC ovarian cancer cells, ES2 ovarian cancer cells, and TC-1 cervical cancer cells. For each cell line, the cells are treated with PTX and varying doses of FA, and then their ATP levels are measured. This indicated the viability of the cells, and the findings for all four cell lines showed that compared to the control, PTX significantly reduced the cancer cell's viability by 40-60%. Furthermore, FA did not create any significant changes in the cell viability levels, verifying that it does not interfere with the chemotherapeutic efficacy of PTX (Figures 3.5 A,B, C and D).

3.3.5 Neuroprotective Effect of FA In Vivo

Next, to examine FA's potential for neuroprotection *in vivo*, a mouse model of PIPN through intravenous administrations of PTX is used. PTX (25mg/kg) was injected intravenously through the tail vein on days 1, 3, and 5 to induce a slight sensory neuropathy similar to the early stages of human CIPN. To examine the ability of FA to prevent PIPN, FA was injected intraperitoneally starting on day 1. FA was administered daily for another 14 days until after the last PTX dose was given. The primary aim was to confirm the *in vitro* results on FA's ability to protect the axon from PIPN, specifically from axonal degeneration, by measuring the density of intraepidermal nerve fibers in the hindlimb medial plantar footpads. The footpads were harvested, cryosectioned, and immunostained with pan-axonal marker anti−protein gene product 9.5 before being mounted on slides. Light microscopy was used to examine the IENFs and their density on each section for each group is calculated (Figures 3.6 A and B). The results showed that the footpad group treated with FA had significantly higher IENF density by threefold, compared to the group treated only with PTX.

After the injections, nociception assays of Hargreaves thermal test and Von Frey mechanical test are performed, which demonstrated that the PTX group was

more sensitive to mechanical and thermal stimuli than the control group (Figures 3.6 C and D). Furthermore, the results of the PTX + FA treatment group showed that FA displayed antinociceptive effects against PTX-induced mechanical allodynia and thermal hyperalgesia in PTX sensory neuropathy modeled mice. The sensory threshold to thermal and mechanical stimuli was higher in the group of mice injected only with FA. To confirm the *in vitro* findings of FA's ability of axonal protection from PTX Induced Neuropathies, medial plantar footpads were harvested then immunostained with pan-axonal marker anti-protein gene product 9.5 to determine IENF densities. (Figures 3.6 C and D) The calculations showed that the footpad group treated with FA had a significantly higher IENF density compared to the group treated only with PTX.

3.3.6 Effect of FA to cellular polyamine levels

Polyamines have considerable importance for the developing and mature nervous system because they exhibit a number of neurophysiological and metabolic effects including the control of nucleic acid and protein synthesis, modulation of ionic channels, and calcium-dependent transmitter release. Therefore the probability that FA has any effect on polyamine levels of neurons is examined.

The results were consistent with previous findings that spermidine was more abundant than putrescine and spermine [111], in rat DRG neurons. The concentrations of spermine, putrescine and spermidine were 0.178±0.007 nM/106, 0.192±0.030 nM/106 and 0.570±0.032 nM/10^6, respectively. The concentrations of spermine and putrescine did not change significantly, however spermidine concentration increased 21% with PTX. FA alone increases spermidine concentrations as compared to control, but the treatment group of 100 nM FA together with PTX creates a peak value of 0.843±0.028 nM/106 cells, which corresponds to 48% higher spermidine levels than control.

3.4 Discusison

Any possible pharmacologic agent that can prevent CIPN will have a great impact on the lives of cancer patients, as it will allow them to have an optimal dose of chemotherapy for prolonged survival and improved quality of life. Furthermore, it can help reduce the significant excess healthcare and resource costs that cancer patients with CIPN suffer from. In this study, Fluocinolone Acetonide (FA), an anti−inflammatory synthetic corticosteroid, is identified as a potential neuroprotective agent that can be used as an adjunct treatment with PTX to prevent PIPN. The drug screening was performed with primary DRG cultures, which represents the original axonal microenvironment that normally consists of Schwann cells, the primary glial cells of the PNS, performing an ideal system for studying cellular and molecular pathways that lead to axonal degeneration. Using an *in vitro* model of PIPN, which is based on the ability of E15 DRG cells to outgrow neurites when exposed to a Neural Growth Factor (NGF), as well as the interference with neurite elongation by toxic substances, 2322 FDA approved drugs (Thermoscientific Spectrum Collection -120606) were screened to ensure safe and clinically feasible application of the therapeutic candidates. Since PTX causes mitotoxic effect in primary afferent sensory neuron axons [78], more than 90% of mitochondria are in the axons in the peripheral nervous system [112], and reduction in ATP levels is correlated with axonal degeneration, ATP assays are used in order to assess the protective effect of each drug against PIPN.

CIPN starts with distal axonal degeneration, and the microenvironment of the DRG cell bodies and distal axons are different from each other *in vivo*. HTCMP therefore provide a more accurate model of the *in vivo* system, in which cell bodies and axons are in different microenvironments. This makes it possible to monitor the disease state, in which cell bodies remains healthy and axons suffer from PTX induced degeneration. Additionally, the embryonic DRG cells allows the culturing of a high content of cells with higher efficiency in isolating neurons in comparison to post-natal animals and are more potent in growing long axons through the microfluidic channels in compartmentalized platforms. However, as the primary cell cultures are more reliable when modeling *in vitro* peripheral neuropathies, they are less manageable and limited

in number. The HTCMP helped to overcome this challenge by facilitating the study of the influence on axonal degeneration and protection by 30 drugs at once. It also allowed the verification of the site of action of FA, which showed that drug administration to the axonal site rather than the somal site resulted in neuroprotection. HTCMP can also be applied to the screening and identification of therapeutic agents against other types of neuropathies such as diabetic neuropathy, neuropathies caused by viruses like HIV, or neuropathies of chemical warfare victims. It provides a powerful solution to the problem of the deficiency of current *in vitro* cell culture methods for understanding and exploring mechanisms distal axonal degeneration induced by neurotoxic agents.

In order for FA to have a clinical significance, it should not hinder the anti-tumor abilities of PTX. To ensure this, FA was administered to four different cancer cell lines together along with PTX. It is demonstrated that FA did not compromise the antineoplastic effect of PTX. PIPN was induced in mice by tail vein injections of 25 mg/kg of PTX every other day for a total of three doses. The rationale for using intravenous injection is that, it models better the human neuropathies than the intraperitoneal administration [85]. FA also showed antinociceptive effects from neuropathic pain, as it diminishes the mechanical and thermal hypersensitivity that is caused by PTX (Figure 3.6A and 3.6B). Along with protecting axons from degeneration and ameliorating neuropathic pain, FA is also known to be an inhibitor of tumor promotion [113–115]. Considering the fact that endogenous polyamines are of considerable importance for the developing and mature nervous system, whether the neuroprotective effect of FA emerges from its ability to increase endogenous polyamine levels is explored. Previous research showed that polyamines play a pivotal role in axonal regeneration. The activity of ODC, the enzyme required for the first and committed step of polyamine synthesis, increases following axonal injury [98, 116], and axonal regeneration is enhanced by administration of exogenous polyamines; whereas blocking the polyamine synthesis inhibits this regeneration [94]. The polyamines are ubiquitous, but they have an uneven distribution in tissues and cells. As reported before [111], spermidine concentration in rat DRG neurons is much more abundant than concentrations of spermine and putrescine. Thus, it can be deduced that spermidine should have a more distinctive function in the nervous system than the other polyamines.

The findings in this research indicate that FA increases the spermidine levels of immortalized DRG neuronal line 50B11 cells. When differentiated in the presence of forskolin, these cells extend long neurites, express neuronal markers, and generate action potentials [117], which makes them a good model for DRG studies, when abundant number of cells are needed. Figure 3.7 demonstrates higher spermidine levels in treatment groups containing varying concentrations of FA alone and also containing PTX. In particular, the spermidine levels at PTX + 100 nM FA were observed to be markedly higher than those in the treatment group with PTX alone. The neuroprotective ability of FA against CIPN emerges from its upsurging of endogenous spermidine concentration, which is consistent with other studies, thereby suggesting that increase in spermidine levels exerts neuroprotective and neuro-regenerative effects. It is reported that in a model system for axotomized sympathetic neurons, where PC12 cells are primed with nerve growth factor, then stripped off the culture dish and replated, spermidine treatment, with or without nerve growth factor, enhanced neurite growth [102]. At *in vivo* model of ONI, spermidine treatment prevented Retinal Ganglionic Cell death and suppressed retinal degeneration. The treatment exerted neuroprotective effects and enhanced optic nerve regeneration following injury by decreasing the accumulation of microglia and reducing the number of activated microglia, and by suppressing iNOS (inducible nitric oxide synthase) upregulation [118, 119]. Also, inhibition of axonal regeneration by MAG and myelin in CNS can be overcome by the synthesis of putrescine (and subsequent conversion to spermidine), which occurs from the pathways of cAMP and Arg I upregulation [120]. Inhibition by MAG can also be overcome through the intrathecal delivery of spermidine [118]. It is also shown that the effect of polyamines on neurite outgrowth and survival originates from the transformation of spermidine to hypusine in the formation of eIF5A [121]. Spermidine has also been shown to be effective in treating neurodegenerative disorders and age induced memory impairment by triggering protective autophagy, a crucial regulator of age-associated pathologies [122]. Spermidine supplementation can also increase stress resistance and decrease age-related oxidative stress markers in several model organisms [123]. The findings suggest FA as a potential treatment not only for CIPN, but also for CNS injuries or degenerations and age-associated neurodegenerative disorders where increased spermidine levels are needed for neuroprotection and regeneration because it triggers a pathway that causes

an increase of spermidine levels in neurons. The mechanisms through which FA increases endogenous spermidine levels and through which spermidine stimulates neurite outgrowth remain to be determined. Polyamine-deficient diets have been shown to reduce chemotherapy-induced cold and mechanical hypersensitivity to pain [124–126]; and targeting polyamine pathways and biosynthesis is a promising area for chemotherapeutics and chemoprevention [127]. However, in these studies, polyamines are usually considered as a group of molecules with similar effects. Different polyamines can have different, even opposite effects, so each polyamine metabolism ought to be considered separately, with respect to their role in the combination in which they naturally occur.

3.5 Summary

Paclitaxel (PTX) is among the most commonly used chemotherapeutic agents that cause chemotherapy-induced peripheral neuropathy (CIPN), a debilitating and serious dose-limiting side effect in peripheral neurons. There are no drugs currently known to be capable of preventing the occurrence of CIPN, and symptomatic therapy is often ineffective. In order to identify therapeutic candidates for axonal protection from Paclitaxel induced peripheral neuropathy (PIPN), neuroprotective drugs were identified from Food and Drug Administration (FDA) approved drug set using *in vitro* ATP assays. To verify neuroprotection, innovative high throughput compartmentalized microfluidic platforms (HTCMP) were used to administer an array of these drugs together with PTX before the onset of axonal degeneration because axons are more susceptible to PTX toxicity than cell bodies. A neuroprotective compound, Flucinolone Acetonide (FA) is identified *in vitro* and validated *in vivo* that it demonstrates axonal protection from PIPN as well as relieving neuropathic pain. Furthermore, it is confirmed with four different cancer cell lines that FA does not interfere with Paclitaxel's antitumor ability.

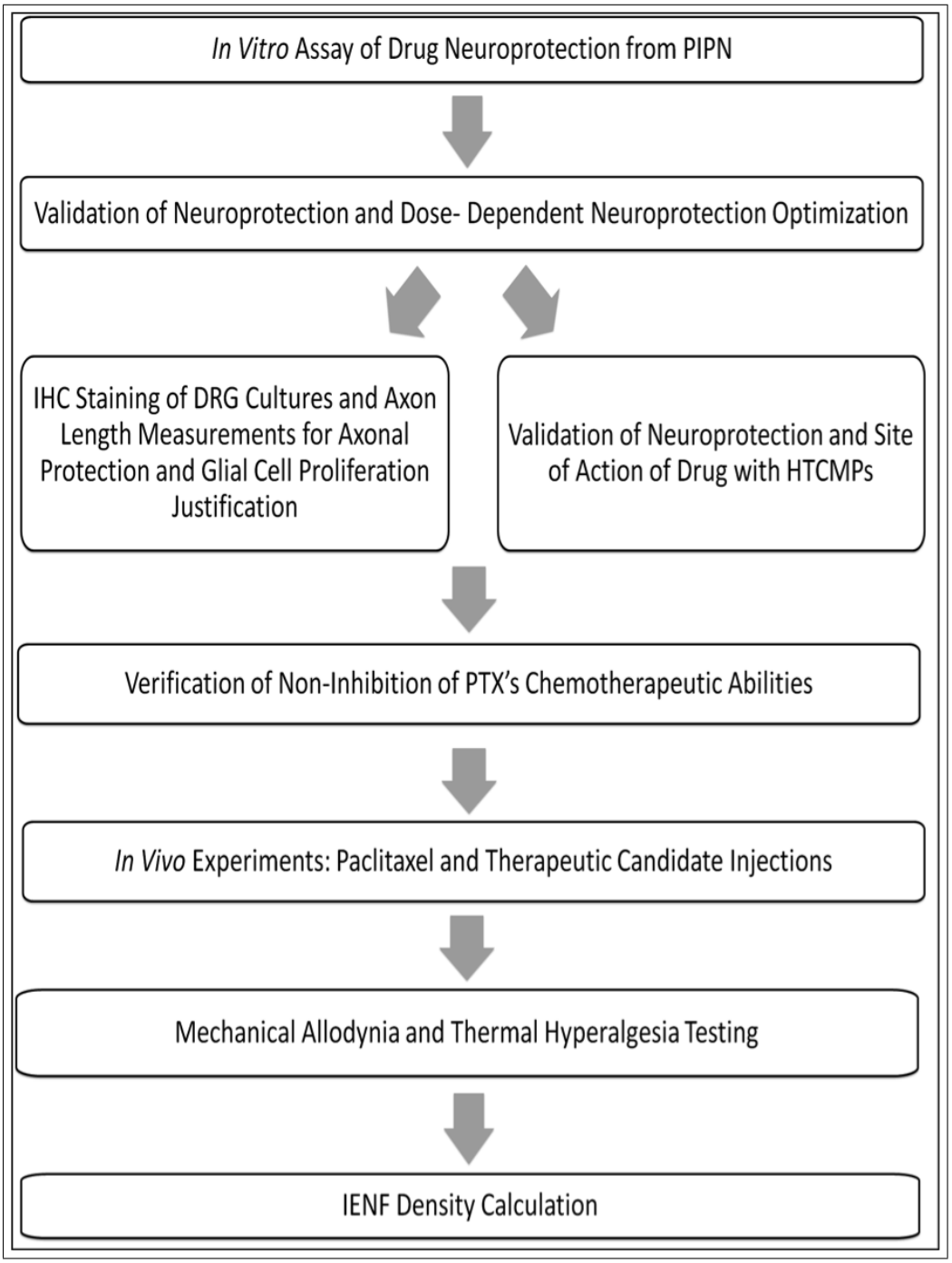

Figure 3.1 Schematic diagram of the protocol used for drug screening against PIPN.

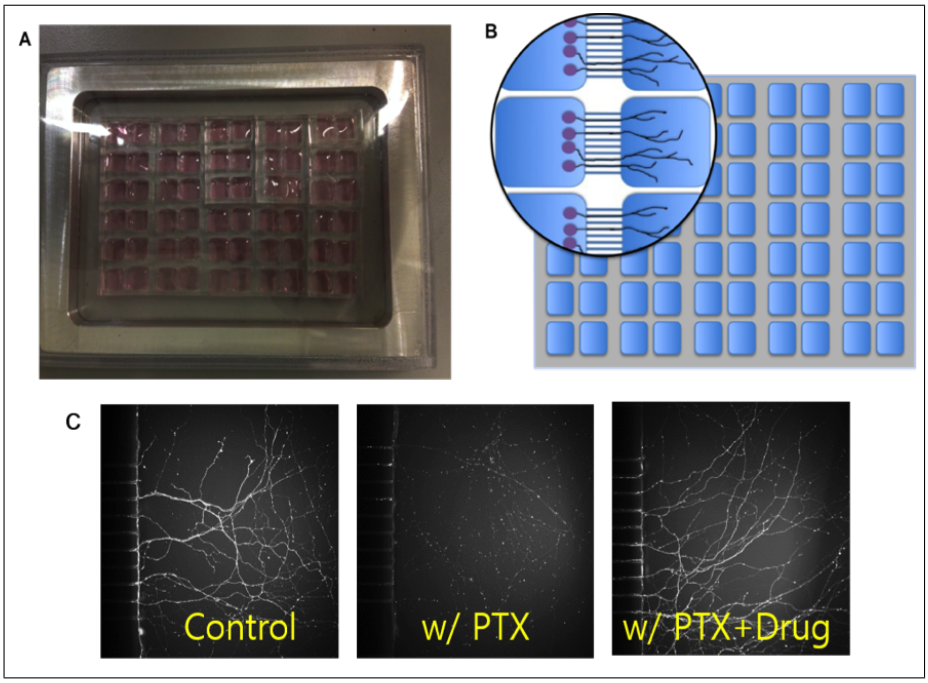

Figure 3.2 A)High throughput compartmentalized microfluidic platform (HTCMP) B) Representational drawing of HTCMP, delineating somal and axonal compartments C) Axonal compartment images of HTCMP's, Control and PTX added to axonal compartment.

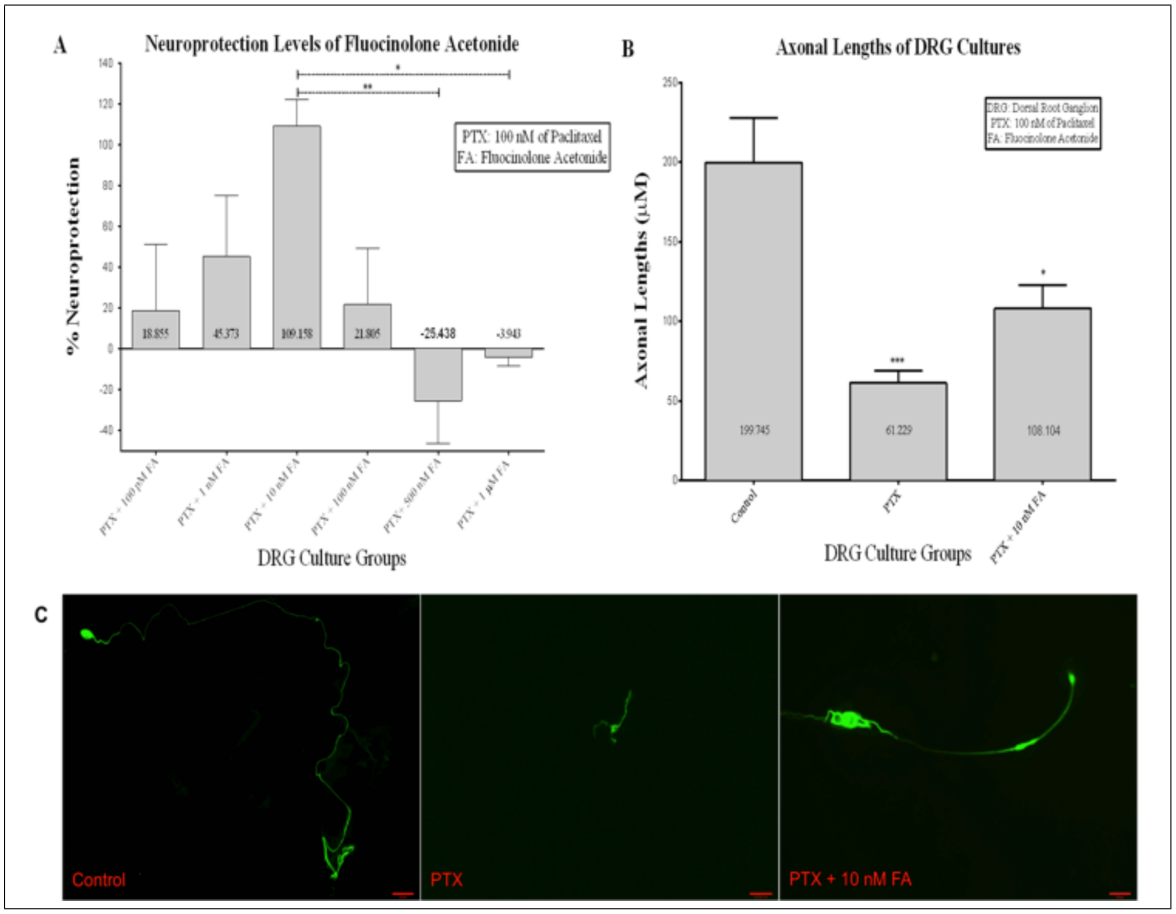

Figure 3.3 Neuroprotection by FA *in vitro* (A) Embryonic DRG cells were cultured, then exposed to PTX with or without various concentrations of FA. ATP levels were measured after 24 h, and converted into percentage neuroprotection values. The data are presented as means ± S.E.M. from four independent experiments. Statistical analysis was done by one-way ANOVA ($p<0.05$). (B) Primary rat DRG neurons were grown in culture and allowed to extend axons for 24 h. Then, they were exposed to PTX or FA for another 24 h. Cells were fixed, stained with anti-bIII-tubulin antibody, and axon lengths were measured. FA at a concentration of 10 nM partially prevented distal axonal degeneration induced by PTX. Statistical analysis was done by one-way ANOVA ($p<0.0001$) using a post-hoc Dunnett's multiple comparison test. The data are presented as means ± S.E.M. from three independent experiments. (C) Images taken of the DRG cultures mentioned in (B) show severe axonal degeneration in the PTX group, compared to reduced degeneration in the PTX 10nM FA group.(Scale bar: 35 μm).

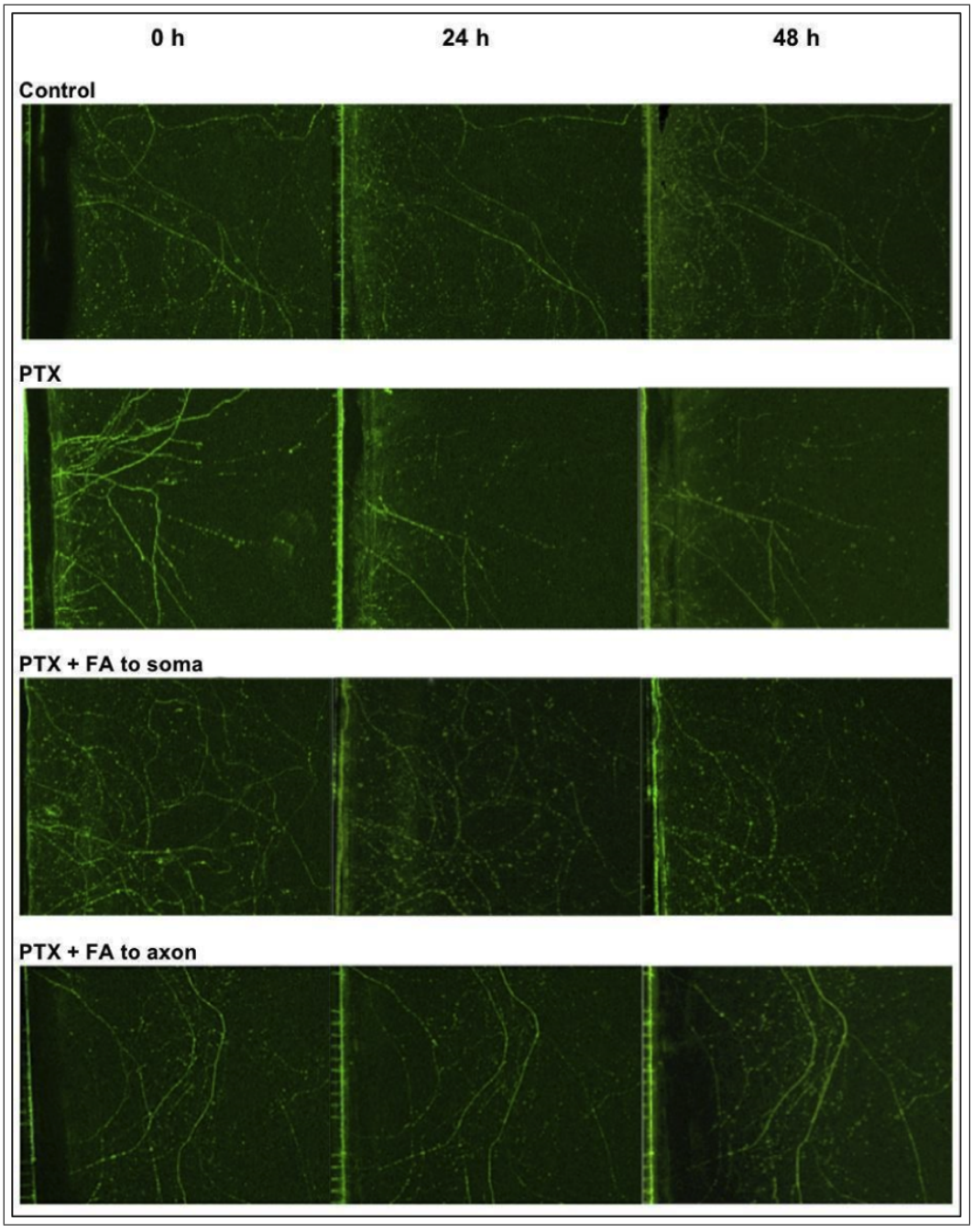

Figure 3.4 Axonal compartment images of HTCMP's. A) Control B) PTX added to axonal compartment C) FA added to somal compartment and PTX is added to axonal site D) FA and PTX both added to axonal site.

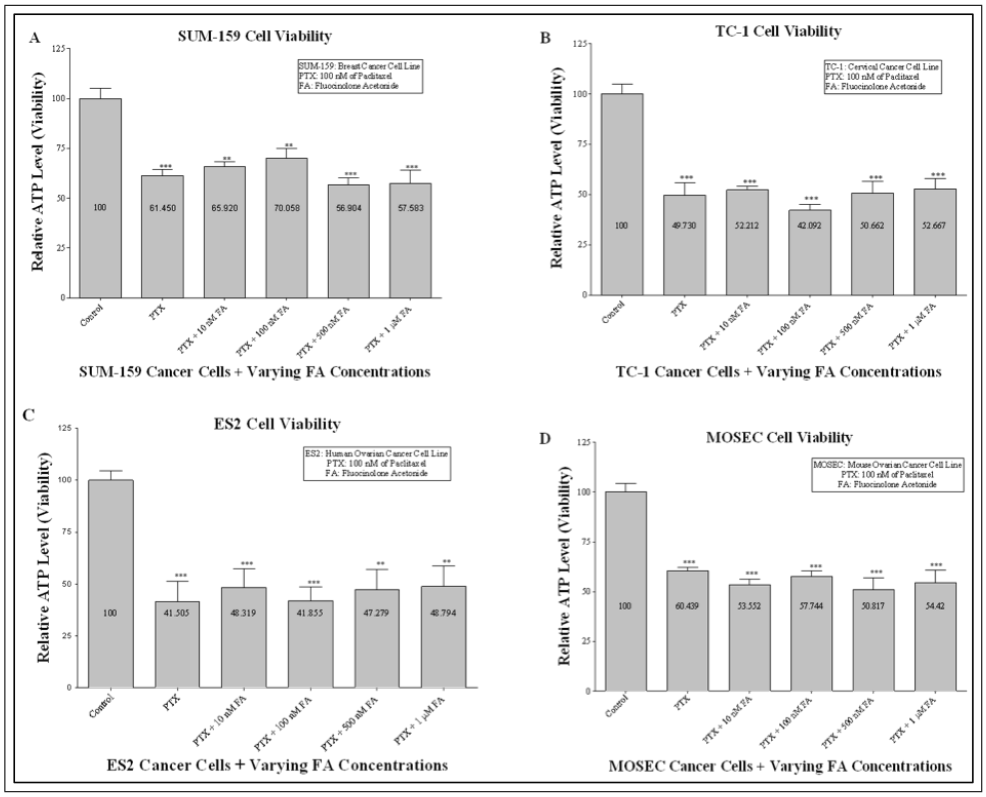

Figure 3.5 FA does not block PTX's chemotherapeutic abilities. When four different cancer cell lines (A-D) were grown in culture and exposed to PTX, their cell viability was reduced by 30-40%. The application of various doses of FA along with PTX did not show any significant change from the PTX only reduction in cell viability. Statistical analysis was done by one-way ANOVA ($p<0.0001$ for all four cancer cells) using a post-hoc Dunnett's multiple comparison test. The data are presented as means ± S.E.M. for each experiment.

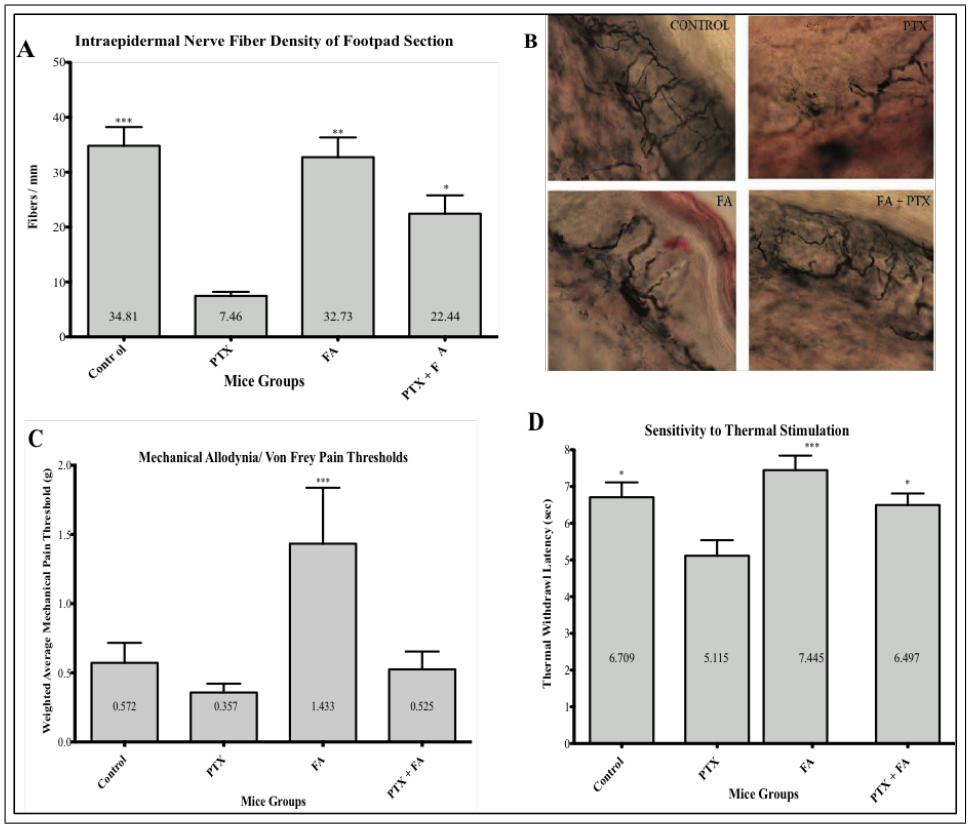

Figure 3.6 Neuroprotection by FA against PIPN in A/J mice. (n = 5-10). Co-administration of FA with PTX partially prevented the development of PIPN as assessed by (A) mechanical pain threshold, (B) thermal withdrawal latency, and (C,D) intraepidermal nerve fiber density. For (A) and (B), statistical analysis was done by one-way ANOVA ($p<0.05$ and $p<0.01$, respectively) using a post-hoc Bonferroni's multiple comparison test between PTX group and PTX + FA group. The data are presented as means ± S.E.M. for each experiment. For IENF density (C), statistical analysis was done by one-way ANOVA ($p<0.01$) using a post-hoc Dunnett's multiple comparison test where PTX served as the control/comparison group in order to observe neuroprotection for PIPN.

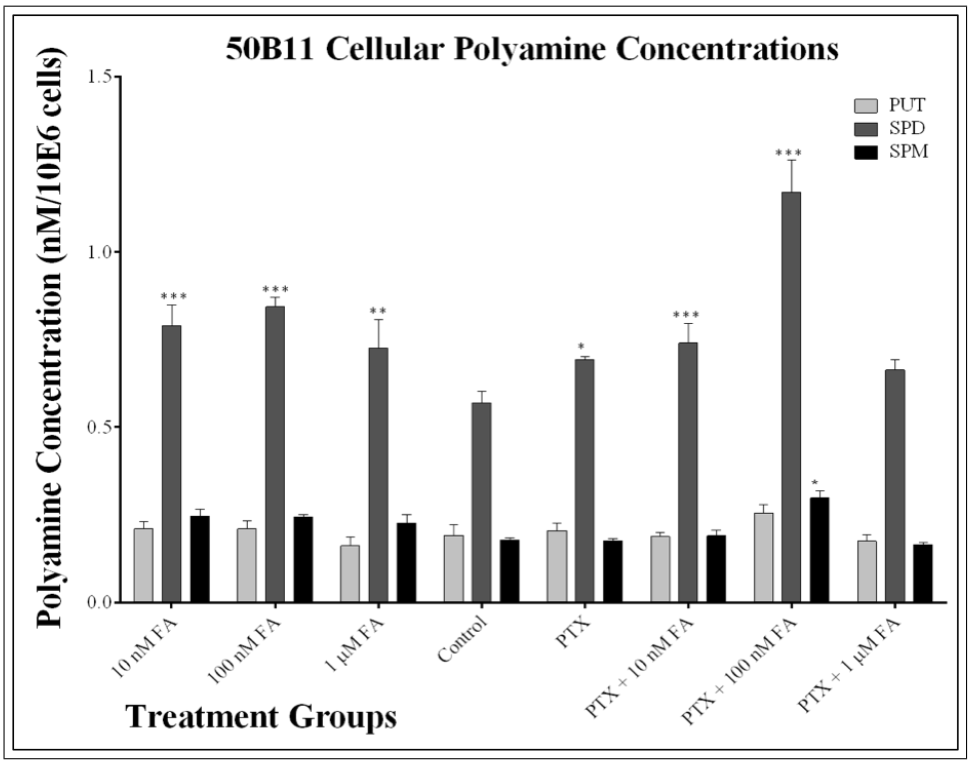

Figure 3.7 Effect of varying concentrations of FA and PTX + FA to 50B11 immortalized DRG cell cultures provided by an HPLC analysis of polyamines (putrescine, spermidine, spermine). Statistical analysis was done by two-way ANOVA ($p<0.0001$) using Bonferroni post tests, comparing each treatment group to control in order to observe the effect of FA on polyamine levels. The data are presented as means ± S.E.M. for three independent experiments.

4. MYELINATION OF MOTOR NEURONS BY OLIGODENDROCYTES DERIVED FROM MOUSE EMBRYONIC STEM CELLS IN A MICROFLUIDIC CELL CULTURE PLATFORM

4.1 Introduction

Severe Spinal cord injury (SCI) results in a serious central nervous system damage that interrupts ascending and descending axonal pathways and results in the loss of neurological function below the site of injury. Neuronal cell death occurs in the primary injury, first by mechanical damage and is then followed by a secondary degenerative stage due to the ensuing inflammation and demyelination processes [128]. Demyelination is the loss of myelin sheath surrounding the axons, which renders CNS axons incapable of passing signals from the brain to other neurons. This demyelination occurs mainly due to the death of endogenous oligodendrocytes, the myelin forming cells in the CNS [129, 130]. Oligodendrocyte progenitor cells (OPCs) are potential targets to replace endogenous oligodendrocytes, as the OPCs are widely considered precursor cells that differentiate into oligodendrocytes during the development and adult stages [131]. However, the mechanism involved in the regulation of OPC differentiation into oligodendrocytes is not fully understood. Moreover, whether the newly formed oligodendrocytes can survive in the demyelinating microenvironment and myelinate axons is still an open question.

Motor neurons are very sensitive to injury. Neurons may die or their axons may be damaged upon injury, thus leading to the loss of neurological function. In the damaged spinal cord, the innate ability to replace lost cells, repair damaged myelin, and regenerate axons is very limited. The formation of glial scar is the main physical and chemical barrier to the regeneration of axons. Reactive astrocytes, the major component of glial scar [132], secrete extracellular matrix (ECM) and inhibitory

molecules such as chondroitin sulfate proteoglycans (CSPGs), which suppress axonal growth [133, 134]. Recent experimental interventions have been tried to overcome the inhibitory environment and to make it more conducive to neuronal growth, such as neutralization of myelin inhibitors [135] and degradation of ECM [136]. However, this solution is are far from clinical applications because only a small portion of neuron fibers regenerate and the length of regenerated axons is still limited [137].

Nevertheless, transplantation of stem cell derived neuron and oligodendrocytes is a potentially effective approach for cell replacement in SCI. Embryonic stem cells (ESCs) are derived from the inner cell mass of the late blastocyst-stage embryos and are capable of self renewal and differentiation into all cell types in the body [138]. The availability of ESCs shows great prospect for clinical therapies in neurodegenerative diseases because of their potential to differentiate into the specialized cell types. Stem cell therapy strategies include: replacement of the damaged neurons and glial cells; re-establishment of neuronal network; production of neurotrophic factors, which are conducive to the survival of host cells and axonal regeneration [139]. Several studies have shown successful transplantation of ESCs into an animal SCI model and reported motor function recovery [140, 141]. Although stem cell derived OPCs and MNs have shown neuroprotective effects in neurological diseases, the ability of stem cell derived OPCs to myelinate stem cell derived motor neuron axons in order to regenerate new neurons with myelination has not been examined.

In this study, oligodendrocytes and motor neurons (MNs) that are differentiated from mESCs are used. A novel co-culture system in a two compartmentalized polydimethylsiloxane (PDMS) microfluidic device, in which the two compartments are connected through microchannels is established. In the experiment, the two cell types were successfully induced in the microfluidic device, and myelination of MNs was observed through MBP expression as well as myelin observation with an electron microscope. This *in vitro* coculture system for MNs and oligodendrocytes not only aids differentiation of mESCs into MNs and oligodendrocytes, but also provides a good system to study the mechanisms of myelination that can provide new knowledge to improve ESC-based myelination therapy. In conclusion, the results have shown that

mESCs derived motor neurons can be myelinated by mESCs derived oligodendrocytes in a microfluidic platform. This *in vitro* co-culture system may be helpful for further study of the mechanisms of demyelination and remyelination that can be used in new ESC based therapies for SCI.

4.2 Materials and Methods

4.2.1 Cell Culture

The general process of mESC differentiation into either oligodendrocytes or motor neurons is shown in Figure 3.1 Briefly, mESCs were cultured in the ESC growth medium that consisted of DMEM, 10%FBS, 10% new-born calf serum, 1x Nucleosides, 2mM L-glutamine (Gibco), 0.1 mM 2-mercaptoethanol (Sigma) and human recombinant leukemia inhibitory factor (LIF 106 units Chemicon). Aggregates were then induced. For motor neuron differentiation, embryoid bodies (EBs) were firstly induced from aggregates in DFK-10 medium consisted DMEM/F12 medium, 10% knockout serum replacement, 1% N2 supplement, glucose (4500mg/L), 2mM L-glutamine (Gibco), Heparin (1U/μl), 0.1 mM 2-mercaptoethanol (Sigma) for 2 days and then by adding retinoic acid (RA) and purmorphamine (Pur) for another 6 days (2-/6+ RA, Pur). At day 9, glial cell derived neurotrophic factor (GDNF) and Brain-derived neurotrophic factor (BDNF) (10ng/ml; Peprotech) were added to the medium for 5-7 days to induce differentiation of EBs into motor neurons. For oligodendrocyte lineage, EBs were induced in the ESC induction medium (ES cell growth medium absence of leukemia inhibitory factor) for 4 days and then treated with RA for another 4 days (4-/4+ RA).

At day 9, EBs were trypsinized and re-suspended in the modified OPC differentiation medium (DMEM with BSA, Pyruvate, progesterone, putrescine, thyroxine, triiodothryonine, insulin, transferring, sodium selenite with basic fibroblast growth factor (FGF2) and Platelet derived growth factor (PDGF) treatment (10ng/ml, Peprotech, USA) for 12-14 days. To achieve further oligodendrocyte maturation, the

growth factors were removed, and the cells were cultured in OPC medium with 0.5% FBS and 0.5% HS (Sato 0.5+0.5) for 1-2 weeks.

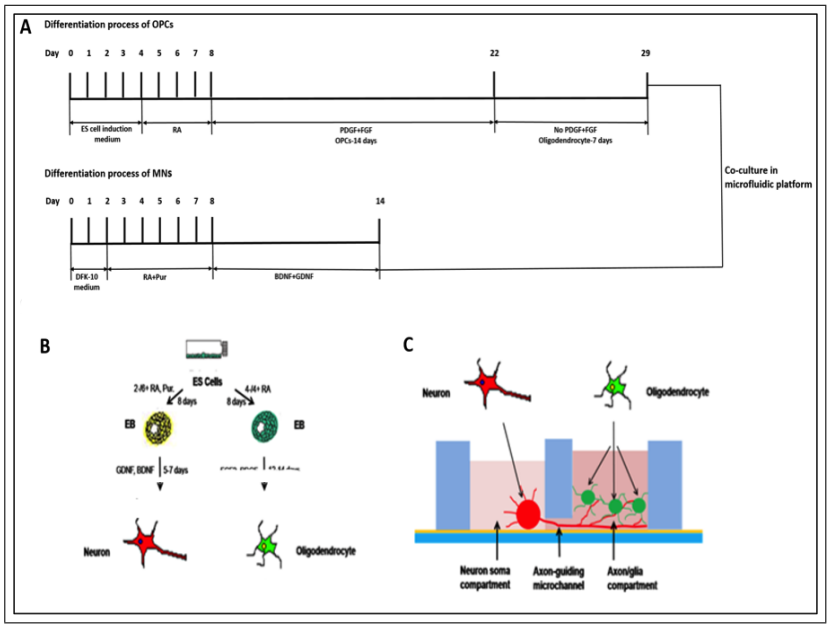

Figure 4.1 Differentiation process of mESCs into either motor neurons or oligodendrocytes and schematic of two-compartmentalized microfluidic chamber (A) For motor neurons (MN) differentiation, EBs were induced from mESCs by adding 2-/6+ RA and Pur for 8 days and followed treatment with GDNF and BDNF for 5 to 7 days. OPCs were derived from EBs by adding FGF2 and PDGF for continuous 12 to 14 days. (B) Soma and axons of MNs are separated in this microfluidic chamber. Only the axons pass through the microchannels and reach the OPCs.

4.2.2 Microfluidic Platform Preparation

Two-compartmentalized microfluidic platforms were prepared according to Yang et al. [142], Briefly; the master mold was fabricated by a two-step photolithographic process. The platform contains 100 parallel microchannels, each with 10 μm-width, 500 μm-length and 2.5 μm-height. Complementary PDMS replicas were formed by pouring PDMS prepolymer (mixed in a 10:1 ration with a cross linking catalyst, Dow Corning, USA) over the silicon master, degasing for 1h and then curing at 70°C in an oven for 1h. Wells were cut at both sides of the channels through a puncher. The chamber was then plasma bonded to the cover glass (22x40mm, ♯1 thickness, Menzel-Glaser, Germany) and left in the oven overnight to improve the bonding.

The wells were sterilized by autoclaving and further cleaned with ethanol and

washed with dd water for several times before use. For mESCs culture, the wells were coated with 100 μg/ml Poly-D-Lysine (PDL) overnight at RT and matrigel for 1h at 37°C.

4.2.3 Immunocytochemistry

mESCs differentiated cultures were washed with 1x PBS and then fixed with 4% paraformaldehyde for 20 mins. After washing 3 times with 1x PBS, the samples were blocked with 10% goat serum (Sigma, USA) and incubated with primary antibodies as Tuj1 (Covance,USA), HB9, Islet1 (DSHB,USA), GFAP (ImmunoStar, USA), A2B5, O1, O4 (gift, USA) MBP, CNPase and neurofilament (Chemicon, USA) overnight at 4°C. Next day, the cultures were incubated with secondary antibodies as Alexa Fluor 488 (Invitrogen, USA) and Cy3-conjugated Affinipure (Jackson ImmunoResearch, USA) after three washes with 1x PBS. The nuclei were counterstained with Hoechst 33342 (Molecular Probes, USA). Images were then taken through a confocal microscope (Olympus FluoviewTM FV-1000).

4.2.4 Electron Microscopy

Three weeks after co-culture of mESCs derived motor neurons and oligodendrocytes, cultures were fixed with 2% paraformaldehyde/2% glutaraldehyde and then prepared for transmission electron microscopy as previously described [142]. Images were taken on a Hitachi, H-7600 TEM at the Electron Microscope unit.

4.3 Results

4.3.1 Schematics of Differentiation of Motor Neurons and OPCs from mESCs

From EBs, MNs and OPCs were induced separately by adding growth factors as GDNF+BDNF or FGF2+PDGF. After that, MNs proceeded to mature in the culture and pass through the microchannel to the other compartment where oligodendrocytes were fully differentiated from OPCs and ready to co-culture with MNs. Figure 4.1B shows clearly how co-culture of MNs and Oligodendrocytes is achieved in the microfluidic chambers. Cell soma and axons are separated in two compartments, which are connected through an array of microchannels. Only the axons of MNs pass through the microchannels and reach the oligodendrocytes, while the cell soma is blocked.

4.3.2 Differentiation of mESCs into Motor Neurons and Oligodendrocytes

At 5-7 days after GDNF and BDNF treatment, mESC derived EBs differentiated into motor neurons, which was verified through immunofluorescence staining with various motor neuron markers. They are positive stained by anti-Tuj1 (green, Figure 4.2A and 4.2C), anti-HB9 (red, Figure 3.2B) and anti-Islet1 (red, Figure 4.2D).

At 14 days after adding growth factors FGF2 and PDGF to induce oligodendrogenesis, cells were characterized by various markers of oligodendrocytes lineage. In Figure 3.3, most of the cells are positively stained by anti-O1 antibody (Figure 3.3A and 3.3C) belonging to the oligodendrocyte lineage and few cells are immunostained with GFAP (Figure 4.3B and 4.3C).

Different stages of oligodendrogenesis from mESC derived EBs were verified by various markers: bipolar shaped A2B5 positive and multipolar shaped NG2 positive cells for the immature oligodendrocyte progenitor cells (Figure 4.3D and 4.3E), O4 positive cells for the preoligodendrocytes (Figure 4.3F), O1 positive cells for the

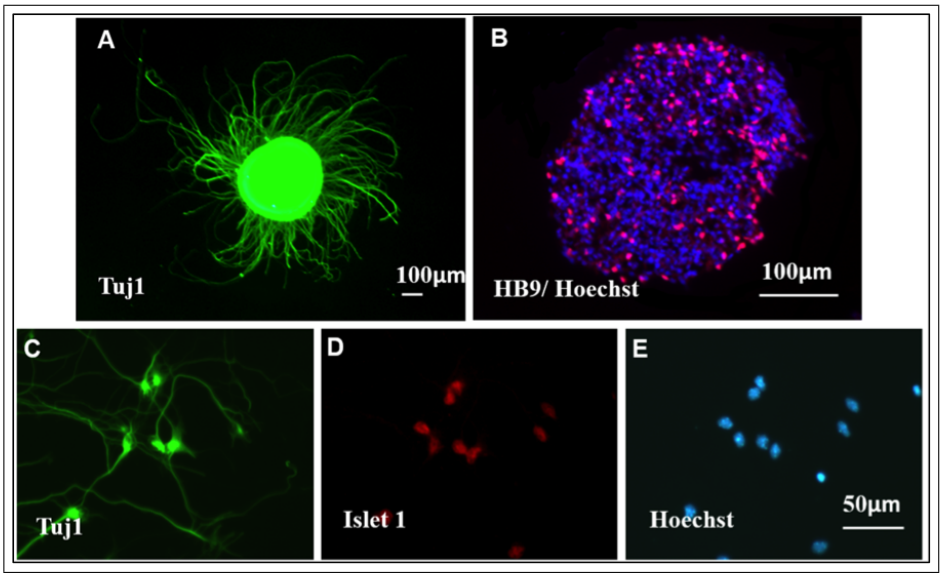

Figure 4.2 Characterization of mESCs derived motor neurons. Immunofluorescence staining for various motor neurons markers: anti-Tuj1 (green), anti-HB9 (red) and anti-Islet-1 (red). Hoechst (blue) was used to identify the nuclei. (Scale bar: 50 μm and 100 μm).

pre-myelinating oligodendrocytes and MBP/CNPase positive cells for the terminally mature oligodendrocytes (Figure 4.3H and 4.3I).

4.3.3 Myelination of axons of motor neurons by oligodendrocytes

Figure 2.4A shows many axons of MNs stretching out from EBs at 7 days after inducing the differentiation in the MN compartment. These axons successfully passed through the microchannels into the oligodendrocyte compartment, while cell bodies were blocked. This compartmentalized chamber separates the axons from cell bodies, which is advantageous for the study of myelination with axons only. After successful establishment of the above MN culture, mESC derived OPCs were placed into the other well. In the Figure 4B, it is observed that processes of MBP+ oligodendrocytes are partially co-localized with the Neurofilament (NF+) axons of MNs (yellow colour) indicating that oligodendrocytes are myelinating the axons to form myelin segments. Further, TEM imaging confirms that these segments are myelin sheaths (Figure 4.4C).

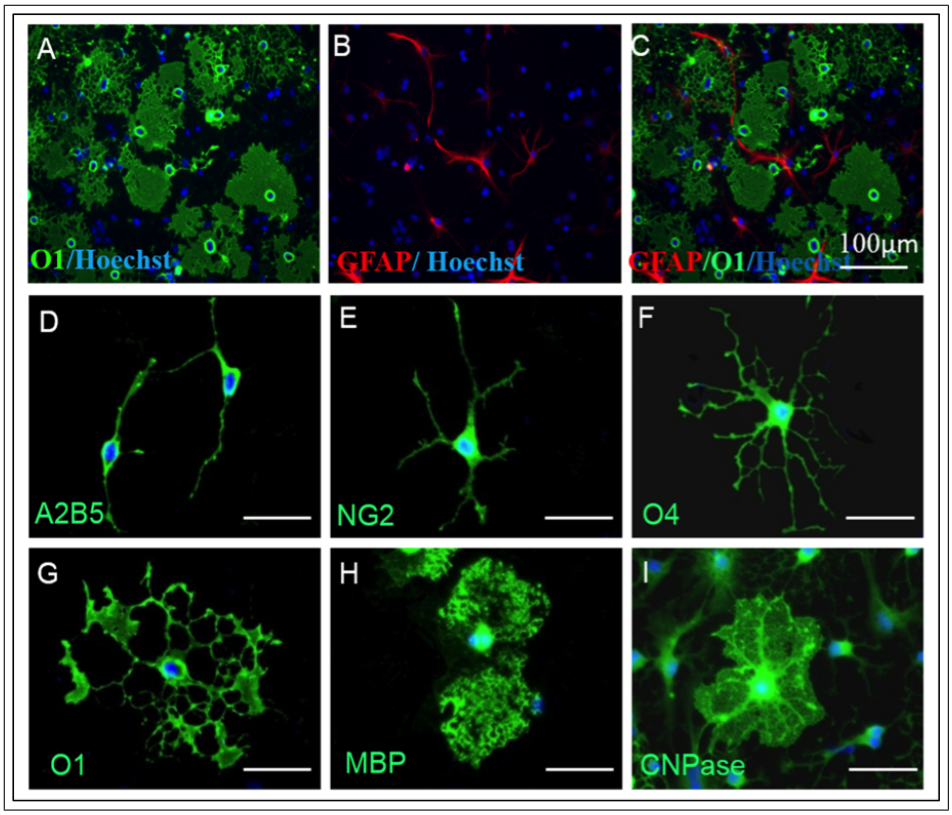

Figure 4.3 Immunofluorescence staining of different markers of oligodendrocyte lineage After 12-14 days of GDNF and BDNF treatment, the cells were stained with anti-O1 (green, A) and anti-GFAP (red, B). Most of the cells are O1+, indicating mESCs are successfully induced to differentiate into oligodendrocytes. Oligodendrogenesis is further confirmed by immunostaining with oligodendrocyte lineage markers like A2B5 (D), NG2 (E), O4 (F), O1 (G), MBP (H) and CNPase (I). All cells are nuclear counterstained with Hoechst (blue). (Scale bar: 100 μm).

4.4 Discussion

In this study, a highly reproducible *in vitro* model for myelination of MNs by oligodendrocytes, both derived from mESCs, is established. This method has some advantages over other techniques. Firstly, mESCs provides a reliable source and large quantities of both dissociated MNs and oligodendrocytes. It is well known that motor neurons are difficult to maintain for extended periods of time in dissociated tissues from mouse/rat spinal cord. As the protocols inducing the differentiation of mESCs into motor neurons are widely established [143, 144], it provides a reproducible method to culture MNs without limitation in cell number. Likewise, the differentiation protocol for mESCs into oligodendrocytes has been well established, so it is also convenient to obtain oligodendrocytes derived from mESCs without limitation in cell number [145, 146].

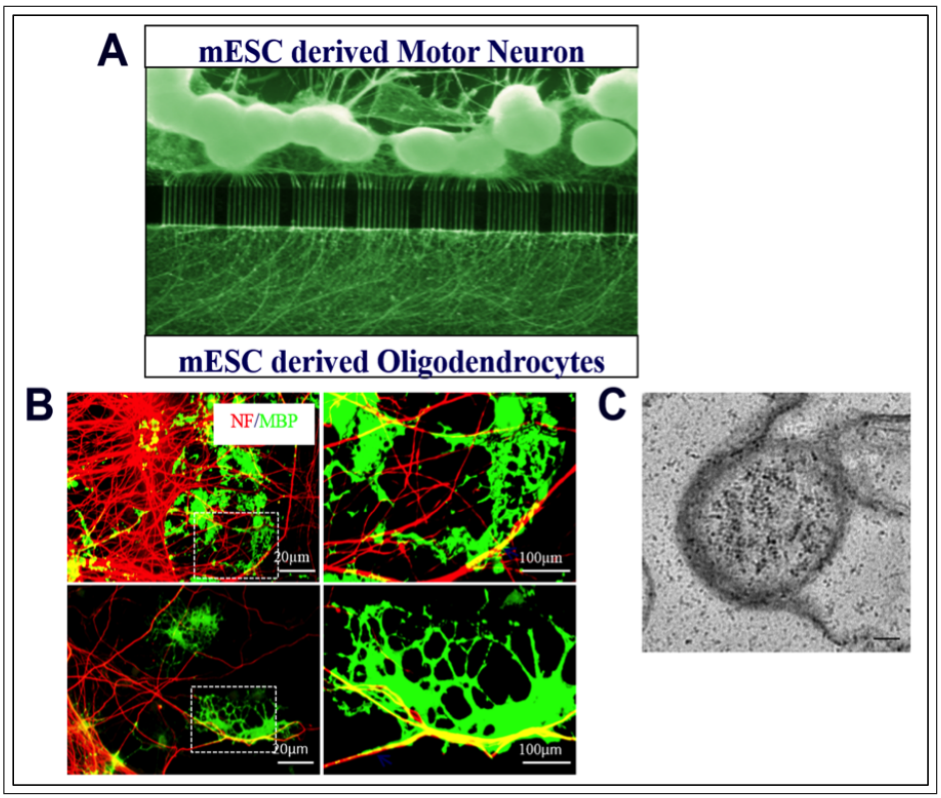

Figure 4.4 Myelination of MN axons by oligodendrocytes (A) Axons from mESCs derived MNs are guided by the microchannels and reach to the oligodendrocyte compartment. (B) Myelin sheaths (yellow colour) are defined as completely overlap between MBP+ oligodendrocyte processes (red) and NF+ axons (green) (Ba and Bc) and higher magnification (Bb and Bd, enlarged image from Ba and Bc in dotted lines). (C) The electron microscope image of a myelinated axon fiber. Multi-layer of myelin (red arrow) around the axon fiber (black arrow) is observed. (Scale bar: 20 μm and 100 μm).

Moreover, an easy but efficient *in vitro* system to study the myelination of stem cell derived motor neurons by oligodendrocytes is described. In the microfluidic platform, two compartments, a soma compartment and an axon/oligodendrocyte compartment are connected by arrays of microchannels separating axons from neuronal soma and dendrites, allowing only the axons to interact with oligodendrocytes. Therefore, this compartmentalized system closely mimics the *in vivo* environment, where axons are myelinated by oligodendrocytes far away from cell bodies. This cannot be accomplished in conventional mixed culture experiments. With this novel culture platform, study of the mechanisms of myelination, such as the effects of growth factors and axon-glia signalling networks, can be easily achieved.

This study may provide some new knowledge useful in ESC therapies. Studies have reported successful transplantation of ESCs into animals and subsequent im-

provement of motor function [140]. However, it is still not clear how to control the proliferation and differentiation of ESCs into the specific cell types and prevent tumor formation. Moreover, the microenvironment around the injury site might not be conducive to the neuronal differentiation of ESCs due to the acute inflammatory condition after injury. The expression of inflammatory cytokines such as TNF-α, IL-1 and IL-6, which are neurotoxic, increase sharply after injury, as reported [147]. It seems to be difficult or impossible to control the environmental signals at the site of implantation. In order to avoid these potential problems, some researchers directly transplanted OPCs into the injury site instead of ESCs and observed enhanced remyelination and recovery of motor function [148]. Since studies have reported that astroglial scar is correlated with the failure of remyelination [149,150], it suggested transplantation of OPCs at the early post-injury period after SCI. However, at the acute phase of injury, macrophages infiltrating from the blood and constitutive microglia are activated and may be toxic to the OPCs. Studies have shown that activated microglia are harmful to OPCs and reduce their survival [151, 152].

Since the final goal of ESC therapy is to form myelinated axon fibers and restore neuronal circuitry in the injury site, one may consider co-transplantation of ESCs derived motor neurons and OPCs. Transplanted motor neurons may replace the lost MNs. Studies have shown that transplanted ESCs derived MNs supported the endogenous neurons survival through secretion of beneficial growth factors in the SCI model [153], spinal muscular atrophy (SMA) and amyotrophic lateral sclerosis (ALS) model [154]. Transplanted OPCs may differentiate into mature oligodendrocytes to myelinate both ESCs derived MNs and constitutive MNs. As shown in this study, ESCs derived oligodendrocytes could myelinate MNs to form myelin around axons. Moreover, ECSs derived OPCs may contribute to functional recovery in SCI through secretion of growth factors [155, 156]. Therefore, it may be beneficial to re-connect the neuron network in the injury center through co-transplantation of MNs and OPCs.

In conclusion, these results have shown that mESCs derived motor neurons can be myelinated by mESCs derived oligodendrocytes in a microfluidic platform. This *in vitro* co-culture system may be helpful for further study of the mechanisms of demyeli-

nation and remyelination that can be used in new ESC based therapies for SCI.

4.5 Summary

Neuronal cell death and demyelination are devastating aspects of neurological diseases, such as multiple sclerosis, and spinal cord injury. Stem cell derived neurons and oligodendrocytes have shown potential as therapeutics for replacement of damaged neurons and remyelination of demyelinated axons in the central nervous system (CNS). However, in some cases, the neurons and axons are damaged so severely that they should be replaced. In this chapter, the hypothesis that stem cell derived oligodendrocytes can myelinate axons of stem cell derived motor neurons in a microfluidic platform, which mimics the isolated *in vivo* environment, is examined. The polydimethylsiloxane (PDMS) microfluidic platform achieves compartmentalization of mouse embryonic stem cells (mESC) derived motor neurons and mESC derived oligodendrocytes, while allowing the axons of the motor neurons to pass through microchannels and reach the oligodendrocytes. It is demonstrated that, axons of mESC derived motor neurons were subjected to myelination by mESC derived oligodendrocytes and it is shown by myelin basic protein immunostaining and electron microscopy. These functioning neuron and oligodendrocyte units may be a very useful tool to study stem cell replacement therapies for nerve injuries where nerve reconstruction would be beneficial.

5. CONCLUSIONS AND FUTURE DIRECTIONS

5.1 Conclusions

The overall objective of this dissertation was to develop *in vitro* compartmentalized microfluidic platforms specifically for peripheral neurons that extend long processes *in vivo* to different microenvironments. The compartmentalized microfluidic platforms allows the differentially manipulation of the cell bodies and axons because they are in physically separated environments and enables elucidation of local mechanisms of axonal degeneration and localized effects of both degenerative and regenerative compounds.

Fluidic isolation in the compartments is examined by characterizing the diffusion profiles of molecules in the device both theoretically and experimentally. A physical axotomy model is created and the regenerative effects of GFLs; the glial cell-line derived nerve growth factor family of ligands are examined post-axotomy. GDNF is found to be the most potent in promoting axon outgrowth and this effect was highest without laminin.

Extending the same design principle, an innovative high throughput compartmentalized microfluidic platform was developed and used to administer an array of drugs concurrently with PTX before the onset of axonal degeneration. Flucinolone Acetonide (FA) is identified *in vitro* and validated *in vivo* that it demonstrates axonal protection from PIPN as well as relieving neuropathic pain. Also it is confirmed with four different cancer cell lines that FA does not interfere with Paclitaxel's antitumor ability.

Stem cell derived neurons are used for replacement of injured neurons but they should be myelinated in order to live and function. In this dissertation, it is demonstrated that motor neurons differentiated from mESCs can be myelinated by oligoden-

drocytes differentiated from mESCs, in a microfluidic platform that also mimics the isolated *in vivo* environment. The myelination is observed through MBP expression and with an electron microscope.

5.2 Potential Use of Compartmentalized Microfluidic Platforms in Reseach

Compartmentalized microfluidic platforms made a significant impact in neurobiological research. The microfluidic devices with different compartments are very promising not only because of their ability of fluidic isolation of cell body and axon, and also photolithography and replicate molding enabled the fabrication of these inexpensive, disposable microfluidic devices made of moldable gels and polymers like PDMS. Furthermore, they facilitate precise control of parameters within the cellular microenvironment and perform highly reproducible analyses.

Compartmentalized microfluidic platforms can be used for the further investigation of local effects of chemicals and factors associated with axonal regeneration in neural cultures as it is demonstrated at Chapter 2, which will contribute to developing growth factor based treatments for promoting sensory axon regeneration. The compartmentalized platforms will help understanding of how cells respond to their local microenvironments and axon specific or cell body specific effects of growth factors necessary for future growth factor-based therapies for enhancing regeneration.

Despite intense research and advances at screening and drug discovery; attempts to find treatments for peripheral neuropathies, are failed due to the inaccurate *in vitro* modeling of neuropathies, which depends on the apoptosis of neurons at the primary screening. However, in many peripheral neuropathies there is no or very little, death of the neuronal cell body. The primary pathology is distal axonal degeneration [157]. HTCMP is an innovative model for *in vitro* assays in drug screening, where distal axonal degeneration can be modeled by manipulating compartments differently. Future

work should be focused on the application of this model of HTCMP to drug screening and identification of therapeutic agents for all neuropathies caused by autoimmune diseases, neuropathies caused by viruses like HIV, alcoholism, chemical warfare victims and especially for diabetic neuropathy. Diabetic neuropathy is the most common form of peripheral neuropathy and becoming an increasing burden where the prevalence of obesity is rising. Unfortunately, there is still no effective treatment for diabetic neuropathy, as in other peripheral neuropathies that all manifests as axonal degeneration of distal sensory fibers, following with a "dying back" pattern of degeneration.

HTCMP will also solve the problem of the deficiency of *in vitro* cell culture methods to understand and explore the underlying mechanisms of distal axonal degeneration. Their compatibility with optical imaging makes them more favorable for understanding neuronal dysfunction and disease better.

Moreover, the *in vivo* tests in Chapter 3 indicated that the antinociceptive effect of FA is very significant at CIPN model of mice and FA alone, so FA should be further studied as a potential painkiller for the symptoms where regular analgesics do not work and also for its potential neuroprotective effect for axonal degenerations other than CIPN. The site of action of FA is found as axonal site but the mechanism of action remains to be further investigated.

It is demonstrated that the axons of mESC derived motor neurons were myelinated by mESC derived oligodendrocytes at compartmentalized microfluidic platforms. This effect should be validated at clinical setting. At future stem cell replacement therapies for nerve injuries, mESC derived oligodendrocytes may be used to support the distal nerve environment by myelinating and replacing the effete denervated Schwann cells which become inadequate for myelination.

5.3 List of publications produced from the thesis

1. Identification of fluocinolone acetonide to prevent paclitaxel induced peripheral neuropathy, A.C. Fışgın, M.G. Joo, P. Xiang, N.V. Thakor, C. Ozturk, A. Hoke, I.H. Yang, *Journal of the Peripheral Nervous System*, Accepted, 2016.

2. Myelination of Motor Neurons Derived from Mouse Embryonic Stem Cells by Oligodendrocytes Derived from Mouse Embryonic Stem Cells in a Microfluidic Compartmentalized Platform., S. Liu, P. Xiang, A.C. Fışgın, V. Belegu, N.V. Thakor, C. Ozturk, A. Hoke, I.H. Yang, *Journal of Stem Cell Research and Therapy*, Vol. 5, 2015.

APPENDIX A. Photolithography

Step	Process	Duration
Degrease and Dehydration Bake	Do a degrease (Acetone, IPA, N2 Dry) followed by 200°C dehydration bake for 10 minutes	~12-13 mins
Cool	Bring down to RT	~10 min
Plasma Treat	200 W, 3 mins exposure for each wafer	~10-15 mins
SU-8 2002	Center wafer, Program (step 1: 500 RPM, Accel: 85, time: 6s step 2: 900 RPM, Accel: 255,time:50s), Apply SU-8 to coat entire wafer, Run Program	~10-15 mins
Soft bake	Hot Plate: RT ramp to 65ºC (1 minute), then ramp to 95ºC (14 min including ramp)	15 mins
Cool	Ramp down to RT slowly	20 min
Exposure	Load bottom mask in aligner, Parameters = Hard Contact, Substrate: 0.50 mm, Resist: 3 µm, Separation: 50 µm, Dose:350 mJ/cm2	~30 min
Post-Expose Bake	Hot Plate: RT ramp to 65ºC (1 minute), then ramp to 95ºC (14 min including ramp), ramp down to RT	~25-30 mins
Develop	Immerse in developer (1-2 min), rinse with IPA, spin dry (2 min), inspect, repeat if necessary	~5 mins
Bake	45°C for 5 mins	5 mins
Plasma Treat	Descum with 300 mTorr, 75 W 20 seconds	20 s
SU-8 3050	Center wafer, Program (1500 RPM, Accel: slow, time: 60s), Pour half-dollar amount of SU-8 onto wafer, Run program	~5-15 mins
Softbake	Hot Plate: RT ramp to 65ºC (1 minute), then ramp to 95ºC (75 min including ramp)	~80 mins
Cool	Bring down to RT slowly and cool	~30 mins
Exposure	Load top mask in aligner, use alignment marks, Parameters = Soft Contact, Substrate: 0.50 mm, Resist: 90 µm, Separation: 250 µm, Dose: 450mJ cm2	~30 mins-120mins
Post-Exposure Bake	Hot Plate: RT ramp to 65ºC (1 minute), then ramp to 95ºC (14 min including ramp)	15 mins
Cool	Ramp down to RT slowly	20 mins
Develop	Immerse in developer (~5 min), sonicate if necessary, rinse with IPA, Spin dry (2 min), inspect	~15 mins
Hard Bake	Hot Plate: RT-->65ºC (1) -->95ºC (4) -->150ºC (overnight)	~12-15 hours
Cool	Bring down to RT slowly and cool	~30 min

Figure A.1 Photolithography steps and processes.

APPENDIX B. Soft Lithography

1. Silane treat master wafer under vacuum.
2. Mix Sylgard 184 (Polydimethylsiloxane (PDMS)) in a ratio of 10:1 base:cross linker for at least 5 minutes, vigorously until well aerated. For microfluidic chambers: 50g base: 5g cross linker.
3. De-gas the aerated mixture in desiccator for 15-20 minutes.
4. Open desiccator to remove remaining bubbles. Repeat degassing if necessary.
5. Pour mixture onto the silicon wafer.
6. Cover and let sit for 5 minutes to remove any bubbles from pouring.
7. Place in oven and bake at 85 C for a minimum of 2 hours.
8. Cool and remove PDMS from wafer/mold.
9. Cut out the PDMS molds into groups that fit into petri dishes by means of a razor blade clean, then punch by dermal biopsy punches to produce the cell culture wells, handle platforms channel side up and maintain this site clean and particle free and plasma bond.

APPENDIX C. Plasma Treatment

1. Ensure devices are clean. Tape clean the devices.
2. Place in sonicator in 100% ethanol, channel side up (the side that will bond to glass up).
3. Set to sonic, time: 5 minutes.
4. Remove from ethanol near hood, place on foil to dry.
5. Tape clean again if necessary or to ensure tight bonding.
6. Open vent to plasma machine and place device channel side up, glass slide (sterile and sonicated in ethanol) inside plasma machine.
7. Close door to plasma chamber, close vent, turn on vacuum pump and pressure gauge, and ensure that oxygen tank is open and let pressure come down to below 150 mTorr.
8. Slowly open gas valve to increase pressure to around 500 mTorr and turn on plasma, and switch power to high.
9. Check that plasma light is purple in color (reflects energy level of plasma). Adjust pressure if necessary set timer to 1 minute and 25 seconds.
10. Work quickly once exposed to atmosphere, flip device over and attach onto exposed side of glass substrate, press to bond.
11. Bake 20 minutes to ensure strong bonding the autoclave prior to surface treatment.

APPENDIX D. Surface Treatment of CMPs for DRG Cultures

1. Dilute Poly-D-Lysine (PDL) to 1 mg/mL stock solution in ultra pure water. Freeze unused PDL in 1 mL aliquots.
2. Dilute solution further to 100 μg/mL to obtain working concentration.
3. Apply 100% ethanol to one side of device, let flow through channel and enter other compartment of device. Since ethanol has lower surface tension than water, this will prevent trapping of air bubbles in the channels. The channels should be controlled with microscope, to ascertain that there is no air bubbles left.
4. Do a minimum of 3 washes with water (alternating sides) to ensure removal of ethanol.
5. Apply either PLL or PDL to one side of device, keeping one side of device slightly elevated to encourage flow.
6. Apply either PLL or PDL to one side of device, keeping one side of device slightly elevated to encourage flow.
7. Let solution flow through channels and coat overnight at 4 C.
8. Remove solution and replace with laminin in PBS (or ultra pure water) at a concentration of 10 μg/mL.
9. Let coat at least 4 hours in incubator preferably overnight.
10. Remove laminin, wash 3x (alternating sides) with drg media.

APPENDIX E. E15 Embryo Isolation and DRG Dissection Procedure

1. Sterilize all dissection instruments by immersing in a jar of 70% ethanol in a tissue culture hood for at least 20 min before using. Leave fine dissection tools (for embryo dissection) in ethanol in the tissue culture hood. Pour approximately 10 ml L-15 media into 3 sterile 100-mm polystyrene petri plates and leave closed in the hood.

2. Working in the hood, anaesthetize pregnant rat by isofluorene.

3. Place rat belly-up on blue diaper and soak abdomen with 70% ethanol to wet fur.

4. With toothed forceps, hold abdominal skin up, and, with large scissors, cut through skin and muscle of abdomen in an upside-down T, with the perpendicular cuts intersecting in the lower abdomen. Be careful not to introduce contamination.

5. Take hold of one horn of the bilateral uterine horns containing the embryos. Lift up with the forceps and cut connective tissue free, creating one long chain of approximately 10 to 15 embryos.

6. Place embryo chain into an empty sterile 100-mm polystyrene petri plate and take to the tissue culture hood. Leave used instruments in dissecting area.

7. Working under a dissecting microscope at a magnification of approximately 1.5X, pick up one end of the embryo chain with the small toothed forceps and use small scissors to cut through the uterine lining so that the amniotic sac containing each embryo protrudes. Try not to pierce the amniotic sac.

8. Cut each sac away from the placenta and let each embryo drop into one of the sterile plates L-15. (Leibovitz L15 Medium is best maintaining the pH at atmospheric conditions). Remove the dirty plate and used instruments from the hood.

9. Using sharp forceps, pinch apart the embryos under the arms or at the waist and place the bottom half into the next plate. Remove used plate and forceps from hood.

10. Use forceps to pinch off and remove legs, tail, and gut, leaving a vertebral column with skin, cartilage, and muscle While doing this, pile up the vertebral column parts on one side of the plate, and the discarded tissues on the other side of the plate.

11. Using ultrafine forceps, pinch away the dorsal attachment, and then draw the DRG away from the neural tube. Place the DRGs in a pile in a clean part of the same plate. Check the DRG pile and remove any extraneous tissues.

REFERENCES

1. Ordovas-Montanes, J., S. Rakoff-Nahoum, S. Huang, L. Riol-Blanco, O. Barreiro, and U. H. von Andrian, "The regulation of immunological processes by peripheral neurons in homeostasis and disease," *Trends Immunol*, Vol. 36, no. 10, pp. 578–604, 2015.

2. Seemann, R., M. Brinkmann, T. Pfohl, and S. Herminghaus, "Droplet based microfluidics," *Rep Prog Phys*, Vol. 75, no. 1, p. 016601, 2012.

3. Park, J. W., B. Vahidi, A. M. Taylor, S. W. Rhee, and N. L. Jeon, "Microfluidic culture platform for neuroscience research," *Nat Protoc*, Vol. 1, no. 4, pp. 2128–36, 2006.

4. Chen, Z. L., W. M. Yu, and S. Strickland, "Peripheral regeneration," *Annu Rev Neurosci*, Vol. 30, pp. 209–33, 2007.

5. Taylor, A. M., M. Blurton-Jones, S. W. Rhee, D. H. Cribbs, C. W. Cotman, and N. L. Jeon, "A microfluidic culture platform for cns axonal injury, regeneration and transport," *Nat Methods*, Vol. 2, no. 8, pp. 599–605, 2005.

6. Park, J. W., H. J. Kim, J. H. Byun, H. R. Ryu, and N. L. Jeon, "Novel microfluidic platform for culturing neurons: culturing and biochemical analysis of neuronal components," *Biotechnol J*, Vol. 4, no. 11, pp. 1573–7, 2009.

7. Ivins, K. J., E. T. Bui, and C. W. Cotman, "Beta-amyloid induces local neurite degeneration in cultured hippocampal neurons: evidence for neuritic apoptosis," *Neurobiol Dis*, Vol. 5, no. 5, pp. 365–78, 1998.

8. Yang, I. H., R. Siddique, S. Hosmane, N. Thakor, and A. Hoke, "Compartmentalized microfluidic culture platform to study mechanism of paclitaxel-induced axonal degeneration," *Exp Neurol*, Vol. 218, no. 1, pp. 124–8, 2009.

9. Taylor, A. M., S. W. Rhee, and N. L. Jeon, "Microfluidic chambers for cell migration and neuroscience research," *Methods Mol Biol*, Vol. 321, pp. 167–77, 2006.

10. Li, N., A. Tourovskaia, and A. Folch, "Biology on a chip: microfabrication for studying the behavior of cultured cells," *Crit Rev Biomed Eng*, Vol. 31, no. 5-6, pp. 423–88, 2003.

11. Hoke, A., "Animal models of peripheral neuropathies," *Neurotherapeutics*, Vol. 9, no. 2, pp. 262–9, 2012.

12. Zeng, H. C., Y. C. Ho, S. T. Chen, H. I. Wu, H. W. Tung, W. L. Fang, and Y. C. Chang, "Studying the formation of large cell aggregates in patterned neuronal cultures," *J Neurosci Methods*, Vol. 165, no. 1, pp. 72–82, 2007.

13. Boucher, T. J., K. Okuse, D. L. Bennett, J. B. Munson, J. N. Wood, and S. B. McMahon, "Potent analgesic effects of gdnf in neuropathic pain states," *Science*, Vol. 290, no. 5489, pp. 124–7, 2000.

14. Kordower, J. H., M. E. Emborg, J. Bloch, S. Y. Ma, Y. Chu, L. Leventhal, J. McBride, E. Y. Chen, S. Palfi, B. Z. Roitberg, W. D. Brown, J. E. Holden, R. Pyzalski, M. D. Taylor, P. Carvey, Z. Ling, D. Trono, P. Hantraye, N. Deglon, and P. Aebischer, "Neurodegeneration prevented by lentiviral vector delivery of gdnf in primate models of parkinson's disease," *Science*, Vol. 290, no. 5492, pp. 767–73, 2000.

15. Meng, X., M. Lindahl, M. E. Hyvonen, M. Parvinen, D. G. de Rooij, M. W. Hess, A. Raatikainen-Ahokas, K. Sainio, H. Rauvala, M. Lakso, J. G. Pichel, H. Westphal, M. Saarma, and H. Sariola, "Regulation of cell fate decision of undifferentiated spermatogonia by gdnf," *Science*, Vol. 287, no. 5457, pp. 1489–93, 2000.

16. Zhou, F. Q., J. Zhong, and W. D. Snider, "Extracellular crosstalk: when gdnf meets n-cam," *Cell*, Vol. 113, no. 7, pp. 814–5, 2003.

17. Vrieseling, E., and S. Arber, "Target-induced transcriptional control of dendritic patterning and connectivity in motor neurons by the ets gene pea3," *Cell*, Vol. 127, no. 7, pp. 1439–52, 2006.

18. Zhou, R., S. Niwa, N. Homma, Y. Takei, and N. Hirokawa, "Kif26a is an unconventional kinesin and regulates gdnf-ret signaling in enteric neuronal development," *Cell*, Vol. 139, no. 4, pp. 802–13, 2009.

19. Mount, H. T., D. O. Dean, J. Alberch, C. F. Dreyfus, and I. B. Black, "Glial cell line-derived neurotrophic factor promotes the survival and morphologic differentiation of purkinje cells," *Proc Natl Acad Sci U S A*, Vol. 92, no. 20, pp. 9092–6, 1995.

20. Zurn, A. D., L. Winkel, A. Menoud, K. Djabali, and P. Aebischer, "Combined effects of gdnf, bdnf, and cntf on motoneuron differentiation in vitro," *J Neurosci Res*, Vol. 44, no. 2, pp. 133–41, 1996.

21. Perrier, J. F., J. Noraberg, M. Simon, and J. Hounsgaard, "Dedifferentiation of intrinsic response properties of motoneurons in organotypic cultures of the spinal cord of the adult turtle," *Eur J Neurosci*, Vol. 12, no. 7, pp. 2397–404, 2000.

22. Ernsberger, U., "The role of gdnf family ligand signalling in the differentiation of sympathetic and dorsal root ganglion neurons," *Cell Tissue Res*, Vol. 333, no. 3, pp. 353–71, 2008.

23. Barati, S., P. R. Hurtado, S. H. Zhang, R. Tinsley, I. A. Ferguson, and R. A. Rush, "Gdnf gene delivery via the p75(ntr) receptor rescues injured motor neurons," *Exp Neurol*, Vol. 202, no. 1, pp. 179–88, 2006.

24. Gordon, T., "The role of neurotrophic factors in nerve regeneration," *Neurosurg Focus*, Vol. 26, no. 2, p. E3, 2009.

25. Andereggen, L., M. Meyer, R. Guzman, A. D. Ducray, and H. R. Widmer, "Effects of gdnf pretreatment on function and survival of transplanted fetal ventral mesencephalic cells in the 6-ohda rat model of parkinson's disease," *Brain Res*, Vol. 1276, pp. 39–49, 2009.

26. Piltonen, M., M. M. Bespalov, D. Ervasti, T. Matilainen, Y. A. Sidorova, H. Rauvala, M. Saarma, and P. T. Mannisto, "Heparin-binding determinants of gdnf reduce its tissue distribution but are beneficial for the protection of nigral dopaminergic neurons," *Exp Neurol*, Vol. 219, no. 2, pp. 499–506, 2009.

27. Narantuya, D., A. Nagai, A. M. Sheikh, J. Masuda, S. Kobayashi, S. Yamaguchi, and S. U. Kim, "Human microglia transplanted in rat focal ischemia brain induce neuroprotection and behavioral improvement," *PLoS One*, Vol. 5, no. 7, p. e11746, 2010.

28. Hoke, A., T. Ho, T. O. Crawford, C. LeBel, D. Hilt, and J. W. Griffin, "Glial cell line-derived neurotrophic factor alters axon schwann cell units and promotes myelination in unmyelinated nerve fibers," *J Neurosci*, Vol. 23, no. 2, pp. 561–7, 2003.

29. Liu, G. S., J. Y. Shi, C. L. Lai, Y. R. Hong, S. J. Shin, H. T. Huang, H. C. Lam, Z. H. Wen, K. S. Hsu, C. H. Chen, S. L. Howng, and M. H. Tai, "Peripheral gene transfer of glial cell-derived neurotrophic factor ameliorates neuropathic deficits in diabetic rats," *Hum Gene Ther*, Vol. 20, no. 7, pp. 715–27, 2009.

30. Zhang, L., Z. Ma, G. M. Smith, X. Wen, Y. Pressman, P. M. Wood, and X. M. Xu, "Gdnf-enhanced axonal regeneration and myelination following spinal cord injury is mediated by primary effects on neurons," *Glia*, Vol. 57, no. 11, pp. 1178–91, 2009.

31. Kaspar, B. K., J. Llado, N. Sherkat, J. D. Rothstein, and F. H. Gage, "Retrograde viral delivery of igf-1 prolongs survival in a mouse als model," *Science*, Vol. 301, no. 5634, pp. 839–42, 2003.

32. Guillot, S., M. Azzouz, N. Deglon, A. Zurn, and P. Aebischer, "Local gdnf expression mediated by lentiviral vector protects facial nerve motoneurons but not spinal motoneurons in sod1(g93a) transgenic mice," *Neurobiol Dis*, Vol. 16, no. 1, pp. 139–49, 2004.

33. Yamasaki, R., M. Tanaka, M. Fukunaga, T. Tateishi, H. Kikuchi, K. Motomura, T. Matsushita, Y. Ohyagi, and J. Kira, "Restoration of microglial function by granulocyte-colony stimulating factor in als model mice," *J Neuroimmunol*, Vol. 229, no. 1-2, pp. 51–62, 2010.

34. Lin, L. F., D. H. Doherty, J. D. Lile, S. Bektesh, and F. Collins, "Gdnf: a glial cell line-derived neurotrophic factor for midbrain dopaminergic neurons," *Science*, Vol. 260, no. 5111, pp. 1130–2, 1993.

35. Tomac, A., J. Widenfalk, L. F. Lin, T. Kohno, T. Ebendal, B. J. Hoffer, and L. Olson, "Retrograde axonal transport of glial cell line-derived neurotrophic factor in the adult nigrostriatal system suggests a trophic role in the adult," *Proc Natl Acad Sci U S A*, Vol. 92, no. 18, pp. 8274–8, 1995.

36. Liu, W. G., G. Q. Lu, B. Li, and S. D. Chen, "Dopaminergic neuroprotection by neurturin-expressing c17.2 neural stem cells in a rat model of parkinson's disease," *Parkinsonism Relat Disord*, Vol. 13, no. 2, pp. 77–88, 2007.

37. Ramaswamy, S., J. L. McBride, C. D. Herzog, E. Brandon, M. Gasmi, R. T. Bartus, and J. H. Kordower, "Neurturin gene therapy improves motor function and prevents death of striatal neurons in a 3-nitropropionic acid rat model of huntington's disease," *Neurobiol Dis*, Vol. 26, no. 2, pp. 375–84, 2007.

38. Evans, J. R., and R. A. Barker, "Neurotrophic factors as a therapeutic target for parkinson's disease," *Expert Opin Ther Targets*, Vol. 12, no. 4, pp. 437–47, 2008.

39. Gardell, L. R., R. Wang, C. Ehrenfels, M. H. Ossipov, A. J. Rossomando, S. Miller, C. Buckley, A. K. Cai, A. Tse, S. F. Foley, B. Gong, L. Walus, P. Carmillo, D. Worley, C. Huang, T. Engber, B. Pepinsky, R. L. Cate, T. W. Vanderah, J. Lai, D. W. Sah, and F. Porreca, "Multiple actions of systemic artemin in experimental neuropathy," *Nat Med*, Vol. 9, no. 11, pp. 1383–9, 2003.

40. Sah, D. W., M. H. Ossipov, A. Rossomando, L. Silvian, and F. Porreca, "New approaches for the treatment of pain: the gdnf family of neurotrophic growth factors," *Curr Top Med Chem*, Vol. 5, no. 6, pp. 577–83, 2005.

41. Schmutzler, B. S., S. Roy, and C. M. Hingtgen, "Glial cell line-derived neurotrophic factor family ligands enhance capsaicin-stimulated release of calcitonin gene-related peptide from sensory neurons," *Neuroscience*, Vol. 161, no. 1, pp. 148–56, 2009.

42. Tomac, A. C., A. D. Agulnick, N. Haughey, C. F. Chang, Y. Zhang, C. Backman, M. Morales, M. P. Mattson, Y. Wang, H. Westphal, and B. J. Hoffer, "Effects of cerebral ischemia in mice deficient in persephin," *Proc Natl Acad Sci U S A*, Vol. 99, no. 14, pp. 9521–6, 2002.

43. Arvidsson, A., Z. Kokaia, M. S. Airaksinen, M. Saarma, and O. Lindvall, "Stroke induces widespread changes of gene expression for glial cell line-derived neurotrophic factor family receptors in the adult rat brain," *Neuroscience*, Vol. 106, no. 1, pp. 27–41, 2001.

44. Kilinc, D., J. M. Peyrin, V. Soubeyre, S. Magnifico, L. Saias, J. L. Viovy, and B. Brugg, "Wallerian-like degeneration of central neurons after synchronized and geometrically registered mass axotomy in a three-compartmental microfluidic chip," *Neurotox Res*, Vol. 19, no. 1, pp. 149–61, 2011.

45. Lonka-Nevalaita, L., M. Lume, S. Leppanen, E. Jokitalo, J. Peranen, and M. Saarma, "Characterization of the intracellular localization, processing, and secretion of two glial cell line-derived neurotrophic factor splice isoforms," *J Neurosci*, Vol. 30, no. 34, pp. 11403–13, 2010.

46. Li, J., C. Klein, C. Liang, R. Rauch, K. Kawamura, and A. J. Hsueh, "Autocrine regulation of early embryonic development by the artemin-gfra3 (gdnf family receptor-alpha 3) signaling system in mice," *FEBS Lett*, Vol. 583, no. 15, pp. 2479–85, 2009.

47. Moriyoshi, K., L. J. Richards, C. Akazawa, D. D. O'Leary, and S. Nakanishi, "Labeling neural cells using adenoviral gene transfer of membrane-targeted gfp," *Neuron*, Vol. 16, no. 2, pp. 255–60, 1996.

48. Hosmane, S., I. H. Yang, A. Ruffin, N. Thakor, and A. Venkatesan, "Circular compartmentalized microfluidic platform: Study of axon-glia interactions," *Lab Chip*, Vol. 10, no. 6, pp. 741–7, 2010.

49. Cui, Q., "Actions of neurotrophic factors and their signaling pathways in neuronal survival and axonal regeneration," *Mol Neurobiol*, Vol. 33, no. 2, pp. 155–79, 2006.

50. Abe, N., and V. Cavalli, "Nerve injury signaling," *Curr Opin Neurobiol*, Vol. 18, no. 3, pp. 276–83, 2008.

51. Ben-Yaakov, K., and M. Fainzilber, "Retrograde injury signaling in lesioned axons," *Results Probl Cell Differ*, Vol. 48, pp. 327–38, 2009.

52. Mills, C. D., A. J. Allchorne, R. S. Griffin, C. J. Woolf, and M. Costigan, "Gdnf selectively promotes regeneration of injury-primed sensory neurons in the lesioned spinal cord," *Mol Cell Neurosci*, Vol. 36, no. 2, pp. 185–94, 2007.

53. Hoke, A., C. Cheng, and D. W. Zochodne, "Expression of glial cell line-derived neurotrophic factor family of growth factors in peripheral nerve injury in rats," *Neuroreport*, Vol. 11, no. 8, pp. 1651–4, 2000.

54. Tsui, C. C., and B. A. Pierchala, "The differential axonal degradation of ret accounts for cell-type-specific function of glial cell line-derived neurotrophic factor as a retrograde survival factor," *J Neurosci*, Vol. 30, no. 15, pp. 5149–58, 2010.

55. Coulpier, M., and C. F. Ibanez, "Retrograde propagation of gdnf-mediated signals in sympathetic neurons," *Mol Cell Neurosci*, Vol. 27, no. 2, pp. 132–9, 2004.

56. Tucker, B. A., M. Rahimtula, and K. M. Mearow, "Laminin and growth factor receptor activation stimulates differential growth responses in subpopulations of adult drg neurons," *Eur J Neurosci*, Vol. 24, no. 3, pp. 676–90, 2006.

57. Plantman, S., M. Patarroyo, K. Fried, A. Domogatskaya, K. Tryggvason, H. Hammarberg, and S. Cullheim, "Integrin-laminin interactions controlling neurite outgrowth from adult drg neurons in vitro," *Mol Cell Neurosci*, Vol. 39, no. 1, pp. 50–62, 2008.

58. Madduri, S., M. Papaloizos, and B. Gander, "Synergistic effect of gdnf and ngf on axonal branching and elongation in vitro," *Neurosci Res*, Vol. 65, no. 1, pp. 88–97, 2009.

59. Airaksinen, M. S., and M. Saarma, "The gdnf family: signalling, biological functions and therapeutic value," *Nat Rev Neurosci*, Vol. 3, no. 5, pp. 383–94, 2002.

60. Vyas, A., Z. Li, M. Aspalter, J. Feiner, A. Hoke, C. Zhou, A. O'Daly, M. Abdullah, C. Rohde, and T. M. Brushart, "An in vitro model of adult mammalian nerve repair," *Exp Neurol*, Vol. 223, no. 1, pp. 112–8, 2010.

61. Pike, C. T., H. G. Birnbaum, C. E. Muehlenbein, G. M. Pohl, and R. B. Natale, "Healthcare costs and workloss burden of patients with chemotherapy-associated peripheral neuropathy in breast, ovarian, head and neck, and nonsmall cell lung cancer," *Chemother Res Pract*, Vol. 2012, p. 913848, 2012.

62. Pachman, D. R., D. L. Barton, J. C. Watson, and C. L. Loprinzi, "Chemotherapy-induced peripheral neuropathy: prevention and treatment," *Clin Pharmacol Ther*, Vol. 90, no. 3, pp. 377–87, 2011.

63. Windebank, A. J., and W. Grisold, "Chemotherapy-induced neuropathy," *J Peripher Nerv Syst*, Vol. 13, no. 1, pp. 27–46, 2008.

64. Argyriou, A. A., J. Bruna, P. Marmiroli, and G. Cavaletti, "Chemotherapy-induced peripheral neurotoxicity (cipn): an update," *Crit Rev Oncol Hematol*, Vol. 82, no. 1, pp. 51–77, 2012.

65. Cavaletti, G., and P. Marmiroli, "Chemotherapy-induced peripheral neurotoxicity," *Nat Rev Neurol*, Vol. 6, no. 12, pp. 657–66, 2010.

66. Crown, J., M. O'Leary, and W. S. Ooi, "Docetaxel and paclitaxel in the treatment of breast cancer: a review of clinical experience," *Oncologist*, Vol. 9 Suppl 2, pp. 24–32, 2004.

67. Bookman, M. A., "Developmental chemotherapy and management of recurrent ovarian cancer," *J Clin Oncol*, Vol. 21, no. 10 Suppl, pp. 149s–167s, 2003.

68. Greco, F. A., r. H A Burris, and J. D. Hainsworth, "Gemcitabine, paclitaxel, and carboplatin for advanced non-small-cell lung cancer," *Oncology (Williston Park)*, Vol. 14, no. 7 Suppl 4, pp. 31–4, 2000.

69. Okano, J., T. Nagahara, K. Matsumoto, and Y. Murawaki, "The growth inhibition of liver cancer cells by paclitaxel and the involvement of extracellular signal-regulated kinase and apoptosis," *Oncol Rep*, Vol. 17, no. 5, pp. 1195–200, 2007.

70. Myrick, D., D. Blackinton, J. Klostergaard, N. Kouttab, A. Maizel, H. Wanebo, and S. Mehta, "Paclitaxel-induced apoptosis in jurkat, a leukemic t cell line, is enhanced by ceramide," *Leuk Res*, Vol. 23, no. 6, pp. 569–78, 1999.

71. Arnal, I., and R. H. Wade, "How does taxol stabilize microtubules?," *Curr Biol*, Vol. 5, no. 8, pp. 900–8, 1995.

72. Milross, C. G., K. A. Mason, N. R. Hunter, W. K. Chung, L. J. Peters, and L. Milas, "Relationship of mitotic arrest and apoptosis to antitumor effect of paclitaxel," *J Natl Cancer Inst*, Vol. 88, no. 18, pp. 1308–14, 1996.

73. Cavaletti, G., E. Cavalletti, P. Montaguti, N. Oggioni, O. D. Negri, and G. Tredici, "Effect on the peripheral nervous system of the short-term intravenous administration of paclitaxel in the rat," *Neurotoxicology*, Vol. 18, no. 1, pp. 137–45, 1997.

74. LaPointe, N. E., G. Morfini, S. T. Brady, S. C. Feinstein, L. Wilson, and M. A. Jordan, "Effects of eribulin, vincristine, paclitaxel and ixabepilone on fast axonal transport and kinesin-1 driven microtubule gliding: implications for chemotherapy-induced peripheral neuropathy," *Neurotoxicology*, Vol. 37, pp. 231–9, 2013.

75. Morfini, G. A., M. Burns, L. I. Binder, N. M. Kanaan, N. LaPointe, D. A. Bosco, J. R H Brown, H. Brown, A. Tiwari, L. Hayward, J. Edgar, K. A. Nave, J. Garberrn, Y. Atagi, Y. Song, G. Pigino, and S. T. Brady, "Axonal transport defects in neurodegenerative diseases," *J Neurosci*, Vol. 29, no. 41, pp. 12776–86, 2009.

76. Ohsumi, S., and Y. Sunada, "Techniques for the neurological examination of taxane-induced neuropathy," *Breast Cancer*, Vol. 11, no. 1, pp. 86–91, 2004.

77. Jaggi, A. S., and N. Singh, "Mechanisms in cancer-chemotherapeutic drugs-induced peripheral neuropathy," *Toxicology*, Vol. 291, no. 1-3, pp. 1–9, 2012.

78. Xiao, W. H., H. Zheng, F. Y. Zheng, R. Nuydens, T. F. Meert, and G. J. Bennett, "Mitochondrial abnormality in sensory, but not motor, axons in paclitaxel-evoked painful peripheral neuropathy in the rat," *Neuroscience*, Vol. 199, pp. 461–9, 2011.

79. Miltenburg, N. C., and W. Boogerd, "Chemotherapy-induced neuropathy: A comprehensive survey," *Cancer Treat Rev*, Vol. 40, no. 7, pp. 872–82, 2014.

80. Melli, G., and A. Hoke, "Dorsal root ganglia sensory neuronal cultures: a tool for drug discovery for peripheral neuropathies," *Expert Opin Drug Discov*, Vol. 4, no. 10, pp. 1035–1045, 2009.

81. Windebank, A. J., A. G. Smith, and J. W. Russell, "The effect of nerve growth factor, ciliary neurotrophic factor, and acth analogs on cisplatin neurotoxicity in vitro," *Neurology*, Vol. 44, no. 3 Pt 1, pp. 488–94, 1994.

82. Jaggi, A. S., V. Jain, and N. Singh, "Animal models of neuropathic pain," *Fundam Clin Pharmacol*, Vol. 25, no. 1, pp. 1–28, 2011.

83. Authier, N., D. Balayssac, F. Marchand, B. Ling, A. Zangarelli, J. Descoeur, F. Coudore, E. Bourinet, and A. Eschalier, "Animal models of chemotherapy-evoked painful peripheral neuropathies," *Neurotherapeutics*, Vol. 6, no. 4, pp. 620–9, 2009.

84. Ward, S. J., S. D. McAllister, R. Kawamura, R. Murase, H. Neelakantan, and E. A. Walker, "Cannabidiol inhibits paclitaxel-induced neuropathic pain through 5-ht(1a) receptors without diminishing nervous system function or chemotherapy efficacy," *Br J Pharmacol*, Vol. 171, no. 3, pp. 636–45, 2014.

85. Zhu, J., W. Chen, R. Mi, C. Zhou, N. Reed, and A. Hoke, "Ethoxyquin prevents chemotherapy-induced neurotoxicity via hsp90 modulation," *Ann Neurol*, Vol. 74, no. 6, pp. 893–904, 2013.

86. Lauria, G., D. R. Cornblath, O. Johansson, J. C. McArthur, S. I. Mellgren, M. Nolano, N. Rosenberg, C. Sommer, and S. E. F. of Neurological, "Efns guidelines on the use of skin biopsy in the diagnosis of peripheral neuropathy," *Eur J Neurol*, Vol. 12, no. 10, pp. 747–58, 2005.

87. Nolano, M., D. A. Simone, G. Wendelschafer-Crabb, T. Johnson, E. Hazen, and W. R. Kennedy, "Topical capsaicin in humans: parallel loss of epidermal nerve fibers and pain sensation," *Pain*, Vol. 81, no. 1-2, pp. 135–45, 1999.

88. Boyette-Davis, J., W. Xin, H. Zhang, and P. M. Dougherty, "Intraepidermal nerve fiber loss corresponds to the development of taxol-induced hyperalgesia and can be prevented by treatment with minocycline," *Pain*, Vol. 152, no. 2, pp. 308–13, 2011.

89. Siau, C., W. Xiao, and G. J. Bennett, "Paclitaxel- and vincristine-evoked painful peripheral neuropathies: loss of epidermal innervation and activation of langerhans cells," *Exp Neurol*, Vol. 201, no. 2, pp. 507–14, 2006.

90. Wu, G., M. Ringkamp, B. B. Murinson, E. M. Pogatzki, T. V. Hartke, H. M. Weerahandi, J. N. Campbell, J. W. Griffin, and R. A. Meyer, "Degeneration of myelinated efferent fibers induces spontaneous activity in uninjured c-fiber afferents," *J Neurosci*, Vol. 22, no. 17, pp. 7746–53, 2002.

91. Scuteri, A., G. Nicolini, M. Miloso, M. Bossi, G. Cavaletti, A. J. Windebank, and G. Tredici, "Paclitaxel toxicity in post-mitotic dorsal root ganglion (drg) cells," *Anticancer Res*, Vol. 26, no. 2A, pp. 1065–70, 2006.

92. Slotkin, T. A., and J. Bartolome, "Role of ornithine decarboxylase and the polyamines in nervous system development: a review," *Brain Res Bull*, Vol. 17, no. 3, pp. 307–20, 1986.

93. Gilad, V. H., W. G. Tetzlaff, J. M. Rabey, and G. M. Gilad, "Accelerated recovery following polyamines and aminoguanidine treatment after facial nerve injury in rats," *Brain Res*, Vol. 724, no. 1, pp. 141–4, 1996.

94. Dornay, M., V. H. Gilad, I. Shiler, and G. M. Gilad, "Early polyamine treatment accelerates regeneration of rat sympathetic neurons," *Exp Neurol*, Vol. 92, no. 3, pp. 665–74, 1986.

95. Gilad, G. M., and V. H. Gilad, "Early polyamine treatment enhances survival of sympathetic neurons after postnatal axonal injury or immunosympathectomy," *Brain Res*, Vol. 466, no. 2, pp. 175–81, 1988.

96. Chu, P. J., H. Saito, and K. Abe, "Polyamines promote neurite elongation of cultured rat hippocampal neurons," *Neurosci Res*, Vol. 19, no. 2, pp. 155–60, 1994.

97. Chu, P. J., H. Saito, and K. Abe, "Polyamines promote regeneration of injured axons of cultured rat hippocampal neurons," *Brain Res*, Vol. 673, no. 2, pp. 233–41, 1995.

98. Makwana, M., and G. Raivich, "Molecular mechanisms in successful peripheral regeneration," *FEBS J*, Vol. 272, no. 11, pp. 2628–38, 2005.

99. Schwartz, M., S. Kohsaka, and B. W. Agranoff, "Ornithine decarboxylase activity in retinal explants of goldfish undergoing optic nerve regeneration," *Brain Res*, Vol. 227, no. 3, pp. 403–13, 1981.

100. Tetzlaff, W., V. H. Gilad, C. Leonard, M. A. Bisby, and G. M. Gilad, "Retrograde changes in transglutaminase activity after peripheral nerve injuries," *Brain Res*, Vol. 445, no. 1, pp. 142–6, 1988.

101. Sebille, A., and M. Bondoux-Jahan, "Motor function recovery after axotomy: enhancement by cyclophosphamide and spermine in rat," *Exp Neurol*, Vol. 70, no. 3, pp. 507–15, 1980.

102. Schreiber, R. C., K. L. Boeshore, G. Laube, R. W. Veh, and R. E. Zigmond, "Polyamines increase in sympathetic neurons and non-neuronal cells after axotomy and enhance neurite outgrowth in nerve growth factor-primed pc12 cells," *Neuroscience*, Vol. 128, no. 4, pp. 741–9, 2004.

103. Oble, D. A., L. Burton, K. Maxwell, T. Hassard, and E. J. Nathaniel, "A comparison of thyroxine- and polyamine-mediated enhancement of rat facial nerve regeneration," *Exp Neurol*, Vol. 189, no. 1, pp. 105–11, 2004.

104. Melli, G., C. Jack, G. L. Lambrinos, M. Ringkamp, and A. Hoke, "Erythropoietin protects sensory axons against paclitaxel-induced distal degeneration," *Neurobiol Dis*, Vol. 24, no. 3, pp. 525–30, 2006.

105. Hargreaves, K., R. Dubner, F. Brown, C. Flores, and J. Joris, "A new and sensitive method for measuring thermal nociception in cutaneous hyperalgesia," *Pain*, Vol. 32, no. 1, pp. 77–88, 1988.

106. Smith, S. B., S. E. Crager, and J. S. Mogil, "Paclitaxel-induced neuropathic hypersensitivity in mice: responses in 10 inbred mouse strains," *Life Sci*, Vol. 74, no. 21, pp. 2593–604, 2004.

107. Schneider, C. A., W. S. Rasband, and K. W. Eliceiri, "Nih image to imagej: 25 years of image analysis," *Nat Methods*, Vol. 9, no. 7, pp. 671–5, 2012.

108. McArthur, J. C., E. A. Stocks, P. Hauer, D. R. Cornblath, and J. W. Griffin, "Epidermal nerve fiber density: normative reference range and diagnostic efficiency," *Arch Neurol*, Vol. 55, no. 12, pp. 1513–20, 1998.

109. Griffin, J. W., J. C. McArthur, and M. Polydefkis, "Assessment of cutaneous innervation by skin biopsies," *Curr Opin Neurol*, Vol. 14, no. 5, pp. 655–9, 2001.

110. Kabra, P. M., H. K. Lee, W. P. Lubich, and L. J. Marton, "Solid-phase extraction and determination of dansyl derivatives of unconjugated and acetylated polyamines by reversed-phase liquid chromatography: improved separation systems for polyamines in cerebrospinal fluid, urine and tissue," *J Chromatogr*, Vol. 380, no. 1, pp. 19–32, 1986.

111. Sabri, M. I., A. I. Soiefer, G. E. Kisby, and P. S. Spencer, "Determination of polyamines by precolumn derivatization with 9-fluorenylmethyl chloroformate and reverse-phase high-performance liquid chromatography," *J Neurosci Methods*, Vol. 29, no. 1, pp. 27–31, 1989.

112. Park, S. B., A. V. Krishnan, C. S. Lin, D. Goldstein, M. Friedlander, and M. C. Kiernan, "Mechanisms underlying chemotherapy-induced neurotoxicity and the potential for neuroprotective strategies," *Curr Med Chem*, Vol. 15, no. 29, pp. 3081–94, 2008.

113. Lichti, U., T. J. Slaga, T. Ben, E. Patterson, H. Hennings, and S. H. Yuspa, "Dissociation of tumor promoter-stimulated ornithine decarboxylase activity and dna synthesis in mouse epidermis in vivo and in vitro by fluocinolone acetonide, a tumor-promotion inhibitor," *Proc Natl Acad Sci U S A*, Vol. 74, no. 9, pp. 3908–12, 1977.

114. Slaga, T. J., A. J. Klein-Szanto, S. M. Fischer, C. E. Weeks, K. Nelson, and S. Major, "Studies on mechanism of action of anti-tumor-promoting agents: their specificity in two-stage promotion," *Proc Natl Acad Sci U S A*, Vol. 77, no. 4, pp. 2251–4, 1980.

115. Schwarz, J. A., A. Viaje, and T. J. Slaga, "Fluocinolone acetonide: a potent inhibitor of mouse skin tumor promotion and epidermal dna synthesis," *Chem Biol Interact*, Vol. 17, no. 3, pp. 331–47, 1977.

116. Gilad, G. M., and V. H. Gilad, "Early rapid and transient increase in ornithine decarboxylase activity within sympathetic neurons after axonal injury," *Exp Neurol*, Vol. 81, no. 1, pp. 158–66, 1983.

117. Chen, W., R. Mi, N. Haughey, M. Oz, and A. Hoke, "Immortalization and characterization of a nociceptive dorsal root ganglion sensory neuronal line," *J Peripher Nerv Syst*, Vol. 12, no. 2, pp. 121–30, 2007.

118. Deng, K., H. He, J. Qiu, B. Lorber, J. B. Bryson, and M. T. Filbin, "Increased synthesis of spermidine as a result of upregulation of arginase i promotes axonal regeneration in culture and in vivo," *J Neurosci*, Vol. 29, no. 30, pp. 9545–52, 2009.

119. Noro, T., K. Namekata, A. Kimura, X. Guo, Y. Azuchi, C. Harada, T. Nakano, H. Tsuneoka, and T. Harada, "Spermidine promotes retinal ganglion cell survival and optic nerve regeneration in adult mice following optic nerve injury," *Cell Death Dis*, Vol. 6, p. e1720, 2015.

120. Cai, D., K. Deng, W. Mellado, J. Lee, R. R. Ratan, and M. T. Filbin, "Arginase i and polyamines act downstream from cyclic amp in overcoming inhibition of axonal growth mag and myelin in vitro," *Neuron*, Vol. 35, no. 4, pp. 711–9, 2002.

121. Huang, Y., D. S. Higginson, L. Hester, M. H. Park, and S. H. Snyder, "Neuronal growth and survival mediated by eif5a, a polyamine-modified translation initiation factor," *Proc Natl Acad Sci U S A*, Vol. 104, no. 10, pp. 4194–9, 2007.

122. Sigrist, S. J., D. Carmona-Gutierrez, V. K. Gupta, A. Bhukel, S. Mertel, T. Eisenberg, and F. Madeo, "Spermidine-triggered autophagy ameliorates memory during aging," *Autophagy*, Vol. 10, no. 1, pp. 178–9, 2014.

123. Wang, I. F., K. J. Tsai, and C. K. Shen, "Spermidine on neurodegenerative diseases," *Cell Cycle*, Vol. 14, no. 5, pp. 697–8, 2015.

124. Rivat, C., P. Richebe, E. Laboureyras, J. P. Laulin, R. Havouis, F. Noble, J. P. Moulinoux, and G. Simonnet, "Polyamine deficient diet to relieve pain hypersensitivity," *Pain*, Vol. 137, no. 1, pp. 125–37, 2008.

125. Ferrier, J., M. Bayet-Robert, B. Pereira, L. Daulhac, A. Eschalier, D. Pezet, J. P. Moulinoux, and D. Balayssac, "A polyamine-deficient diet prevents oxaliplatin-induced acute cold and mechanical hypersensitivity in rats," *PLoS One*, Vol. 8, no. 10, p. e77828, 2013.

126. Balayssac, D., J. Ferrier, B. Pereira, B. Gillet, C. Petorin, J. Vein, F. Libert, A. Eschalier, and D. Pezet, "Prevention of oxaliplatin-induced peripheral neuropathy by a polyamine-reduced diet-neuroxapol: protocol of a prospective, randomised, controlled, single-blind and monocentric trial," *BMJ Open*, Vol. 5, no. 4, p. e007479, 2015.

127. Nowotarski, S. L., P. M. Woster, and J. R A Casero, "Polyamines and cancer: implications for chemotherapy and chemoprevention," *Expert Rev Mol Med*, Vol. 15, p. e3, 2013.

128. Beattie, M. S., Q. Li, and J. C. Bresnahan, "Cell death and plasticity after experimental spinal cord injury," *Prog Brain Res*, Vol. 128, pp. 9–21, 2000.

129. Emery, E., P. Aldana, M. B. Bunge, W. Puckett, A. Srinivasan, R. W. Keane, J. Bethea, and A. D. Levi, "Apoptosis after traumatic human spinal cord injury," *J Neurosurg*, Vol. 89, no. 6, pp. 911–20, 1998.

130. Abe, Y., T. Yamamoto, Y. Sugiyama, T. Watanabe, N. Saito, H. Kayama, and T. Kumagai, "Apoptotic cells associated with wallerian degeneration after experimental spinal cord injury: a possible mechanism of oligodendroglial death," *J Neurotrauma*, Vol. 16, no. 10, pp. 945–52, 1999.

131. Polito, A., and R. Reynolds, "Ng2-expressing cells as oligodendrocyte progenitors in the normal and demyelinated adult central nervous system," *J Anat*, Vol. 207, no. 6, pp. 707–16, 2005.

132. Fawcett, J. W., and R. A. Asher, "The glial scar and central nervous system repair," *Brain Res Bull*, Vol. 49, no. 6, pp. 377–91, 1999.

133. Matsui, F., and A. Oohira, "Proteoglycans and injury of the central nervous system," *Congenit Anom (Kyoto)*, Vol. 44, no. 4, pp. 181–8, 2004.

134. Bradbury, E. J., L. D. Moon, R. J. Popat, V. R. King, G. S. Bennett, P. N. Patel, J. W. Fawcett, and S. B. McMahon, "Chondroitinase abc promotes functional recovery after spinal cord injury," *Nature*, Vol. 416, no. 6881, pp. 636–40, 2002.

135. Bregman, B. S., E. Kunkel-Bagden, L. Schnell, H. N. Dai, D. Gao, and M. E. Schwab, "Recovery from spinal cord injury mediated by antibodies to neurite growth inhibitors," *Nature*, Vol. 378, no. 6556, pp. 498–501, 1995.

136. Yick, L. W., P. T. Cheung, K. F. So, and W. Wu, "Axonal regeneration of clarke's neurons beyond the spinal cord injury scar after treatment with chondroitinase abc," *Exp Neurol*, Vol. 182, no. 1, pp. 160–8, 2003.

137. Bradbury, E. J., and S. B. McMahon, "Spinal cord repair strategies: why do they work?," *Nat Rev Neurosci*, Vol. 7, no. 8, pp. 644–53, 2006.

138. Evans, M. J., and M. H. Kaufman, "Establishment in culture of pluripotential cells from mouse embryos," *Nature*, Vol. 292, no. 5819, pp. 154–6, 1981.

139. Mothe, A. J., and C. H. Tator, "Advances in stem cell therapy for spinal cord injury," *J Clin Invest*, Vol. 122, no. 11, pp. 3824–34, 2012.

140. McDonald, J. W., X. Z. Liu, Y. Qu, S. Liu, S. K. Mickey, D. Turetsky, D. I. Gottlieb, and D. W. Choi, "Transplanted embryonic stem cells survive, differentiate and promote recovery in injured rat spinal cord," *Nat Med*, Vol. 5, no. 12, pp. 1410–2, 1999.

141. Kimura, H., M. Yoshikawa, R. Matsuda, H. Toriumi, F. Nishimura, H. Hirabayashi, H. Nakase, S. Kawaguchi, S. Ishizaka, and T. Sakaki, "Transplantation of embryonic stem cell-derived neural stem cells for spinal cord injury in adult mice," *Neurol Res*, Vol. 27, no. 8, pp. 812–9, 2005.

142. Yang, I. H., D. Gary, M. Malone, S. Dria, T. Houdayer, V. Belegu, J. W. McDonald, and N. Thakor, "Axon myelination and electrical stimulation in a microfluidic, compartmentalized cell culture platform," *Neuromolecular Med*, Vol. 14, no. 2, pp. 112–8, 2012.

143. Wu, C. Y., D. Whye, R. W. Mason, and W. Wang, "Efficient differentiation of mouse embryonic stem cells into motor neurons," *J Vis Exp*, no. 64, p. e3813, 2012.

144. Wichterle, H., I. Lieberam, J. A. Porter, and T. M. Jessell, "Directed differentiation of embryonic stem cells into motor neurons," *Cell*, Vol. 110, no. 3, pp. 385–97, 2002.

145. Jiang, P., V. Selvaraj, and W. Deng, "Differentiation of embryonic stem cells into oligodendrocyte precursors," *J Vis Exp*, no. 39, 2010.

146. Liu, S., Y. Qu, T. J. Stewart, M. J. Howard, S. Chakrabortty, T. F. Holekamp, and J. W. McDonald, "Embryonic stem cells differentiate into oligodendrocytes and myelinate in culture and after spinal cord transplantation," *Proc Natl Acad Sci U S A*, Vol. 97, no. 11, pp. 6126–31, 2000.

147. Hausmann, O. N., "Post-traumatic inflammation following spinal cord injury," *Spinal Cord*, Vol. 41, no. 7, pp. 369–78, 2003.

148. Keirstead, H. S., G. Nistor, G. Bernal, M. Totoiu, F. Cloutier, K. Sharp, and O. Steward, "Human embryonic stem cell-derived oligodendrocyte progenitor cell transplants remyelinate and restore locomotion after spinal cord injury," *J Neurosci*, Vol. 25, no. 19, pp. 4694–705, 2005.

149. Butt, A. M., and M. Berry, "Oligodendrocytes and the control of myelination in vivo: new insights from the rat anterior medullary velum," *J Neurosci Res*, Vol. 59, no. 4, pp. 477–88, 2000.

150. Linington, C., B. Engelhardt, G. Kapocs, and H. Lassman, "Induction of persistently demyelinated lesions in the rat following the repeated adoptive transfer of encephalitogenic t cells and demyelinating antibody," *J Neuroimmunol*, Vol. 40, no. 2-3, pp. 219–24, 1992.

151. Miller, B. A., J. M. Crum, C. A. Tovar, A. R. Ferguson, J. C. Bresnahan, and M. S. Beattie, "Developmental stage of oligodendrocytes determines their response to activated microglia in vitro," *J Neuroinflammation*, Vol. 4, p. 28, 2007.

152. Pang, Y., L. Campbell, B. Zheng, L. Fan, Z. Cai, and P. Rhodes, "Lipopolysaccharide-activated microglia induce death of oligodendrocyte progenitor cells and impede their development," *Neuroscience*, Vol. 166, no. 2, pp. 464–75, 2010.

153. Rossi, S. L., G. Nistor, T. Wyatt, H. Z. Yin, A. J. Poole, J. H. Weiss, M. J. Gardener, S. Dijkstra, D. F. Fischer, and H. S. Keirstead, "Histological and functional benefit following transplantation of motor neuron progenitors to the injured rat spinal cord," *PLoS One*, Vol. 5, no. 7, p. e11852, 2010.

154. Wyatt, T. J., S. L. Rossi, M. M. Siegenthaler, J. Frame, R. Robles, G. Nistor, and H. S. Keirstead, "Human motor neuron progenitor transplantation leads to endogenous neuronal sparing in 3 models of motor neuron loss," *Stem Cells Int*, Vol. 2011, p. 207230, 2011.

155. Zhang, Y. W., J. Denham, and R. S. Thies, "Oligodendrocyte progenitor cells derived from human embryonic stem cells express neurotrophic factors," *Stem Cells Dev*, Vol. 15, no. 6, pp. 943–52, 2006.

156. Sharp, J., J. Frame, M. Siegenthaler, G. Nistor, and H. S. Keirstead, "Human embryonic stem cell-derived oligodendrocyte progenitor cell transplants improve recovery after cervical spinal cord injury," *Stem Cells*, Vol. 28, no. 1, pp. 152–63, 2010.

157. Hoke, A., and R. Mi, "In search of novel treatments for peripheral neuropathies and nerve regeneration," *Discov Med*, Vol. 7, no. 39, pp. 109–12, 2007.